QUASAR Deliverable D4.2

Cooperation Strategies for Secondary Users

Project Number:	INFSO-ICT-248303
Project Title:	Quantitative Assessment of Secondary Spectrum Access - QUASAR
Document Type:	

Document Number:	ICT-248303/QUASAR/WP4/D4.2/120331
Contractual Date of Delivery:	31.03.2012
Actual Date of Delivery:	05.04.2012
Editors:	Chao Wang (KTH EES)
Participants:	Vladimir Atanasovski (UKIM), Liljana Gavrilovska (UKIM), Maksym Girnyk (KTH EES), Bisera Jankuloska (UKIM), Riku Jäntti (Aalto), Konstantinos Koufos (Aalto), Jonas Kronander (Ericsson AB), Xia Li (RWTH), Valentina Pavlovska (UKIM), Marina Petrova (RWTH), Muhammad Imadur Rahman (Ericsson AB), Valentin Rakovic (UKIM), Lars K. Rasmussen (KTH EES), Kalle Ruttik (Aalto), Ljiljana Simić (RWTH), Chao Wang (KTH EES)
Workpackage:	WP4
Estimated Person Months:	24 MM
Security:	PU[1]
Nature:	Report
Version:	1.0
Total Number of Pages:	91
File:	QUASAR_D4.2_120331.doc

Abstract

In this deliverable, we focus on cognitive radio systems with multiple secondary users. We investigate novel strategies that allow the secondary users to be *aware* and *cooperate* with each other in order to reduce harmful interference to the primary system and also enhance the secondary system's spectral efficiency and communication quality. To this end, we introduce two secondary relaying schemes by

[1] Dissemination level codes: **PU** = Public
PP = Restricted to other programme participants (including the Commission Services)
RE = Restricted to a group specified by the consortium (including the Commission Services)
CO = Confidential, only for members of the consortium (including the Commission Services)

exploiting the concept of cooperative communications within the secondary system. In addition, we propose an adaptive power allocation strategy, which can jointly assign transmit powers to multiple secondary users. We also investigate four models that permit secondary users to collaboratively perform sensing in multiple spectrum bands. Finally, we use two potential solutions to enable secondary user cooperation so that the available spectrum opportunity can be shared in more efficient fashions. We provide sound theoretic analysis to explicitly exhibit the advantages of allowing multiple secondary users to interact with each other. Our results imply that seeking secondary-user cooperation can serve as a promising solution to reduce interference and improve performance in next-generation cognitive radio systems. In particular, the bottleneck posed by the aggregated interference may be mitigated by secondary cooperation. The strategies proposed and analyzed in this deliverable would pave the way for further research on approaches to realizing more efficient and reliable cooperation among secondary users.

Keywords List

Secondary user cooperation, secondary relaying, coordinated power allocation, cooperative multi-band sensing, cooperative spectrum sharing

Executive Summary

The main target of WP4 is to understand the impact of allowing multiple secondary users to share the available spectrum opportunity. In our previous deliverable D4.1 [1], we have provided methods and solutions to handle the sharing problems for scenarios with *unaware* secondary users. In other words, each secondary user does not have any knowledge regarding other secondary users in the vicinity so that no potential interaction among secondary users is feasible. We have observed that the aggregated interference from several secondary transmitters is a key problem and a bottleneck for secondary communication. Estimating and controlling it by keeping it at an acceptably low level is of crucial importance. Introducing *cooperation* between secondary users (or systems) may potentially serve as an effective approach to facilitate this task. Therefore, in this deliverable, we aim to take a further step by allowing different secondary users to be *aware* and *cooperate* with each other. The main focus of this deliverable is to investigate novel secondary-user cooperation strategies in order to tackle the bottleneck, i.e. to reduce harmful interference to the primary system and enhance the secondary system's spectral efficiency and communication quality.

In this deliverable, we first consider exploiting the concept of cooperative communications in the secondary system such that certain users can serve as relays and assist other users' transmissions. We propose two secondary relaying schemes in Chapter 2. In Chapter 3 we introduce a novel adaptive coordinated power allocation strategy for the secondary system, aiming at maximizing the sum rate of all secondary users while protecting potential primary users in a given area. Chapter 4 focuses on cooperative multi-band sensing, i.e. the multi-band sensing decision is made by all secondary users that cooperate. We present performance evaluations of four selected sensing models. Finally, Chapter 5 is dedicated to two novel cooperative strategies such that secondary users can relay for each other or exchange certain information in order to share the available spectrum opportunity in more efficient fashions.

More specifically, by exploiting potential cooperation among secondary by letting some nodes serve as relays and assist in other secondary users' transmission it is shown that the interference introduced by the secondary system to the primary system may be reduced. Or, equivalently, the performance in terms of throughput of the secondary system can be improved without increasing the probability of causing harmful interference. The two proposed cooperative secondary relaying schemes confirm the positive impact of considering secondary user cooperation on the secondary performance in terms of higher throughput or higher diversity.

By introducing cooperation, via coordination of secondary users, and exploiting information on which secondary users are transmitting and at what locations, it is shown that a novel optimization approach allows the secondary transmit powers to be higher than what is allowed in the current proposed regulation by the ECC. This, while ensuring protection of primary receivers. Hence, the secondary throughput may be increased. The amount of the increase in performance will depend strongly on the details of the scenario and no figures may be stated with enough confidence.

Even though spectrum sensing is deemed as a non-prioritized solution for secondary TVWS applications it may be utilized as a complementary spectrum availability detection approach capable of increasing the efficiency of the detection process of the database approach. Moreover, sensing methods may still be preferred as detection techniques for other situations, e.g., where Programme Making Special Events (PMSE) devices are granted a prioritized status but not required to be registered in a database. The spectrum sensing process (facilitated with cooperation and multi-band approach) may also complement the database spectrum opportunity detection approach by providing more updated information on the spectrum usage in these bands. For these reasons various benefits of cooperative multi-band sensing is investigated in this deliverable and a key finding is that multi-band sensing does increase the reliability compared to the

single-band sensing case. Further, when the number of cooperative nodes is increased in a novel control scheme we find that the introduced cooperation leads to an increased throughput of the secondary system. When a MAC protocol is used for reporting of sensing results, the control signalling can dominate the sensing overhead in some scenarios. This emphasizes the importance of using an efficient reporting MAC in cooperative sensing.

The introduced cooperative spectrum sharing algorithms result in increased secondary system performance at the cost of increased computational complexity and signalling overhead. A first novel sharing scheme achieves a manageable computational complexity to allow real time beamforming to clusters of secondary users, limiting the interference in other directions. A second proposed sharing scheme has the benefit of allowing a larger number of secondary users to be served by access points than what can be supported without the novel scheme. Further, only a small increase in secondary throughput is observed in this latter scheme for the investigated scenarios but this increase is expected to be significant in even denser secondary deployments.

The QUASAR project initially set out to investigate some general questions regarding secondary cooperation; how much of the available opportunistic capacity needs to be spent on sensing and control signalling, how much may be gained by introducing multiple-access, and how much gain may be realized through the use of advanced adaptive strategies. It turns out that the gains that may be achieved differ between the proposed solutions and are very scenario dependent. The results given in this deliverable may be seen as a first step of address the above general questions. More research is needed to put definite numbers on, and with confidence answer the above questions in a more general setting.

However, the presented results explicitly exhibit the advantages of allowing multiple secondary users to interact with each other. Thus we conclude that seeking secondary-user cooperation can serve as a promising solution to reduce interference and improve performance in next-generation cognitive radio systems. The strategies proposed and analyzed in this deliverable would pave the way for further research on approaches to realizing more efficient and reliable cooperation among secondary users.

Contributors

First name	Last name	Affiliation	Email
Maksym	Girnyk	KTH EES	mgyr@kth.se
Lars K.	Rasmussen	KTH EES	lkra@kth.se
Chao	Wang	KTH EES	chaowang@kth.se
Vladimir	Atanasovski	UKIM	vladimir@feit.ukim.edu.mk
Liljana	Gavrilovska	UKIM	liljana@feit.ukim.edu.mk
Bisera	Jankuloska	UKIM	bisera@feit.ukim.edu.mk
Valentina	Pavlovska	UKIM	valenpav@feit.ukim.edu.mk
Valentin	Rakovic	UKIM	valentin@feit.ukim.edu.mk
Ljiljana	Simić	RWTH	lsi@inets.rwth-aachen.de
Marina	Petrova	RWTH	pma@inets.rwth-aachen.de
Xia	Li	RWTH	xia@inets.rwth-aachen.de
Konstantinos	Koufos	Aalto	Konstantinos.koufos@aalto.fi
Kalle	Ruttik	Aalto	Kalle.ruttik@aalto.fi
Riku	Jäntti	Aalto	Riku.jantti@aalto.fi
Jonas	Kronander	Ericsson AB	jonas.kronander@ericsson.com
Muhammad Imadur	Rahman	Ericsson AB	muhammad.imadur.rahman@ericsson.com

Table of contents

Abbreviations

ACK	Acknowledgement
ARQ	Automatic Repeat Request
ASI	Accumulated Secondary Interference
AWGN	Additive White Gaussian Noise
BOI	Backward Overhearing Interference
BPCU	Bits per Channel Use
BS	Base Station
CCC	Common Control Channel
CMS	Cooperative Multi-band Sensing
CMSS	Cooperative Multi-band Spectrum Sensing
CR	Cognitive Radio
DMSS	Distributed Multi-band Spectrum Sensing
DMT	Diversity-Multiplexing Tradeoff
EGC	Equal Gain Combining
ENG	Electronic News Gathering
FC	Fusion Centre
FDMA	Frequency Division Multiple Access
FDSS	Frequency Division Spectrum Sharing
FOI	Forward Overhearing Interference
GOI	General Overhearing Interference
LICQ	Linear Independent Constraint Qualification
MAC	Multiple-Access
MCKP	Multiple Choice Knapsack Packing
MDS-FFNC	Maximum Distance Separable Finite Field Network Code
MRC	Maximum Ratio Combining
MV	Majority Voting
NACK	Negative Acknowledgement
NBS	Nash Bargaining Solution
NCBC	Network Coordinated Beamforming with user Clustering
NCBF	Network Coordinated Beamforming
PMSE	Programme Making Special Events
PSD	Power Spectrum Density
PU	Primary User
QoS	Quality of Service
RSG	Random Sampling Grid
SAP	Secondary Access Point
SIC	Successive Interference Cancellation

SIMO	Single-Input Multiple-Output
SINR	Signal-to-Interference-plus-Noise Ratio
SIR	Signal to Interference Ratio
SNR	Signal-to-Noise Ratio
SPRT	Sequential Probability Ratio Test
SU	Secondary User
TDMA	Time Division Multiple Access
TRS	Total Random Sampling
UE	User Equipment
UL	Uplink
VCO	Voltage Controlled Oscillator
WLAN	Wireless Local Area Network
WSD	White Space Device

1 Introduction

As new wireless applications and services emerge rapidly, the demand of higher data rates and reliability in wireless communications is endless. Besides densifying the networks, another natural approach to achieve such requirements is to use more bandwidth. On the one hand, the wireless spectrum is becoming an increasingly more precious commodity. On the other hand, a scan of the radio spectrum reveals the presence of so-called *spectrum holes*, where the spectrum is used inefficiently and thus valuable bandwidth resources are wasted. The concept of *cognitive radio* (CR) [2] was proposed to allow users to sense and learn the surrounding spectrum environment and dynamically adapt transmission strategies to increase spectral efficiency [3].

In general, a typical CR scenario consists of two co-exist systems: *A primary system*, which represents a deployed system with license to operate within a certain spectrum band, and a *secondary system,* intending to use the primary system's band to conduct its own operation. Clearly, a crucial requirement behind the CR concept is that the harmful interference introduced by the secondary system to the primary system must be kept to a certain satisfactory level. In other words, the concept of CR tends to seek effective spectrum sharing solutions (or secondary spectrum usage opportunities) such that the service requirements of both the primary and the secondary system are met, with priority towards the primary system. *Underlay*, *interweave*, and *overlay* are three major primary-secondary spectrum sharing strategies [4].

The main target of WP4 is to understand the impact of allowing multiple secondary users (or multiple secondary systems) to access/share the available spectrum opportunity. In our previous deliverable D4.1 [1], we have provided methods and solutions to handle the sharing problems for scenarios with *unaware* secondary users. In other words, each secondary user does not have any knowledge regarding other secondary users in the vicinity so that no potential interaction among secondary users is feasible. In this deliverable, we aim to take a further step by allowing different secondary users to be *aware* and *cooperate* with each other. Such user cooperation may be carried out in different levels and forms. For instance, some users may potentially be dedicated to assist other users' transmissions. Different secondary users may decide their resource allocation strategy together. They may also jointly perform multi-band sensing to reach more accurate opportunity sensing decisions. Certainly, through proper interactions the available spectrum opportunity can be shared in more efficient ways. Thus the main focus of this deliverable is to investigate novel secondary-user cooperation strategies in order to reduce harmful interference to the primary system and enhance spectral efficiency and communication quality within the secondary system.

More specifically, in Chapter 2 we consider exploiting the concept of cooperative communications [5] in the secondary system such that certain users can serve as relays and assist some target users' transmissions. We study two secondary relaying schemes. We first focus on an underlay primary-secondary spectrum sharing setup, in which the secondary network has a tandem structure while the primary system may have different receivers that can be interfered by the secondary transmissions. We provide the optimal power allocation strategy for the secondary system in order to maximize its throughput, without introducing more interference to the primary system. In addition, we also propose a secondary relaying scheme for an overlay primary-secondary spectrum sharing setup, where multiple secondary relays are used to assist in the communications between multiple secondary sources and a common secondary destination. Unlike the first scheme, in which the secondary system always operates in the primary system's band, here the secondary access is conducted in an opportunistic manner: The secondary relays transmit using the band owned by the primary system only when the secondary sources require their assistance. We employ network coding and Automatic Repeat Request (ARQ) feedback signals in the secondary system to efficiently obtain spatial diversity. Due to the fact that the use of relays effectively reduces the negative

impact of fading, in both schemes we observe the performance enhancement brought by considering secondary-user cooperation.

In Chapter 3 we introduce a novel adaptive coordinated power allocation strategy for the secondary system. The strategy allocates transmit powers to secondary transmitters, that will transmit simultaneously on the same band, while protecting potential primary users in a given area. It does so by maximizing the sum rate of the secondary communication links. For being applicable the strategy needs the secondary transmissions to be orthogonal, and hence it applies in particular to the cellular uplink case. The strategy is shown by numerical simulations to produce efficient power allocations while at the same time effectively protect primary users. The advantage of this strategy is that it dynamically incorporates the additional margin of the interference threshold, related to having multiple secondary transmitters. The margin does not need to be specified in advance, and hence is not needed to be based on worst case assumptions as is otherwise common, cf. the proposed method of SE43 to calculate the maximally allowed transmit power [6]. This coordinated cooperative dynamic approach to the handling of the multiple secondary transmitters allows larger secondary transmit powers and hence better secondary communication performance, compared to methods based on worst case assumptions.

Spectrum sensing, which enables secondary users to sense and inspect vacant spectrum opportunities for secondary usage, is certainly one of the key CR functionalities. Although latest secondary spectrum access study (including the QUASAR project) shows that the database approach is preferable to spectrum sensing in static environments (e.g. TVWS), the process of spectrum sensing may prove vital for accurate and up-to-date databases population especially in more dynamic environments. Since performing sensing in multiple spectrum bands can provide significantly higher opportunity detection probability than sensing in a single band, multi-band sensing has been considered as an easier and safer approach for spectrum opportunity detection. Thus our focus in Chapter 4 is on cooperative multi-band sensing, i.e. the multi-band sensing decision is made from all secondary users that cooperate. We present performance evaluations of four selected sensing models in this chapter. Specifically, in a *Distributed Multi-band Spectrum Sensing* (DMSS) model, each secondary user measures only one band but the sensing decision is reached from multiple users' observations. We investigate the minimal required number of sensed bands in multiband environment under certain constraints for the interference at the primary system and service outage probability. The *energy efficient multiband spectrum sensing* model stems on the DMSS scenario and, furthermore, investigates the optimal number of users that should be allocated for reliable measurement in each frequency band. This allows maximization of the achievable throughput and minimization of the total spent power. Unlike the DMSS model, where each user targets a single band, the *Cooperative Multi-band Spectrum Sensing* (CMSS) model requires each secondary user to conduct sensing in multiple bands before a joint decision is made by multiple users. In this model we investigate the optimal sensing duration and optimal number of collaborating nodes that satisfy the required spectrum sensing reliability and maximize the opportunistic throughput in the secondary cognitive network for different fusion rules. Finally, we consider a *Fast Cooperative Spectrum Sensing* (FCSS) model to evaluate the multi-band spectrum sensing by taking into account the multiple access protocols including TDMA and CSMA/CA during data fusion. We examine the most suitable sensor assignment strategy per band and optimal number of sensing nodes that maximize the opportunistic throughput.

The final part of this deliverable, Chapter 5, is dedicated to novel strategies that enable multiple secondary users to cooperate with each other in order to efficiently share the available spectrum opportunity (with database based spectrum opportunity detection) and in the same time foster reliable primary users' protection. Network MIMO has been seen as a promising method for cooperative spectrum sharing. For instance, the Network Coordinated Beamforming (NCBF) technique permits multiple systems to put their

antennas together and create a large antenna array. It thus enables multiple systems to jointly and efficiently access the same spectrum at the same time. But in general this technique requires high processing power. To handle this issue, we propose a *Network Coordinated Beamforming with user Clustering* (NCBC) scheme based on network MIMO NCBF technique and a User Clustering (UC) strategy. Our NCBC scheme effectively reduces the computational complexity of NCBF so that it would be suitable for real time spectrum sharing in secondary systems. In addition, we introduce a spectrum sharing scheme among secondary WiFi-like systems who intend to operate in TV white space. We consider a unique combination of a game theory based power allocation strategy and a simple channel allocation algorithm. The proposed scheme is able to maximize the number of supported secondary users. In other words, it realizes efficient available spectrum usage among secondary users.

2 Secondary Cooperation through Relaying

2.1 Introduction

It is well known that wireless communications suffer from the fading phenomenon. Due to path loss, shadowing, and multi-path fading between a wireless source-destination pair, a large transmit power might be required to guarantee a certain quality of service (QoS). Clearly, large transmit power means high energy consumption and high interference to other systems operating at the same time in the same frequency band. Many investigations have been conducted to tackle this issue. Introducing relays to assist in wireless communications has been considered as one of the promising solutions [5]. The conventional usage of relays is to place them in advantageous positions to reduce the negative impact of large-scale fading. In the last decade much interest has been attracted to their ability of handling also small-scale fading: relays can provide spatial diversity by delivering information via new fading paths. Certainly the relaying functions can be performed by fixed relay stations. However, a more attractive approach for future wireless systems can be allowing different users to act as relays for each other [5]. For instance, in a cellular network, at one time instant a mobile terminal A near the cell boundary intends to communicate with the serving base station (BS) located at the cell centre. A high transmit power is expected to reach high-speed and low-error transmission. If another mobile terminal B, which locates in between and is currently inactive, can relay A's signal to the BS, potentially the expected transmit power of A can be significantly reduced. At another time instant when B starts communicating with the BS, another mobile terminal (possible A) may provide assistance. Therefore, by seeking relays we are actually seeking *cooperation* among different terminals.

In this section, we borrow the above idea and introduce relays to assist in the communication of secondary system in cognitive radio scenarios. In other words, we allow cooperation among secondary users and investigate the impact of such an assumption on the secondary system's performance. We first consider an underlay primary-secondary spectrum sharing scenario, in which a secondary source intends to deliver information to a secondary destination using a primary system's spectrum band. The primary system may potentially have multiple receivers. To guarantee the service quality of the primary system the aggregate secondary interference (ASI) at all the primary receivers should be limited to below a certain level. We place full-duplex decode-and-forward relays between the secondary source-destination pair (so that the secondary system has a tandem topology). Clearly, the relays create multiple hops, each of which has a shorter propagation length than that of the direct source-destination link. However, they also introduce extra interference to both the primary system and secondary system itself. We study power allocation strategies for the secondary system in order to maximize its throughput, under the constraint of strictly limited interference to external users (i.e. primary receivers). We show that the optimal approach is to assign power to each secondary node such that each hop has identical capacity and the interference power constraint is satisfied with equality. Since in general a closed-form solution of the power allocation problem is difficult to attain (but it can be solved numerically), we provide high-SNR and low-SNR approximations to the solution. Our results exhibit that using relays (or user cooperation) is able to provide throughput enhancement of the secondary system, under certain conditions.

In addition, we propose another secondary cooperation scheme based on the overlay primary-secondary spectrum sharing strategy. (In fact this scheme can also be applicable to *out of band relaying scenarios* in which the relays operate in bands other than those where the main communication is done.) We consider a point-to-point primary system and a multi-user secondary system. In principle the two systems operate in different spectrum bands, which are respectively termed primary band and secondary band in this deliverable. Due to the fading phenomenon, the performance of the secondary system is limited. We can use relays to provide enhanced performance

and apply network coding on top of channel coding to efficiently use the channel. However, due to the fact that in most practical systems relays cannot receive and transmit simultaneously in the same frequency band (i.e. the so-called *half-duplex limitation*), some extra channels in the secondary band have to be reserved for relay operation. Such a requirement will lead to a spectral inefficiency when compared with direct source-destination communication without relaying, especially in the high signal-to-noise (SNR) ratio region. To handle this issue, we consider aligning the relays' operation with that of the primary system. In order to compensate the interference introduced by the secondary relaying, we require the secondary destination to help the primary system to boost its signal power. In other words, the secondary relays and the primary system share the primary band through overlay sharing strategy. Since the direct source-destination channels in the secondary band can be good enough to support high-quality communication, the use of the secondary relays may not always be necessary. Thus we also consider exploiting Automatic Repeat Request (ARQ) feedback signals from the secondary destination to avoid unnecessary secondary relays' activation. The secondary relays are used only if the secondary sources require assistance. Therefore, unlike the first scheme in which the secondary system always operates together with the primary system, here the secondary access of the primary band is conducted in an opportunistic fashion. The energy consumption of the secondary system is minimized. In addition, the considered multi-user secondary system may allow spectral efficient multiple access. We show that by permitting multiple secondary sources to transmit non-orthogonally, the performance can be further enhanced. Our results also explicitly display the advantage of considering user cooperation in the secondary system.

2.2 **Power allocation in multi-hop underlay CR networks**

2.2.1 **System model**

We consider a *K*-hop secondary system with a tandem topology as illustrated in Fig. 2-1. Nodes 1 and $K+1$ denote the secondary source and destination, respectively. Nodes $2,\cdots,K$ denote intermediate relays. Assume the relay nodes to operate in *full-duplex* mode. Namely, relays can receive and transmit information simultaneously in the same frequency band. Transmission from node i to node $i+1$ is said to be *overheard* if the signal from node i reaches node j ($j \neq i+1$). In certain scenarios overhearing may be helpful leading to increased diversity. However, in this section we assume that node $i+1$ knows only its incoming channel from node i. Thus it treats its overheard signals as interference. Overhearing interference can come from the nodes downstream referred to as *forward overhearing interference* (FOI). Interference from upstream nodes is called *backward overhearing interference* (BOI). If both FOI and BOI are present we refer to this case as *general overhearing interference* (GOI), as illustrated in Fig. 2-1. In the case of BOI, we assume that the channel gains to downstream nodes are smaller (in absolute value) than those to upstream nodes. For instance, this can be achieved by using directional antenna transmissions with main lobes directed upstream [7].

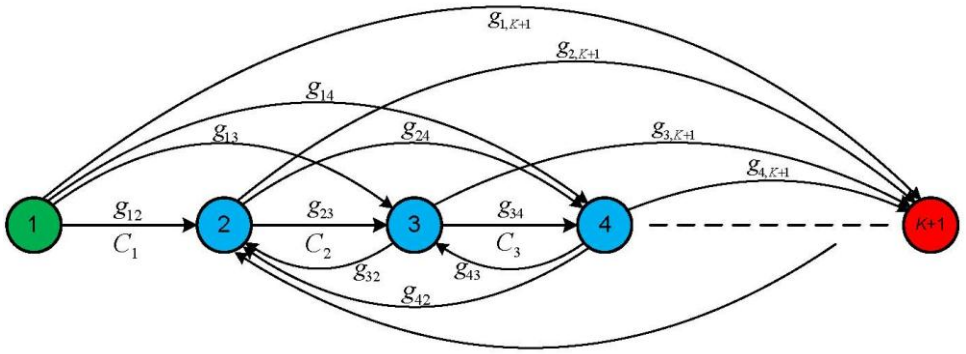

Fig. 2-1: Multi-hop transmission with overhearing upstream and downstream.

The links of the primary and secondary networks, as well as inter-network links, are additive white Gaussian noise (AWGN) channels subject to slow fading such that the channel gains are random but constant during a transmission suite from source to destination. The transmit power of CRN node i is denoted as P_i and the noise variance is σ^2. The channel gain $g_{i,j}$ between nodes i and j in the CRN absorbs path-loss and Rayleigh fading effects. The channel gain $\tilde{g}_{i,j}$ between node i in the secondary network and node j in the *primary* network is defined similarly. We also assume that all channel gains are known at the secondary source before the transmission starts, which can be obtained with an initial training phase. In this way, the secondary source can determine the optimal power allocation and forward the allocation information upstream as overhead with the message. The remaining nodes can also get information of the channel gains of their incoming links during the training phase to implement the regenerative relaying. Thus, according to the network model, the capacity of link i is

$$C_i = \log_2\left(1+\frac{g_{i,i+1}P_i}{\sigma^2+\sum_{j=1}^{L_f} g_{i-j,i+1}P_{i-j}+\sum_{j=1}^{L_b} g_{i+1+j,i+1}P_{i+1+j}}\right), \tag{2-1}$$

where L_f and L_b are corresponding maximum numbers of hops that create FOI and BOI. Suppose the primary network consists of M receivers operating simultaneously with the secondary network within the same area. In order to limit the ASI to the primary network the secondary system has a constraint

$$\sum_{i=1}^{K}\sum_{j=1}^{M}\tilde{g}_{i,j}P_i \le \gamma\,. \tag{2-2}$$

We denote $\varphi_i = \sum_{j=1}^{M}\tilde{g}_{i,j}$ and rewrite the ASI constraint in the following form

$$\sum_{i=1}^{K}\varphi_i P_i \le \gamma\,. \tag{2-3}$$

2.2.2 **Optimal power allocation**

From [8] we know that the end-to-end throughput of the network with a single source and a single sink is determined by the minimum capacity of the channels in the network. Since overhearing links cannot be helpful for information transmission, then in the case of the tandem topology the capacity is determined by the weakest link, i.e.,

$C = \min\{C_1, \ldots, C_K\}$. Therefore, the end-to-end throughput maximization problem for a given channel realization becomes

$$\begin{aligned} \max \quad & \min\{C_1, \ldots, C_K\} \\ \text{s.t.} \quad & \sum_{i=1}^{K} \varphi_i P_i \le \gamma \\ & P_i \ge 0, \quad \forall i. \end{aligned} \tag{2-4}$$

Unfortunately, since a function of type $f(x) = \log_2\left(1 + \frac{a}{b + cx}\right)$ with a, b, and c constants is not concave, the problem above is not a convex optimization problem. However, for this problem we have the following result.

Theorem 2-1. For a multi-hop tandem secondary network with a constraint on the ASI the end-to-end throughput is maximized if and only if the capacities of all channels of the network are equal, i.e.,

$$C_1 = \ldots = C_K, \tag{2-5}$$

and the ASI constraint is met with equality, i.e.,

$$\sum_{i=1}^{K} \varphi_i P_i = \gamma. \tag{2-6}$$

Proof: See appendix A.1.

Theorem 1 suggests that any violation of either (2-5) or (2-6) will immediately lead to sub-optimal solution. Therefore, in order to find the power allocation that achieves the maximum throughput we have to solve a system of $K-1$ non-linear equations (2-5) subject to the ASI constraint (2-6). For a large number of hops in the network it is difficult to find a closed-form solution; however, the problem can be solved numerically.

Furthermore, in order to simplify the solution we can use a high-SNR approximation based on the fact that at high SNR network performance is GOI-limited and the influence of noise vanishes. Thus, if $\min_{i,j}\{g_{i,j} P_i\} >> \sigma^2$ the latter can be neglected and the capacities become

$$C_i = \log_2\left(1 + \frac{g_{i,i+1} P_i}{\sum_{j=1}^{L_f} g_{i-j,i+1} P_{i-j} + \sum_{j=1}^{L_b} g_{i+1+j,i+1} P_{i+1+j}}\right). \tag{2-7}$$

According to Theorem 2-1, from (2-7) we get $K-1$ equalities with K unknowns, while one more equation is formed by the ASI constraint (2-6). Therefore, we can compute the optimal P_i^*. In general, this system is easier to solve than (2-1).

Similarly, at low SNR we can use the fact that the network performance is noise-limited and hence, we can neglect the GOI. The capacities become

$$C_i = \log_2\left(1 + \frac{g_{i,i+1} P_i}{\sigma^2}\right). \tag{2-8}$$

From (2-8) we get a system of $K-1$ equalities, subject to the ASI constraint (2-6) and thus, we can compute P_i^*.

2.2.3 **Examples**

For illustration, we now give a few examples as follows.

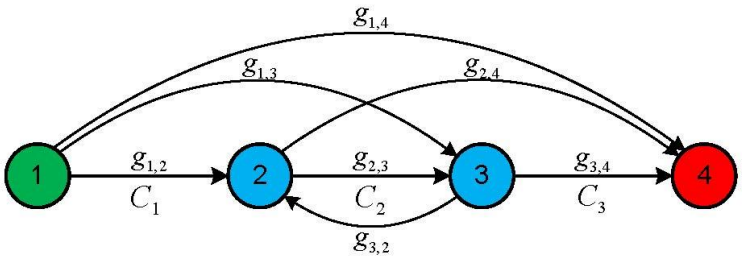

Fig. 2-2: 3-hop transmission with overhearing upstream and downstream.

2.2.3.1 3-Hop Network with General Overhearing

Consider a 3-hop network with possible one hop GOI which contains both FOI and BOI components of the interference as shown in Fig. 2-2. We assume that two-hop FOI is weak and can be disregarded, i.e., $L_f = 1$ and $L_b = 1$. For this setting the link capacities are given by

$$C_1 = \log_2\left(1+\frac{g_{12}P_1}{\sigma^2+g_{32}P_3}\right), \tag{2-9a}$$

$$C_2 = \log_2\left(1+\frac{g_{23}P_2}{\sigma^2+g_{13}P_1}\right), \tag{2-9b}$$

$$C_3 = \log_2\left(1+\frac{g_{34}P_{31}}{\sigma^2+g_{24}P_2}\right). \tag{2-9c}$$

From Theorem 2-1 we know that in order to obtain optimal P_1^*, P_2^* and P_3^* we have to solve the system of equations above, together with (2-6). Unfortunately, (2-9) has no direct closed-form solution; however, this can be done numerically. Moreover, to simplify the solution we may use two following approximations.

2.2.3.2 High-SNR Regime

When the transmit power is large, the network performance becomes interference-limited and therefore, if $\min_{i,j}\{g_{i,j}P_i\} >> \sigma^2$ the latter is negligible and the channel capacities become

$$C_1 = \log_2\left(1+\frac{g_{12}P_1}{g_{32}P_3}\right), \tag{2-10a}$$

$$C_2 = \log_2\left(1+\frac{g_{23}P_2}{g_{13}P_1}\right), \tag{2-10b}$$

$$C_3 = \log_2\left(1+\frac{g_{34}P_{31}}{g_{24}P_2}\right). \tag{2-10c}$$

Let $r=\frac{g_{12}}{g_{32}}$, $s=\frac{g_{23}}{g_{13}}$ and $q=\frac{g_{34}}{g_{24}}$. Thus, we can find that

$$\frac{P_1}{P_3}=\sqrt[3]{\frac{sq}{r^2}},\ \frac{P_2}{P_1}=\sqrt[3]{\frac{rq}{s^2}},\ \sum_{i=1}^{3}\varphi_i P_i=\gamma. \tag{2-11}$$

Solving the system of equations (2-11) provides the optimal power allocation at high SNR

$$P_1^*=\frac{\gamma\sqrt[3]{\frac{sq}{r^2}}}{\varphi_1\sqrt[3]{\frac{sq}{r^2}}+\varphi_2\sqrt[3]{\frac{q^2}{sr}}+\varphi_3} \tag{2-12a}$$

$$P_2^*=\frac{\gamma\sqrt[3]{\frac{q^2}{sr}}}{\varphi_1\sqrt[3]{\frac{sq}{r^2}}+\varphi_2\sqrt[3]{\frac{q^2}{sr}}+\varphi_3} \tag{2-12b}$$

$$P_3^*=\frac{\gamma}{\varphi_1\sqrt[3]{\frac{sq}{r^2}}+\varphi_2\sqrt[3]{\frac{q^2}{sr}}+\varphi_3} \tag{2-12c}$$

2.2.3.3 Low-SNR Regime

When SNR is low, the network performance is noise-limited and hence, we can neglect the interference from overhearing. The capacity expressions are simplified to

$$C_1=\log_2\left(1+\frac{g_{12}P_1}{\sigma^2}\right), \tag{2-13a}$$

$$C_2=\log_2\left(1+\frac{g_{23}P_2}{\sigma^2_1}\right), \tag{2-13b}$$

$$C_3=\log_2\left(1+\frac{g_{34}P_{31}}{\sigma^2}\right). \tag{2-13c}$$

Equating capacities in (2-13) we obtain a system of equations

$$\frac{P_1}{P_3}=\frac{g_{23}}{g_{12}},\ \frac{P_1}{P_3}=\frac{g_{34}}{g_{23}},\quad \sum_{i=1}^{3}\varphi_i P_i=\gamma. \tag{2-14}$$

Solving (2-14) we get the optimal transmit powers at low SNR

$$P_1^*=\frac{\gamma g_{23}g_{34}}{\varphi_1 g_{23}g_{34}+\varphi_2 g_{34}g_{12}+\varphi_3 g_{12}g_{23}} \tag{2-15a}$$

$$P_2^*=\frac{\gamma g_{34}g_{12}}{\varphi_1 g_{23}g_{34}+\varphi_2 g_{34}g_{12}+\varphi_3 g_{12}g_{23}} \tag{2-15b}$$

$$P_3^*=\frac{\gamma g_{12}g_{23}}{\varphi_1 g_{23}g_{34}+\varphi_2 g_{34}g_{12}+\varphi_3 g_{12}g_{23}} \tag{2-15c}$$

2.2.4 **Numerical results**

In this section we present numerical results for the 3-hop network with GOI illustrated in Fig. 2-2. The received power is subject to path-loss with path-loss exponent $\alpha = 4$, and channel gains are modelled as i.i.d. complex Gaussian entries, *CN* (0,1). The distance between the transmitter and the receiver is normalized to one. The primary network is assumed to have similar line topology with $M = 4$ receivers. The distance between the primary network and the secondary network is similarly set to one. The noise variance is chosen to be $\sigma^2 = 1$ mW. Backward channel gain is modelled as $g_{32} = Gg_{23}$, where antenna directivity attenuation G is set to 0.2.

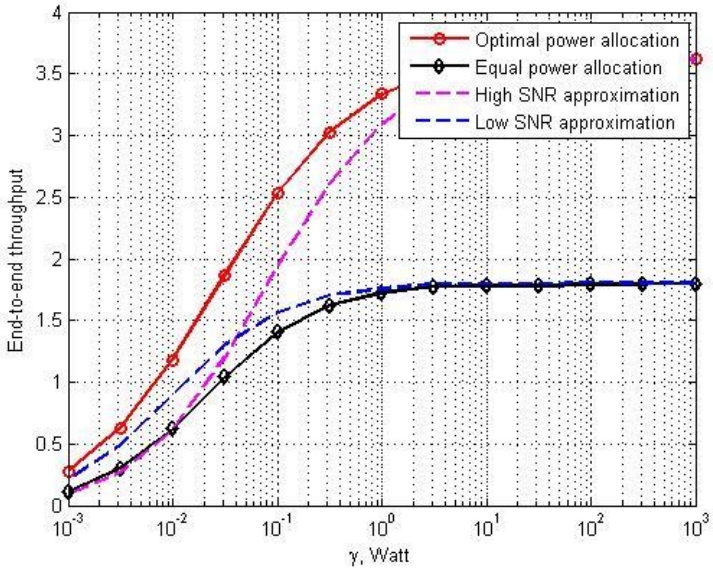

Fig. 2-3: End-to-end throughput for different power strategies

We note that the tolerable ASI threshold γ is linearly related to the transmission power in (2-6). Since we consider the interference-limited networks, we use γ as x-label for plots. For instance, Fig. 2-3 shows the performance of the optimal power allocation found by solving (2-9) as well as high- and low-SNR approximation solutions (2-12) and (2-15), respectively in comparison with equal power allocation. The approximations are much easier to solve. Low-SNR approximation is suitable for γ values less than 10 mW, while the High-SNR approximation tends to the optimal solution for large γ values.

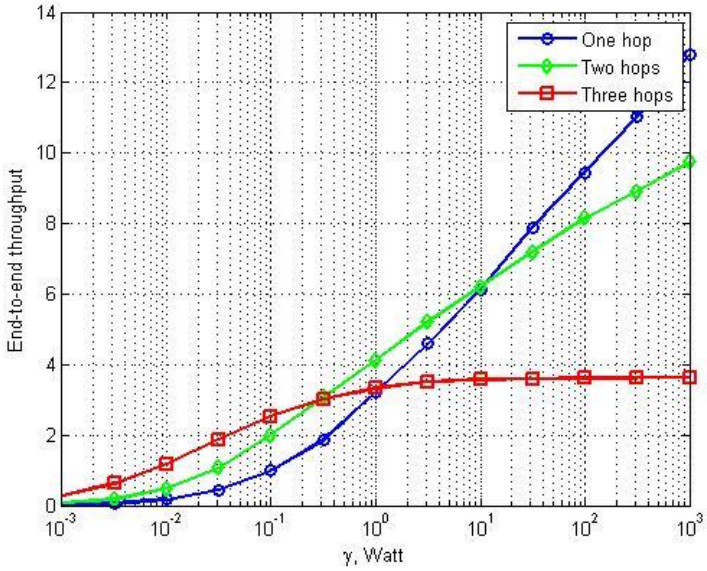

Fig. 2-4: End-to-end throughput for different number of hops

We note that the low-SNR and equal power solutions are suboptimal in the high-SNR region due to neglecting GOI which becomes significant as the SNR increases. Fig. 2-4 illustrates the system performance for different number of hops when the distance between the source and the destination is fixed to $d=3$, similarly to the previous case. We can observe that for small γ values 3-hop transmission performs better than the other strategies. This is because it splits the link into three regenerative channels with smaller pathloss components due to shorter distances between the transmitter and the receiver at each hop. However, having more hops, the system has more interfering nodes and therefore, it drops faster to the interference-limited mode. This explains the behaviour of curves for large γ values. Direct transmission from the source to the destination in this case is not affected by any interference and thus, outperforms transmission strategies with multiple hops. Thus, using multi-hop transmission leads to interference-limited performance at high SNR. On the other hand, multi-hop transmission allows reducing the power of each node, thereby reducing the interference to the primary system, which allows delivery of a message over longer distances when the tolerable interference threshold of the primary system is low.

2.3 **Coded secondary relaying in overlay CR networks**

2.3.1 **System model**

In this subsection, we consider a wireless cognitive radio network consisting of a primary system (e.g. a TV broadcasting system) with a single source-destination pair (denoted as S_p and D_p), and a secondary system (e.g. a cellular system) with two sources S_1 and S_2, two half-duplex DF relays R_1 and R_2, and a common destination D_s, displayed in Fig. 2-5 Two orthogonal spectrum bands (or different time intervals) are reserved for these two systems' operations respectively. The primary source continuously sends information to its destination in the primary band. There exists a certain cooperation (cognition) between the two systems such that D_s knows the transmit signals from S_p in advance. This can be realized by, for instance, connecting the secondary destination (e.g. the base station of a cellular system) with the primary source (e.g. the TV station of a TV broadcasting system) using a high-speed wire line [4]. Thus D_s is able to

transmit the primary signals together with S_p to boost the receive signal power at D_p. We assume that D_s can shield its reception from its own transmission. If any secondary terminal sends information to D_s in the primary band, D_s can also receive this information without being interfered by the transmission of S_p or itself. In the secondary band, the secondary sources intend to deliver independent messages I_1 and I_2 respectively to the secondary destination. In this section we mainly focus on the performance of the secondary system. If D_s is able to successfully recover both I_1 and I_2, we say the *communication is successful*. Otherwise, error event occurs and the *communication fails*.

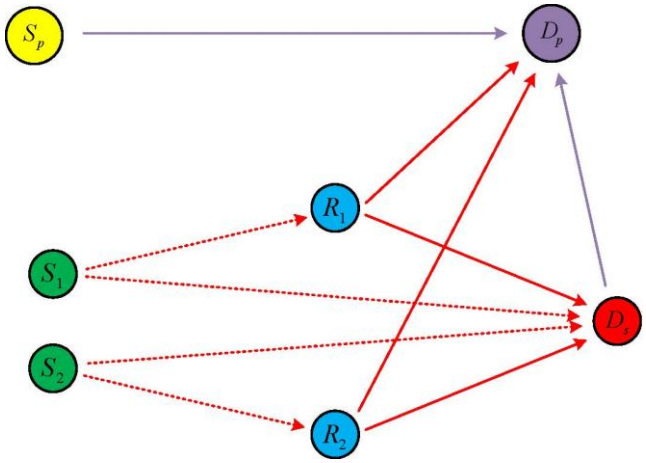

Fig. 2-5: System model. Purple lines denote the transmissions of primary signals. Red lines denote the transmissions of secondary signals. Solid and dash lines denote operations in primary and secondary bands, respectively.

We assume narrow-band transmissions in a slow, flat Rayleigh fading environment. Denote the channel fading coefficient between nodes a and b in the primary band as $g_{a,b} \sim CN(0, \lambda_{p:a,b})$, and denote that in the secondary band as $h_{a,b} \sim CN(0, \lambda_{s:a,b})$, in which $\lambda_{p:a,b} = x_{a,b}^{-\tau_p}$, $\lambda_{s:a,b} = x_{a,b}^{-\tau_s}$, $x_{a,b}$ denotes the distance between a and b, and τ_p (τ_s) is the path loss exponent in the primary band (secondary band). For presentation simplicity, we assume $\lambda_{s:S_i,D_s} = \lambda_0$, $\lambda_{s:S_i,R_j} = \lambda_1$, $\lambda_{p:R_j,D_s} = \lambda_2$ (i.e. $x_{S_1,D_s} = x_{S_2,D_s}$, $x_{S_1,R_j} = x_{S_2,R_j}$, $x_{R_1,D_s} = x_{R_2,D_s}$, $\forall i, j \in \{1,2\}$. Extending the results to more general cases is straightforward.

We consider a symmetric secondary network. Each of the secondary sources transmits with an expected average rate $\bar{R}$ bits per channel use (BPCU). Thus if one scheme requires B frequency/time slots (unit channels) within the secondary band to deliver I_1 and I_2 to D_s, each message should contain $\hat{R} = B\bar{R}$ bits information in order to meet the expected rate. In addition, we normalize the average noise power at each receiver to be one. The primary source transmits with power ρ_p, each secondary source transmits with power ρ_s, each secondary relay transmits with power $\rho_r = \kappa\rho_s$ ($\kappa \geq 0$), and

potentially the secondary destination transmits the primary signals with power ρ_{d_1} and ρ_{d_2} to compensate the interference introduced by the two secondary relays respectively.

2.3.2 **Transmission process**

To permit each secondary relay to jointly transmit multiple source messages and to obtain good diversity performance, we apply the class of *maximum distance separable finite field network codes* (MDS-FFNCs) [9], [10] on top of channel coding in the secondary relays. Specifically, the network coding functions employed at R_1 and R_2 tend to add I_1 and I_2 in *GF*(4) to generate new transmit messages (i.e. network codewords) I_1+I_2 and I_1+2I_2, respectively. Thus the knowledge of any two messages within the set $\{I_1, I_2, I_1+I_2, I_1+2I_2\}$ can guarantee recovering both I_1 and I_2.

We use $X_a = f_a(I)$ ($a \in \{S_1, S_2, R_1, R_2\}$) to denote the signal (channel codeword) transmitted from node a, where $f_a(I)$ denotes node a's channel encoding function of message I. To conduct the communication of the secondary system, the secondary sources first broadcast their signals $X_{S_1} = f_{S_1}(I_1)$ and $X_{S_2} = f_{S_2}(I_2)$ (orthogonally or non-orthogonally) within the secondary band. If D_s correctly decodes both X_{S_1} and X_{S_2} (through Cyclic Redundancy Check, CRC, checking), it sends back a 1-bit positive acknowledgement (ACK) signal to the relays to notify successful communication and thus the relays remain silent. Otherwise, if D_s cannot decode either X_{S_1} or X_{S_2}, D_s feeds back a 1-bit negative acknowledgement (NACK) signal. Upon receiving this NACK signal R_1 is activated to forward its received messages using the primary band. If R_1 decodes both X_{S_1} and X_{S_2}, it sends $X_{R_1} = f_{R_1}(I_1+I_2)$. If R_1 decodes only one codeword X_{S_j} ($j \in \{1,2\}$), it transmits $X_{R_1} = f_{R_1}(I_j)$ to D_s. Otherwise, R_1 remains silent if it recovers neither I_1 nor I_2.

To compensate the interference generated from R_1, D_s also transmits the primary signals to D_p, using power ρ_{d_1}. The average SINR at D_p is calculated by $\frac{\rho_p \left| g_{S_p,D_p} \right|^2 + \rho_{d_1} \left| g_{D_s,D_p} \right|^2}{\rho_r \left| g_{R_1,D_p} \right|^2 + 1}$ [4]. In order to guarantee the communication quality of the primary system, D_s should properly chose its transmit power ρ_{d_1} to satisfy the following condition

$$\Pr\left\{ \frac{\rho_p \left| g_{S_p,D_p} \right|^2 + \rho_{d_1} \left| g_{D_s,D_p} \right|^2}{\rho_r \left| g_{R_1,D_p} \right|^2 + 1} \geq SINR_{th} \right\} \geq p_{th} \tag{2-16}$$

in which $\Pr\{A\}$ denotes the probability that event A occurs, $SINR_{th}$ denotes a pre-agreed SINR threshold, and p_{th} is an acceptable probability that the average SINR at the primary destination should be larger than $SINR_{th}$.

With the received signals from S_1, S_2, and R_1, if D_s recovers both I_1 and I_2, it sends an ACK signal to keep R_2 silent. Otherwise, it sends a NACK signal to activate R_2.

Similarly, if R_2 recovers both I_1 and I_2 from the sources, it transmits $X_{R_2} = f_{R_2}(I_1 + 2I_2)$ in the primary band. If it knows only X_{S_j} ($j \in \{1,2\}$), R_2 transmits $X_{R_2} = f_{R_2}(I_j)$. Otherwise, it remains silent. To protect the primary system, the power ρ_{d_2} from D_s should be chosen to satisfy

$$\Pr\left\{ \frac{\rho_p \left| g_{S_p,D_p} \right|^2 + \rho_{d_2} \left| g_{D_s,D_p} \right|^2}{\rho_r \left| g_{R_2,D_p} \right|^2 + 1} \geq SINR_{th} \right\} \geq p_{th} \tag{2-17}$$

If D_s still cannot recover I_1 and I_2 after the transmission of R_2, error event occurs and the secondary communication fails.

In this subsection, we assume that D_s can always choose sufficiently large power to retransmit the primary signals so that the conditions (2-16) and (2-17) can always be satisfied. (In general if the knowledge of the channels between the secondary system and the primary system is perfectly known at D_s, its required power can be directly computed. If this knowledge is not available, some worst case scenarios should be considered. For instance, the secondary system may choose a critical user to be the target primary destination [4]. The secondary system has to increase its power consumption to relay the primary signals or to reduce its service requirement to protect the primary system.) Our focus is mainly on the impact of operating the secondary relays in the primary band and exploiting ARQ signals from D_s on the error performance of the secondary system.

2.3.3 **Secondary system performance analysis**

We consider two different multiple access strategies among the two secondary sources. We start our performance analysis from the simple orthogonal transmission.

2.3.3.1 Orthogonal secondary source transmission

The two sources access the secondary band *orthogonally*. $B = 2$ frequency/time slots in the secondary band are required to finish the transmission so that each message contains $\hat{R} = 2\overline{R}$ bits information. Following the description provided in the above section, it can be seen that the communication fails only if D_s cannot recover the source messages after both relays' transmissions. In other words, if D_s can use its received signals from all the four transmitting terminals S_1, S_2, R_1, and R_2 to recover I_1 and I_2, the secondary communication would be successful. We use $\Im_j \subseteq \{I_1, I_2\}$ ($j \in \{1,2\}$) to denote the set of source messages that can be recovered by R_j. Clearly, the overall error probability at D_s can be calculated by

$$P_e = \sum_{\Im_1, \Im_2 \subseteq \{I_1, I_2\}} P_{\Im_1} P_{\Im_2} P_{e|\Im_1,\Im_2} \tag{2-18}$$

where $P_{\Im_j}$ denotes the probability that a specific set $\Im_j$ occurs, and $P_{e|\Im_1,\Im_2}$ is the error probability at D_s given $\Im_1$ and $\Im_2$.

We assume the channel codes employed on the physical layer to be sufficiently strong such that erroneous decoding happens only if *outage event* occurs. Consequently, at each receiver error probability is dominated by *outage probability*. In addition, for

computation simplicity, we do not apply maximum ratio combining (MRC) at D_s even though the relays can potentially use the same channel code as a source to encode the same message, e.g. $f_{R_1}(I_1) = f_{S_1}(I_1)$. Clearly, if MRC is applicable at D_s, the error performance can be further enhanced.

In the secondary band the probability that R_j can correctly decode X_{S_i} is calculated as $\Pr\left\{\log\left(1+\rho\left|h_{S_i,R_j}\right|^2\right) > \hat{R}\right\} = e^{-\frac{\eta}{\lambda_1}}$ in which $\rho = \rho_s$ denotes the average transmit SNR, and $\eta = \frac{2^{2\bar{R}}-1}{\rho}$. Similarly, the probability that D_s correctly decodes X_{S_i} can be calculated as $\Pr\left\{\log\left(1+\rho\left|h_{S_i,D_s}\right|^2\right) > \hat{R}\right\} = e^{-\frac{\eta}{\lambda_0}}$. In the primary band, D_s can correctly decode X_{R_j} with probability $\Pr\left\{\log\left(1+\kappa\rho\left|h_{R_j,D_s}\right|^2\right) > \hat{R}\right\} = e^{-\frac{\eta}{\kappa\lambda_2}}$.

As a result, we can have

$$P_{\Im_j} = \left(e^{-\frac{\eta}{\lambda_1}}\right)^{|\Im_j|}\left(1-e^{-\frac{\eta}{\lambda_1}}\right)^{2-|\Im_j|} \tag{2-19}$$

where $|\Im_j|$ denotes the cardinality of set $\Im_j$.

Different decoding patterns at the relays would lead to different approaches to calculate $P_{e|\Im_1,\Im_2}$. Now we individually consider the following seven cases to derive $P_{e|\Im_1,\Im_2}$.

Case 1): $\Im_1 = \phi$ & $\Im_2 = \phi$. No relay transmits anything. The communication is successful only when D_s decodes both X_{S_1} and X_{S_2}. Thus

$$P_{e|\Im_1,\Im_2} = 1-e^{-\frac{2\eta}{\lambda_0}} \tag{2-20}$$

Case 2): $\Im_1 = \{I_1\}$ & $\Im_2 = \phi$. In this case $X_{R_1} = f_{R_1}(I_1)$, and R_2 does not transmit even if it receives a NACK signal from D_s. The communication is successful if D_s decodes the set of signals $\{X_{S_1}, X_{S_2}\}$, or $\{X_{S_2}, X_{R_1}\}$. We have

$$P_{e|\Im_1,\Im_2} = 1-\left(e^{-\frac{2\eta}{\lambda_0}} + e^{-\left(\frac{\eta}{\lambda_0}+\frac{\eta}{\kappa\lambda_2}\right)} - e^{-\left(\frac{2\eta}{\lambda_0}+\frac{\eta}{\kappa\lambda_2}\right)}\right). \tag{2-21}$$

The situations $\Im_1 = \{I_2\}$ & $\Im_2 = \phi$, $\Im_1 = \phi$ & $\Im_2 = \{I_1\}$, and $\Im_1 = \phi$ & $\Im_2 = \{I_2\}$ lead to the same $P_{e|\Im_1,\Im_2}$.

Case 3): $\Im_1 = \{I_1, I_2\}$ & $\Im_2 = \phi$. Here $X_{R_1} = f_{R_1}(I_1 + I_2)$ and R_2 does not transmit anything. The communication is successful if D_s decodes any of the following sets $\{X_{S_1}, X_{S_2}\}$, $\{X_{S_1}, X_{R_1}\}$, and $\{X_{S_2}, X_{R_1}\}$. As a result,

$$P_{e|\Im_1,\Im_2} = 1-2e^{-\left(\frac{\eta}{\lambda_0}+\frac{\eta}{\kappa\lambda_2}\right)}\left(1-e^{-\frac{\eta}{\lambda_0}}\right)-e^{-\frac{2\eta}{\lambda_0}} \tag{2-22}$$

The error probability is the same if $\Im_1=\phi$ & $\Im_2=\{I_1,I_2\}$.

Case 4): $\Im_1=\{I_1\}$ & $\Im_2=\{I_1\}$. In this case $X_{R_1}=f_{R_1}(I_1)$ and $X_{R_2}=f_{R_2}(I_1)$. The communication is successful if D_s decodes X_{S_2}, and also decodes at least one signal within the set $\{X_{S_1},X_{R_1},X_{R_2}\}$. Then

$$P_{e|\Im_1,\Im_2} = 1-e^{-\frac{\eta}{\lambda_0}}\left(1-\left(1-e^{-\frac{\eta}{\lambda_0}}\right)\left(1-e^{-\frac{\eta}{\kappa\lambda_2}}\right)^2\right) \tag{2-23}$$

The situation $\Im_1=\{I_2\}$ & $\Im_2=\{I_2\}$ has the same $P_{e|\Im_1,\Im_2}$.

Case 5): $\Im_1=\{I_1\}$ & $\Im_2=\{I_2\}$. Now $X_{R_1}=f_{R_1}(I_1)$ and $X_{R_2}=f_{R_2}(I_2)$. The communication is successful if D_s decodes at least one signal within $\{X_{S_1},X_{R_1}\}$, and it also decodes at least one signal within $\{X_{S_2},X_{R_2}\}$. We have

$$P_{e|\Im_1,\Im_2} = 1-\left(e^{-\frac{\eta}{\lambda_0}}+e^{-\frac{\eta}{\kappa\lambda_2}}-e^{-\left(\frac{\eta}{\lambda_0}+\frac{\eta}{\kappa\lambda_2}\right)}\right)^2. \tag{2-24}$$

The same $P_{e|\Im_1,\Im_2}$ holds when $\Im_1=\{I_2\}$ & $\Im_2=\{I_1\}$.

Case 6): $\Im_1=\{I_1,I_2\}$ & $\Im_2=\{I_2\}$. Then $X_{R_1}=f_{R_1}(I_1+I_2)$ and $X_{R_2}=f_{R_2}(I_2)$. The communication is successful if *i)* D_s decodes at least one signal within $\{X_{S_2},X_{R_2}\}$, and also at least one signal within $\{X_{S_1},X_{R_1}\}$, or *ii)* D_s cannot decode either X_{S_2} or X_{R_2}, but it decodes both X_{S_1} and X_{R_1}.

$$P_{e|\Im_1,\Im_2} = 1-\left(e^{-\frac{\eta}{\lambda_0}}+e^{-\frac{\eta}{\kappa\lambda_2}}-e^{-\left(\frac{\eta}{\lambda_0}+\frac{\eta}{\kappa\lambda_2}\right)}\right)^2-e^{-\left(\frac{\eta}{\lambda_0}+\frac{\eta}{\kappa\lambda_2}\right)}\left(1-e^{-\frac{\eta}{\lambda_0}}\right)\left(1-e^{-\frac{\eta}{\kappa\lambda_2}}\right). \tag{2-25}$$

The situations $\Im_1=\{I_1,I_2\}$ & $\Im_2=\{I_1\}$, $\Im_1=\{I_1\}$ & $\Im_2=\{I_1,I_2\}$, and $\Im_1=\{I_2\}$ & $\Im_2=\{I_1,I_2\}$ have the same expression of $P_{e|\Im_1,\Im_2}$.

Case 7): $\Im_1=\{I_1,I_2\}$ & $\Im_2=\{I_1,I_2\}$. In this final case both relays can recover both source messages so that $X_{R_1}=f_{R_1}(I_1+I_2)$ and $X_{R_2}=f_{R_2}(I_1+2I_2)$. As we mentioned earlier, D_s can recover both I_1 and I_2 if the signals transmitted from any two of the four transmitting terminals can be decoded. In other words, the communication fails if at most one signal within $\{X_{S_1},X_{S_2},X_{R_1},X_{R_2}\}$ can be decoded at D_s. Consequently

$$P_{e|\Im_1,\Im_2} = \left(1-e^{-\frac{2\eta}{\lambda_0}}\right)\left(1-e^{-\frac{\eta}{\kappa\lambda_2}}\right)^2+2e^{-\frac{\eta}{\kappa\lambda_2}}\left(1-e^{-\frac{\eta}{\lambda_0}}\right)^2\left(1-e^{-\frac{\eta}{\kappa\lambda_2}}\right). \tag{2-26}$$

The overall error probability P_e thus can be calculated by substituting equations (2-19)-(2-26) into (2-18).

To more clearly see the spectral efficiency of the considered scheme, in the high SNR region we permit $\overline{R}$ to scale with SNR and use the *diversity-multiplexing tradeoff* (DMT) [11] to characterize the negative slope of the log-log plot of P_e versus SNR. Specifically, define diversity gain d and multiplexing gain r as [11]

$$d = -\lim_{\rho\to\infty} \frac{\log P_e(\rho)}{\log \rho} \text{ and } r = \lim_{\rho\to\infty} \frac{\overline{R}(\rho)}{\log \rho}. \quad (2\text{-}27)$$

The curve $d(r)$, the tradeoff between d and r, is termed DMT.

We use $\doteq$ to denote the exponential equality operator [11]: $W \doteq \rho^b$ is equivalent to $b = \lim_{\rho\to\infty} \frac{\log W}{\log \rho}$. Setting $\overline{R} = r \log \rho$, we can have $\eta = \frac{2^{2\overline{R}} - 1}{\rho} \doteq \rho^{-(1-2r)}$ and $1 - e^{-\frac{\eta}{c}} \approx \frac{\eta}{c} \doteq \rho^{-(1-2r)}$, in which c can be any finite constant, and the approximation holds in the high-SNR region. Therefore, it is not difficult to show that for high SNR, the overall error probability derived from (2-18) can be expressed as $P_e \doteq \rho^{-3(1-2r)}$. The achievable DMT thus is

$$d(r) = 3(1-2r). \quad (2\text{-}28)$$

The maximal diversity gain is 3 and the maximal multiplexing gain is $\frac{1}{2}$. Compared to direct source-destination transmission without relaying, the error probability is substantially improved without spectral efficiency loss (see Fig. 2-6 and Fig: 2-7).

Now we analyze the probability that the relays should be activated, i.e., the probability that D_s has to spend power to compensate the interference introduced by the relays. To minimize the system complexity, we assume that D_s does not know the decoding pattern at the relays after the sources' transmission. Then as long as D_s sends back a NACK signal to request the assistance from a relay, D_s starts transmitting the primary signals even through the relay may not interfere D_p when it is unable to recover any source message.

Use P_{d_j} to denote the probability that D_s has to compensate the interference introduced by R_j. After the sources broadcast their signals, D_s sends back a NACK signal to activate R_1 if it cannot decode the signals directly from at least one source. Therefore, we have

$$P_{d_1} = 1 - e^{-\frac{2\eta}{\lambda_0}}. \quad (2\text{-}29)$$

In addition, if after the transmission of R_1, D_s still cannot recover I_1 and I_2, R_2 should be activated and D_s starts to consume power to compensate interference. Different decoding patterns at R_1 would lead to different decoding processes at D_s. Use $\overline{P}_{e|\Im_1}$ to denote the error probability at D_s after R_1's transmission, given $\Im_1$. We have

$$P_{d_2} = \sum_{\Im_2 \subseteq \{I_1, I_2\}} P_{\Im_1} \overline{P}_{e|\Im_1} . \quad (2\text{-}30)$$

It is not difficult to see that $\overline{P}_{e|\Im_1} = P_{e|\Im_1,\phi}$. Substituting (2-19)-(2-22) in (2-30) leads to P_{d_2} (the performance will be shown in Fig. 2-8).

2.3.3.2 Non-orthogonal secondary source transmission

To further improve the performance, in this subsection we permit the secondary sources to transmit *non-orthogonally* within the secondary band. Since $B=1$ slot in the secondary band suffices to finish the transmission, each message contains $\hat{R} = \overline{R}$ bits information. For fair comparison with the previous orthogonal scheme, each source transmits with $\rho_s = \frac{\rho}{2}$ so that the average sum transmit power remains the same. Both relays and D_s perform successive interference cancellation (SIC) to decode the signals from the sources. If D_s directly decodes X_{S_1} and X_{S_2}, no relay is activated. Otherwise, R_1 is activated to forward its received messages. R_2 is used only if the communication is not successful after R_1's transmission.

Consider a 2×1 symmetric multiple-access (MAC) channel, in which each transmitter transmits with power $\frac{\rho}{2}$ and rate $\hat{R}$. The probability that the receiver decodes the signal from *only* the first transmitter, through SIC, is [12]

$$p_{1,\lambda} = \frac{1}{2^{\hat{R}}} \left(e^{-\frac{2^{\hat{R}}-1}{\lambda\rho/2}} - e^{-\frac{2^{2\hat{R}}-1}{\lambda\rho/2}} \right), \quad (2\text{-}31)$$

where λ is the variance of the channel gains. By symmetry, the probability that the receiver decodes only the second transmitter's signal can also be expressed by $p_{1,\lambda}$. The probability that the receiver decodes neither transmitter's signal is [12]

$$p_{2,\lambda} = 1 - \frac{1}{2^{\hat{R}}} e^{-\frac{2^{\hat{R}}-1}{\lambda\rho/2}} - e^{-\frac{2^{2\hat{R}}-1}{\lambda\rho/2}} \left(1 - \frac{1}{2^{\hat{R}}} + \frac{\left(2^{\hat{R}}-1\right)^2}{\lambda\rho/2} \right). \quad (2\text{-}32)$$

Thus $2p_{1,\lambda} + p_{2,\lambda}$ denotes the probability that the receiver cannot decode at least one transmitter's signal.

For the considered scheme, the overall error probability at D_s can also be calculated by equation (2-18). According to (2-31) and (2-32), we can calculate $P_{\Im_j}$ as follows,

$$P_{\phi} = p_{2,\lambda_1}, \quad (2\text{-}33)$$

$$P_{\{I_1\}} = P_{\{I_2\}} = p_{1,\lambda_1}, \quad (2\text{-}34)$$

$$P_{\{I_1,I_2\}} = 1 - 2p_{1,\lambda_1} - p_{2,\lambda_1} . \quad (2\text{-}35)$$

Let $\eta = \frac{2^{\hat{R}}-1}{\rho} = \frac{2^{\bar{R}}-1}{\rho}$, and $i_1, i_2, j \in \{1,2\}$, $i_1 \neq i_2$. Following the discussions we provided in the above subsection, regarding the different decoding patterns at the relays we also consider the seven cases to derive $P_{e|\Im_1,\Im_2}$.

Case 1): $\Im_1 = \phi$ & $\Im_2 = \phi$.

$$P_{e|\Im_1,\Im_2} = 2p_{1,\lambda_0} + p_{2,\lambda_0}. \tag{2-36}$$

Case 2): $\Im_{i_1} = \{I_j\}$ & $\Im_{i_2} = \phi$.

$$P_{e|\Im_1,\Im_2} = p_{1,\lambda_0}\left(2 - e^{-\frac{\eta}{\kappa\lambda_2}}\right) + p_{2,\lambda_0}. \tag{2-37}$$

Case 3): $\Im_{i_1} = \{I_1, I_2\}$ & $\Im_{i_2} = \phi$.

$$P_{e|\Im_1,\Im_2} = 2p_{1,\lambda_0}\left(1 - e^{-\frac{\eta}{\kappa\lambda_2}}\right) + p_{2,\lambda_0}. \tag{2-38}$$

Case 4): $\Im_{i_1} = \{I_j\}$ & $\Im_{i_2} = \{I_j\}$.

$$P_{e|\Im_1,\Im_2} = p_{1,\lambda_0}\left(2 - 2e^{-\frac{\eta}{\kappa\lambda_2}} + e^{-\frac{2\eta}{\kappa\lambda_2}}\right) + p_{2,\lambda_0}. \tag{2-39}$$

Case 5): $\Im_{i_1} = \{I_1\}$ & $\Im_{i_2} = \{I_2\}$

$$P_{e|\Im_1,\Im_2} = 2p_{1,\lambda_0}\left(1 - e^{-\frac{\eta}{\kappa\lambda_2}}\right) + p_{2,\lambda_0}\left(1 - e^{-\frac{2\eta}{\kappa\lambda_2}}\right). \tag{2-40}$$

Case 6): $\Im_{i_1} = \{I_1, I_2\}$ & $\Im_{i_2} = \{I_j\}$.

$$P_{e|\Im_1,\Im_2} = p_{1,\lambda_0}\left(2 - 3e^{-\frac{\eta}{\kappa\lambda_2}} + e^{-\frac{2\eta}{\kappa\lambda_2}}\right) + p_{2,\lambda_0}\left(1 - e^{-\frac{2\eta}{\kappa\lambda_2}}\right). \tag{2-41}$$

Case 7): $\Im_1 = \{I_1, I_2\}$ & $\Im_2 = \{I_1, I_2\}$.

$$P_{e|\Im_1,\Im_2} = 2p_{1,\lambda_0}\left(1 - 2e^{-\frac{\eta}{\kappa\lambda_2}} + e^{-\frac{2\eta}{\kappa\lambda_2}}\right) + p_{2,\lambda_0}\left(1 - e^{-\frac{2\eta}{\kappa\lambda_2}}\right). \tag{2-42}$$

The overall error probability thus can be calculated by substituting (2-33)-(2-42) into (2-18). Setting $\bar{R} = r\log\rho$, we can approximate $P_{1,\lambda}$ as $P_{1,\lambda} \doteq \rho^{-(1-r)}$ and approximate $P_{2,\lambda}$ as $P_{2,\lambda} \doteq \rho^{-2(1-2r)}$. It can be shown that the overall error probability at D_s can be expressed as $P_e \doteq \rho^{-(2(1-2r)+\min\{1-r,2(1-2r)\})}$. Thus the DMT is

$$d(r) = 2(1-2r) + \min\{1-r, 2(1-2r)\}. \tag{2-43}$$

Permitting the sources to transmit non-orthogonally obtains a better DMT than requiring them to transmit orthogonally.

Now we derive the probability that D_s should spend power to compensate interference from the relays. It is easy to see

$$P_{d_1} = 2p_{1,\lambda_0} + p_{2,\lambda_0}. \quad (2\text{-}44)$$

Furthermore, since $\overline{P}_{e|\Im_1} = P_{e|\Im_1,\phi}$, substituting (2-33)-(2-38) into (2-30) leads to P_{d_2}.

2.3.4 **Numerical results**

In this section, we show the performance of the proposed secondary relaying strategy. We normalize the distance between S_i ($i \in \{1,2\}$) and D_s to one (i.e. $x_{S_i,D_s} = 1$) and we assume the relays locate in the middle between the secondary sources and D_s (i.e. $x_{S_i,R_j} = x_{R_j,D_s} = 0.5$). The path loss exponents are set to $\tau_p = \tau_s = 4$. In addition, we set $\kappa = x_{S_i,D_s}^{-\tau_s} / x_{R_j,D_s}^{-\tau_p}$ so that the average received powers at D_s from each source and each relay are the same. In other words, we require each relay to transmit with power $\rho_r = \rho_s / 16$.

We consider three benchmark protocols.

1) *Direct transmission*: The sources orthogonally communicate with D_s without the assistance of relays. $B = 2$ and the error probability at D_s is $P_e = 1 - e^{-2(2^{2\overline{R}}-1)/\lambda_0\rho}$. The achievable DMT is $d(r) = 1 - 2r$.

2) *Conventional Relaying*: The two relays are used to assist the sources in the secondary band. $B = 4$ slots in the secondary band are required to finish transmission. The error probability can be analyzed following the analysis provided in Section 2.3.3.1, but with $\hat{R} = 4\overline{R}$. The achievable DMT is $d(r) = 3(1 - 4r)$.

3) *Secondary Relaying without ARQ*: The relays operate in the primary band. But no ARQ feedback signal from D_s is exploited. The error performance is the same as that for the proposed secondary relaying with orthogonal source transmission. D_s always transmits primary signals to compensate interference, i.e. $P_{d_2} = P_{d_2} = 1$. The energy consumption of the secondary system is high, especially for high SNR.

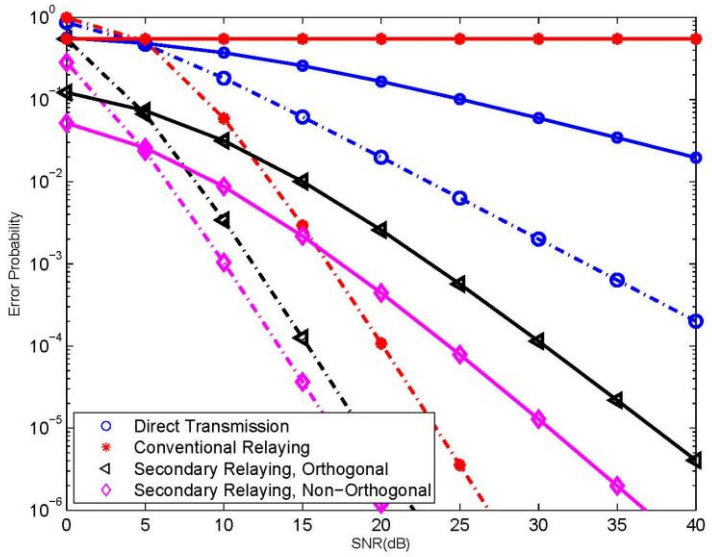

Fig. 2-6: Error performance comparison. Dashed lines represent the performance when the average rate is fixed at 1/2 BPCU. Solid lines represent the performance when the multiplexing gain is chosen as 1/4.

We plot the error performance comparison in Fig. 2-6. When the average transmission rate is fixed (i.e. $r=0$), the conventional relaying protocol can provide sufficiently better error performance than direct transmission. However, due to its low spectral efficiency, if we chose $r=1/4$, the diversity gain is 0 so that the error probability does not change with changing SNR. The performance is even worse than direct transmission. The proposed secondary relaying strategy can attain better performance than these two protocols in both cases. High communication reliability is obtained without spectral efficiency loss. And clearly, permitting the secondary sources to transmit non-orthogonally outperforms requiring them to transmit orthogonally, especially when $r>0$.

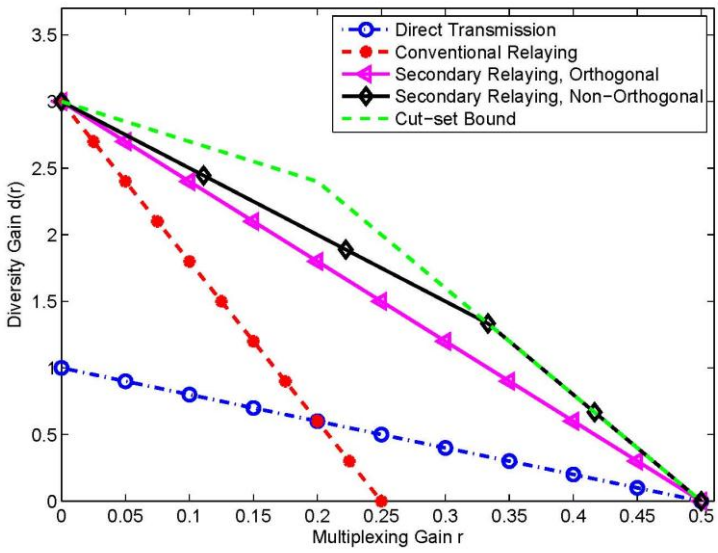

Fig: 2-7. DMT comparison.

The advantages of the proposed secondary relaying strategy in terms of DMT or high-SNR error performance can be seen from Fig: 2-7. Interestingly, when $\frac{1}{3} \le r \le \frac{1}{2}$, allowing the secondary sources to transmit non-orthogonally achieves the DMT derived through cut-set bound analysis [13]. This means that the protocol is *optimal* in terms of DMT when $\frac{1}{3} \le r \le \frac{1}{2}$.

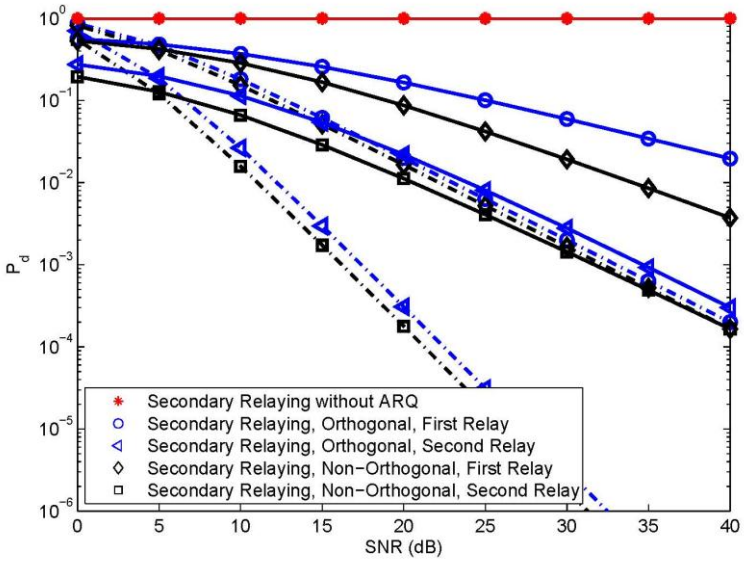

Fig. 2-8: The probability that secondary destination spends power to compensate interference. Dashed lines represent the performance when average rate is fixed at 1/2 BPCU. Solid lines represent the performance when when the multiplexing gain is chosen as 1/4.

We also plot the probability that D_s should transmit the primary signals to compensate interference in Fig. 2-8. Clearly, exploiting ARQ feedback signals from D_s can significantly reduce unnecessary energy consumption of the secondary system. Again, permitting the secondary sources to non-orthogonally broadcast their messages performs better.

2.4 **Summary**

In this chapter we consider exploiting potential cooperation among secondary users such that some nodes can serve as relays and assist in some other secondary users' transmissions. Since the use of relays is an effective solution to tackle the negative impact of fading in wireless communication systems, the considered secondary user cooperation strategy can potentially decrease the secondary system's transmit power. Thus the interference introduced by the secondary system to the primary system can be reduced. Or equivalently, the performance of the secondary system can be improved without increasing interference. We have studied two secondary relaying schemes in this chapter. The first one follows the underlay primary-secondary spectrum sharing setup. The secondary users access the primary band without interacting with the primary system. The second one takes a step further. The secondary system also cooperates with the primary system by relaying the primary signals, i.e. an overlay primary-secondary spectrum sharing setup. Our results in both schemes have confirmed the positive impact of considering secondary user cooperation on the secondary system's

performance (in terms of higher throughput or higher diversity). The performance gains presented in this chapter are obtained based on the assumption that the path gains from secondary transmitters to primary receivers are known to the secondary system. In practice, if such channel knowledge is not perfectly available (e.g. only the statistics or imperfectly estimated versions of the channel gains are available), the secondary system may need to consider a more strict constraint on its transmit power. In other words, the secondary system needs to pose a reduced performance requirement to protect the primary system.

3 Transmit Power Adaptation Strategy for TVWS

An adaptation strategy is a strategy in which the secondary users adapt in various ways to the environment to reach a desired outcome. Here we consider the case where secondary users cooperate to appropriately adapt their transmissions or secondary opportunity usage to reach a better result, individually or as a collective, than would have been possible without the cooperation.

In this section a specific adaptation strategy is presented. The strategy is aiming to enhance the total capacity of the collective of secondary users using TV white spaces for communication. This is achieved by coordination of the secondary transmit powers in such a way that the total aggregated interference towards primary receivers is kept under control.

3.1 Introduction

In recent years, the FCC in the US has opened up the opportunity for secondary usage of the TV broadcast band in the US, under a set of conditions. Further Ofcom in UK is well on its way to finalizing a rule set that allows secondary usage of the TV broadcast bands in the UK. In Europe the regulatory standardization group CEPT SE43 finalized a report outlining the requirements for operating as a secondary user in the TV white spaces. Thus, the process of opening up TV white spaces for secondary usage around the globe is well under way.

One commonality to the rules in place in the US and the proposed rules in Europe and UK is that a way to getting access to the TV white spaces, i.e., perform secondary transmissions in the TV bands, is to access a geo-location database. The geo-location database provides a secondary user, sometimes also referred to as a white space device (WSD), with a list of TV channels (and in the CEPT SE43 proposal [6], an associated maximal output power) that is allowed to be used by the secondary user at its location.

A more elaborate approach to geo-location database functionality has been proposed by CEPT SE43 [6]. This is referred to as the master-slave approach, in which a master (BS) can make database requests for its associated slaves (UEs). This enables easier operation of a standard cellular system in the TV white spaces since the UEs need not send requests to the database. In CEPT SE43 terminology a base station (BS) is a master WSD and user equipment (UE) is a slave WSD. The master WSD is responsible for allocating TV channels and associated output powers to the slave WSDs.

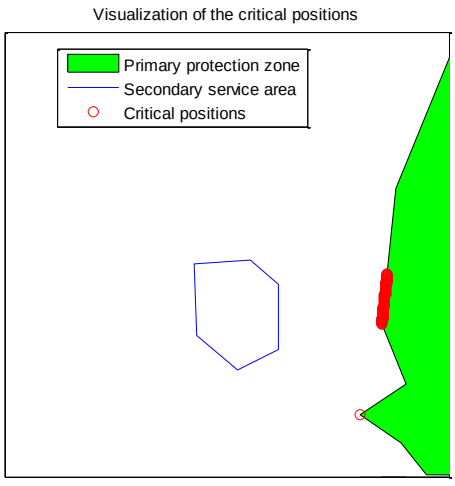

Fig. 3-1: An example visualization of a set of critical positions located along the TV coverage for a secondary service area

The approach outlines a procedure where a master WSD queries a geo-location database for channels, critical positions, and interference thresholds, i.e., the maximally allowed aggregated interference, generated from the master and slave WSDs at the respective critical position. An example set of critical positions is illustrated in Fig. 3-1. A critical position is defined as a point on the primary service coverage area which is closest to some point of the secondary service area. Based on this information the master WSD derives a set of constraints for each allowed channel that are to be respected by the uplink (UL) power allocation procedure in the secondary system. These constraints dictate that the total aggregated interference generated at a critical position must be kept below the specified maximally allowed aggregated interference.

One way of taking into account the probability distribution of the total aggregated interference at a critical point is by setting the maximally allowed aggregated interference at a much lower value, i.e., to introduce an additional fixed margin. This fixed margin is introduced at the geo-location database which does not have information on the number and locations of the slaves WSDs intending to transmit on the channel under consideration. Hence the margin must be decided using worst case assumptions leading to very conservative decisions, i.e., large values. A large margin implies that the secondary system is overly constrained in its UL power allocation.

The point being that it is suboptimal to set the margin at the geo-location database if the distribution of the total aggregated interference at critical positions is to be accounted for.

The cooperation between secondary systems is handled by the geo-location database. Since the SUs are required to inform the database regarding their output powers, the SUs are explicitly cooperative with other SUs via the geo-location database manager.

3.2 **A power adaptation strategy**

The power adaptation strategy introduces a method to find the optimal power allocation for multiple simultaneous uplink (UL) transmissions for a cellular system operating in TV white spaces, i.e., the UL power allocation respect the constraints imposed by primary user protection.

It introduces an iterative method to dynamically adjust a margin to the interference threshold, specified by the geo-location database, so that the probability of causing an aggregated interference towards any of the critical locations is kept below a specified threshold. The aggregated interference probability distribution can typically *not* be obtained analytically, hence the proposed iterative approach.

The operation of the master WSD contains the following steps:

1. The master WSD queries the database for information on the available channels, the corresponding critical positions and corresponding interference thresholds.
2. The master WSD estimates, e.g., via use of pilots in nearby previously set up white space channels and extrapolation or via calculation using appropriate channel models, the channel gains between the master WSD and all slave WSDs.
3. The master WSD calculates or estimates, by use of appropriate channel models, all channel gains between all combinations of slave WSDs and critical positions.
4. The master WSD sets an initial margin for the aggregated interference, i.e., the aggregated interference must be below what the primary receiver can tolerate plus the initial margin.

5. The master WSD maximizes the sum rate or some other suitable criterion of the UL transmissions by solving a standard convex optimization problem with constraints on the maximally allowed aggregated interference with the margin added, using known methods.
6. The master WSD evaluates whether the UL (i.e., slave WSD) power allocation generates a probability distribution of the aggregated interference that yields a sufficiently low, but not too low, probability of exceeding the interference threshold at all critical positions. This can be done by Monte Carlo evaluation; use the desired powers, take the uncertainties into account and see what the probability of exceeding the threshold is.
    - If the probability of causing excessive interference is too high the margin is increased and if the probability is too low (meaning that higher power levels can be used) the margin is decreased. Then the process continues at step 5.
    - If the probability is in a predefined range the iterative procedure stops (go to step 7). The obtained power allocation is the optimal allocation that protects the primary receivers at the specified level.
7. The master WSD informs the slave WSDs of the UL transmit powers.
8. The WSDs use the specified transmit powers when transmitting in UL.

Steps 1 and 2 could be performed simultaneously or in the opposite order.

3.3 **Scenario**

The present study considers a master WSD providing radio access to a set of served slave WSDs. The master WSD may be a cellular base station with three sectors as illustrated in Fig. 3-2, and the slave WSDs may be served UEs. Also, the master WSD may be a WLAN access point and the slaves may be served WLAN clients. In Fig. 3-2 a single critical position is also indicated at a distance d away from the base station.

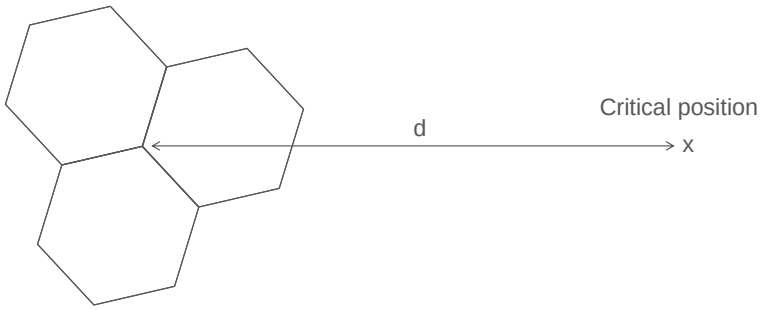

Fig. 3-2: Illustration of a cellular system and a critical position x a distance d away from the base station (master WSD) serving 3 sectors

A critical position is a position within a TV broadcast coverage area where the aggregated interference generated by the transmissions from the secondary system (master WSD and slave WSDs) is expected to be the largest. The critical positions may be the set of positions in the TV broadcast coverage area that are closest to the master WSD service area, as illustrated in Fig. 3-1. In the query to the geo-location database, the master WSD specifies its service area and in the reply the geo-location database specifies, for each allowed channel the corresponding set of critical positions. Optionally, the positions of the transmitters for which a power allocation is desired can be submitted, potentially with an associated uncertainty, or a "worst case position" (with a certain confidence). Along with each critical position an interference threshold is specified in the reply. The probability that the total aggregated interference caused by

secondary systems exceeds this interference threshold must be limited by a threshold which may be pre-defined or optionally given in the geo-location database reply.

The present solution addresses optimization of power allocation to slave WSDs. As an example, this power allocation may be for the UL in a cellular system, or for any type of WS transmissions.

Fig. 3-3 illustrates schematically the useful secondary communication links (arrows in black) and the generated interference towards a primary receiver at a critical location x (red arrows). This figure illustrates the UL in a cellular system.

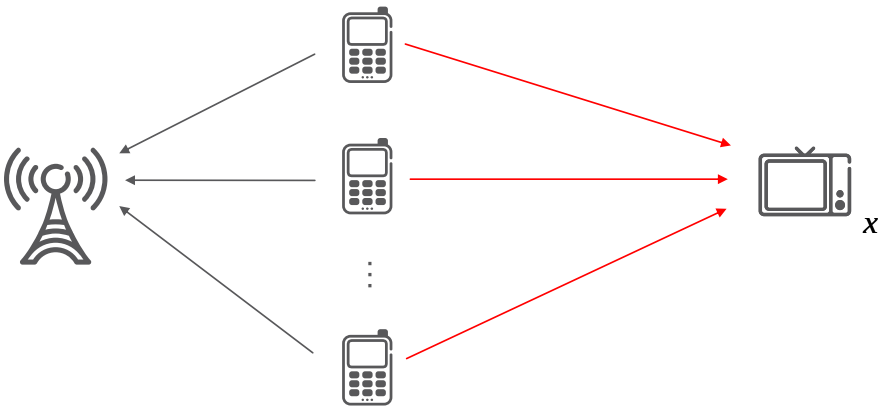

Fig. 3-3: Schematic illustration of the UL transmission scenario.

3.4 **Optimization problem**

The optimization problem illustrated here is the sum rate maximization of UL. Other optimization criteria can be considered also. In efficient communication schemes UL transmission schemes may be considered as orthogonal, i.e., the interference between the different UL transmissions may be neglected or assumed to be constant. This implies that the optimization problem we want to solve, i.e., rate maximization, may be stated as:

$$\begin{aligned} \text{Maximize} \quad & \sum_{n=1}^{N} \log_2\left(1+\frac{G_{nn}p_n}{W_n+I}\right) \\ \text{subject to} \quad & \Pr\left(\sum_{n=1}^{N} G_{x_i n}p_n > I_{th}\right) < \varepsilon, \text{ for all critical positions } x_i \\ & 0 < p_n < p_{\max}, \forall n \end{aligned} \tag{3-1}$$

where N is the number of slave WSDs, p_n is the transmit power of slave WSD n, $G_{x_i n}$ is the channel gain between the slave WSD n and the primary receiver at the critical position x_i, and G_{nn} is the channel gain between the WSD n and the master WSD. I_{th} is the interference threshold, obtained from the geo-location database, below which the aggregated interference caused by the secondary transmissions towards the primary receiver must be kept with a probability of $(1-\varepsilon)$. Further, W_n is the noise and I is interference (due to the TV broadcast transmissions, etc.) at the master WSD. $p_{\max}$ is the maximal possible output power of the slave WSDs, dictated by hardware limitations or regulatory specifications.

It should be noted that the optimization procedure also straightforwardly generalizes to situations where with different margins and/or interference thresholds for each critical

position are specified as well as to situations where different slave WSDs have different maximal possible transmit powers.

This problem is possible to reformulate as a convex optimization problem:

$$\begin{aligned} \text{Maximize} \quad & \sum_{n=1}^{N} \log_2\left(1+\frac{G_{nn}p_n}{W_n+I}\right) \\ \text{subject to} \quad & \sum_{n=1}^{N} G_{x_i n}p_n < I_{th} - I_{\text{margin}}, \text{ for all critical positions } x_i \\ & 0 < p_n < p_{\max}, \forall n \end{aligned} \tag{3-2}$$

where the margin I_{margin} have been introduced. The optimal setting of I_{margin}, that makes (3-2) equivalent with (3-1), will depend on the threshold ε as well as the number of WSDs N and the associated propagation models. The problem (3-2) is easy to solve using standard methods for solving convex optimization problems (e.g., the cvx toolbox for Matlab, [14]).

The original problem (3-1) is solved by using an iterative method to find the I_{margin} so that

$$P_{HI,x} \equiv \Pr\left(\sum_{n=1}^{N} G_{x_i n}p_n > I_{th} - I_{margin}\right) < \varepsilon, \text{ for all critical positions } x_i \tag{3-3}$$

is fulfilled. To maximize the UL capacity the probability should not be too low either so the I_{margin} is actually iteratively updated until the maximal aggregated interference position satisfies

$$P_{HI}^{\max} \equiv \max_{x_i} \Pr\left(\sum_{n=1}^{N} G_{x_i n}p_n > I_{th} - I_{margin}\right) \in \left[\varepsilon - \varepsilon', \varepsilon\right] \tag{3-4}$$

is fulfilled. The ε' is a parameter that is typically much lower than ε. In the example realization below the acceptable probability interval is chosen to be [0.95%, 1%]. This condition may be evaluated using the well known Fenton Wilkinson method, see e.g., [15], for approximation of the sum of the log-normal distributions of each interfering signal. Also, the probability may be estimated using standard Monte-Carlo methods.

The way the margin I_{margin} is updated is by choosing an initial value of zero dB, i.e. $I_{\text{margin}}^{(0)}$ = 0 dB, and choosing a maximal margin value $I_{\text{margin}}^{\max}$ that is very large, e.g. 120 dB. Then in each iteration

- if the probability $P_{HI}^{\max}$ is larger than ε, the minimal margin value is set to $I_{\text{margin}}^{\min} = I_{\text{margin}}^{(n)}$ and then the margin is increased to

$$I_{\text{margin}}^{(n+1)} = I_{\text{margin}}^{(n)} + \frac{1}{2}\left(I_{\text{margin}}^{\max} - I_{\text{margin}}^{\min}\right) \tag{3-5}$$

- if the probability $P_{HI}^{\max}$ is lower than $\varepsilon - \varepsilon'$, the maximal margin value is set to $I_{\text{margin}}^{\max} = I_{\text{margin}}^{(n)}$ and then the margin is decreased to

$$I_{\text{margin}}^{(n+1)} = I_{\text{margin}}^{(n)} - \frac{1}{2}\left(I_{\text{margin}}^{\max} - I_{\text{margin}}^{\min}\right) \tag{3-6}$$

The new value $I_{\text{margin}}^{(n+1)}$ is then used as I_{margin} in the convex optimization problem Eq.(3-2) to find the power allocation and subsequently to evaluate the validity of the solution (power allocation) via the constraint Eq.(3-3).

The iterative optimization process is illustrated in Fig. 3-4 below. Prior to what is shown in this figure the master WSD queries the geo-location database for the relevant information (specified above). The master WSD queries the database. Then the master WSD does the following:

1. The master WSD estimates, e.g., via use of pilots, the channel gains between the master WSD and all slave WSDs.
2. The master WSD calculates or estimates all channel gains between all combinations between slave WSDs and critical positions, using e.g., a pre-defined propagation model, antenna diagrams, etc. The estimation of the channel gains may be improved if, e.g., there is some feedback mechanism from the primary receivers implemented or if there is measurement equipment deployed by e.g., the secondary system operator, for measuring the aggregated interference at representative critical positions.
3. The master WSD sets an initial margin for the aggregated interference, e.g., $I_{\text{margin}}^{(0)}$ = 0 dB.
4. The master WSD maximizes the sum rate or some other appropriate criterion of the UL transmissions by solving a standard convex optimization problem with constraints on the maximally allowed aggregated interference with the margin added, using standard methods for convex optimization.
5. The master WSD evaluates for all critical positions whether the UL (i.e., slave WSD) power allocation results in a probability distribution of the aggregated interference that yields a sufficiently low, but not too low, probability of exceeding the interference threshold, i.e.,

$$P_{HI,x_i} < \varepsilon, \forall x_i, \quad P_{HI}^{\max} \in [\varepsilon - \varepsilon', \varepsilon] \tag{3-7}$$

   a. If the probability of exceeding the interference threshold is too high the margin is increased and if the probability is too low the margin is decreased. Then the process continues at step 4.
   b. If the probability is within a predefined range the iterative procedure stops (go to step 7). And the obtained power allocation is the optimal allocation that protects the primary receivers at the specified level.
6. The master WSD informs the slave WSDs of the UL transmit powers.
7. The WSDs use the specified transmit powers when transmitting in UL, i.e., from the slave WSDs to the master WSD.

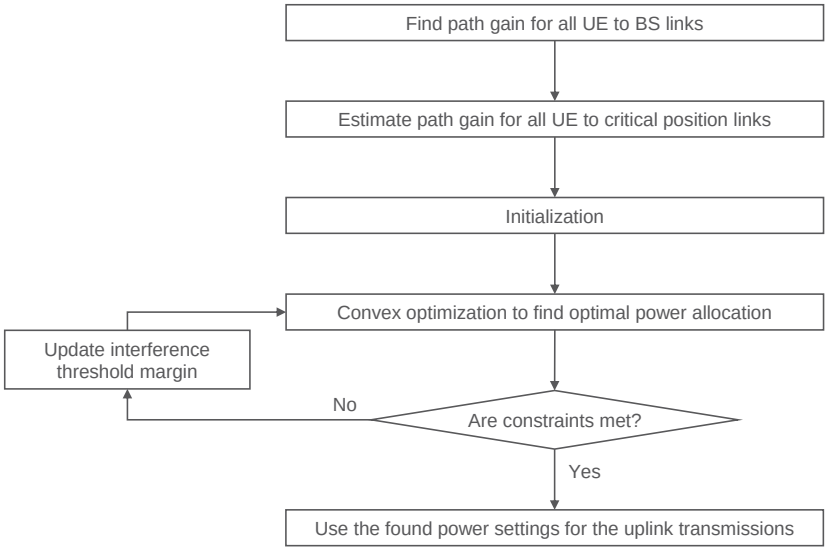

Fig. 3-4: Schematic flow diagram of the iterative process followed to find the optimal power allocation that respects the aggregated interference constraints.

3.5 **Numerical realization of the optimization algorithm**

In this section an example realization is presented to give evidence that the above outlined method for allocating powers performs as indicated.

In the example realization, five slave WSDs, i.e., $N=5$, are allocated transmit powers for UL. This setup in the example is visualized in Fig. 3-5. The critical positions are assumed to be the, in the figure visible part of the TV coverage contour (the line in red).

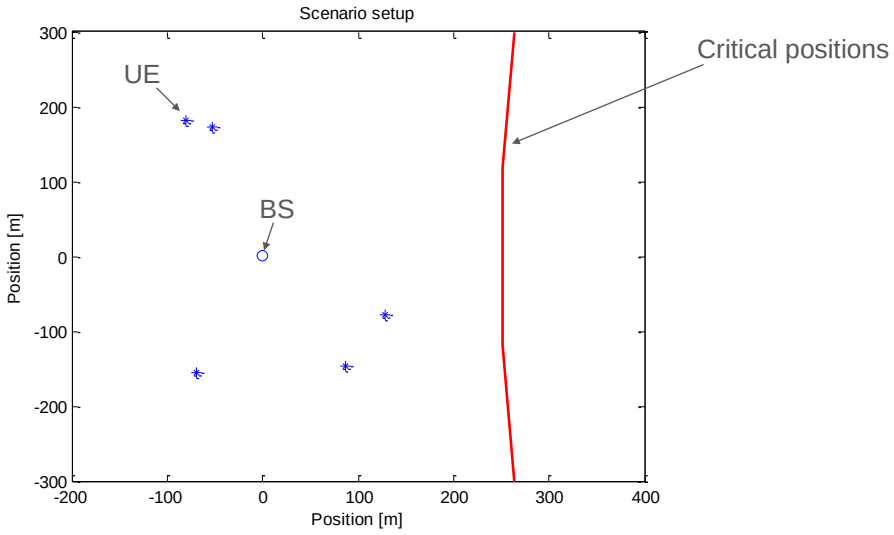

Fig. 3-5: The studied example scenario

In the simulations an interference threshold of I_{th} = - 57 dBm and an acceptable interval for the probability of harmful interference $[\varepsilon-\varepsilon',\varepsilon]$ = $[0.95\%,1\%]$ is assumed. The aggregated interference and probability of harmful interference have been calculated using the Fenton-Wilkinson approximation, first introduced in [15] and further described in [16] and [17]. The optimization procedure converges in this realization rather quickly

to a margin of 11 dB. The optimal power allocation for a maximum slave WSD transmit power of $p_{\max}$ = 20 dBm, is found to be:

$$p_1 = 6.76 \text{ dBm}$$
$$p_2 = 12.72 \text{ dBm}$$
$$p_3 = 20.00 \text{ dBm}$$
$$p_4 = 20.00 \text{ dBm}$$
$$p_5 = 20.00 \text{ dBm}$$

This UL power allocation generates the mean aggregated interference shown in Fig. 3-6.

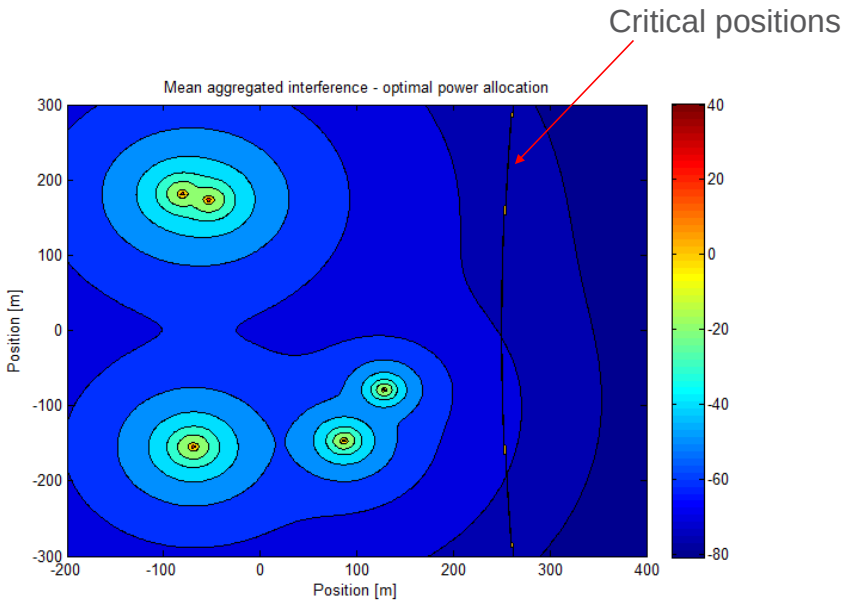

Fig. 3-6: The mean aggregated interference when the optimal power allocation is used at the slave WSDs.

Further, the mean aggregated interference along the contour (left to right correspond to down to up direction in Fig. 3-6) is shown in Fig. 3-7, where it is verified that the solution of the convex optimization problem Eq.(3-2) with the correct margin indeed respects the constraints in Eq.(3-2).

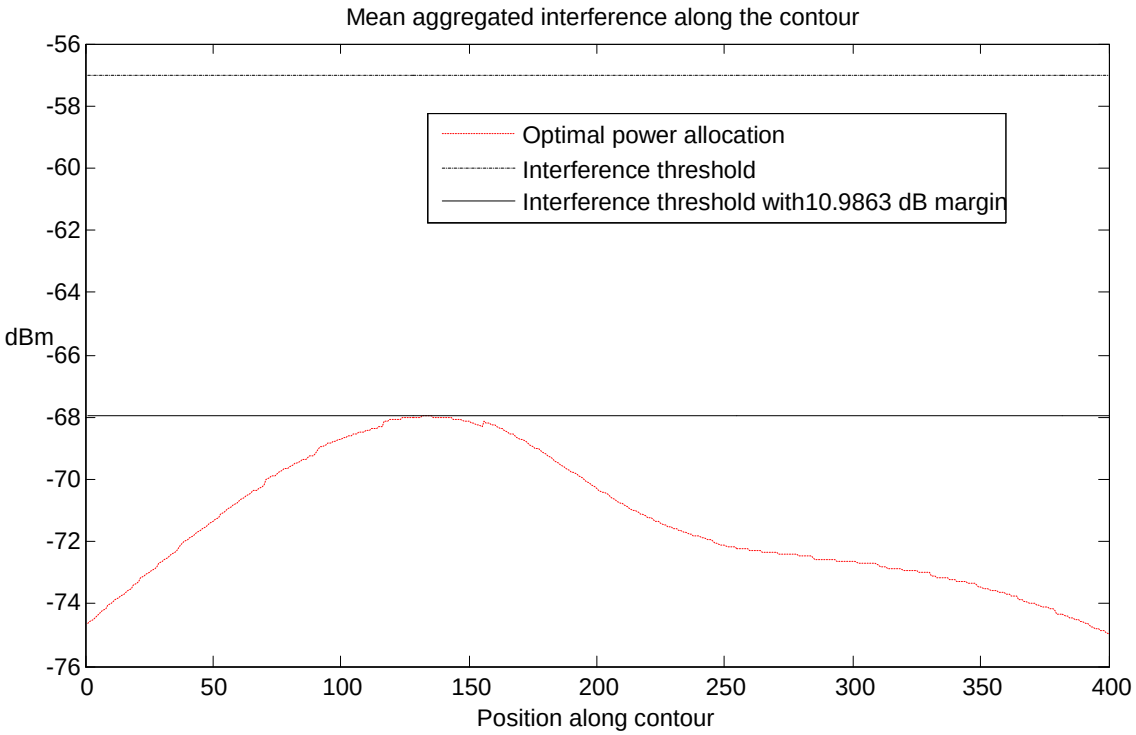

Fig. 3-7: The obtained mean aggregated interference along the TV coverage contour, i.e., the critical positions.

Fig. 3-8 shows the probability of exceeding the interference threshold at the critical positions along the contour. Indeed the maximum probability of interference at any critical location is 0.96%, i.e., within the acceptable interval.

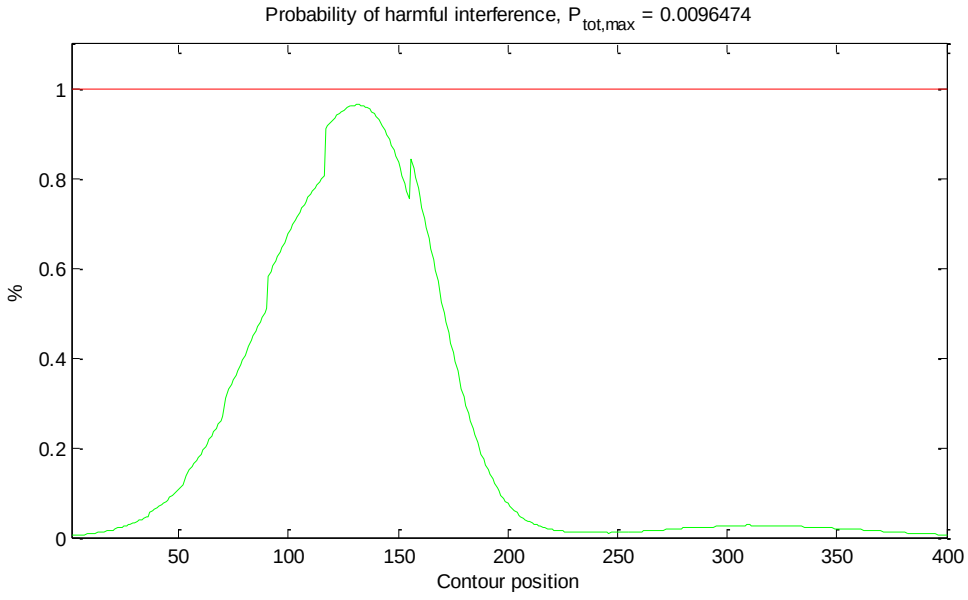

Fig. 3-8: The probability of causing harmful interference, i.e., of the aggregated interference to be above the interference threshold for the optimal power allocation in the example scenario, along the TV coverage contour (critical positions).

Fig. 3-9 shows the region in which the probability of exceeding the interference threshold is above 1%. The coverage contour, i.e, the set of critical positions, is almost tangential to this region at the critical position having the maximal probability of harmful interference. This is to be expected from a well behaving power allocation process since this indicates that the slave WSD powers are set so that the maximal capacity (sum rate) in UL is achieved without violating the primary protection requirements.

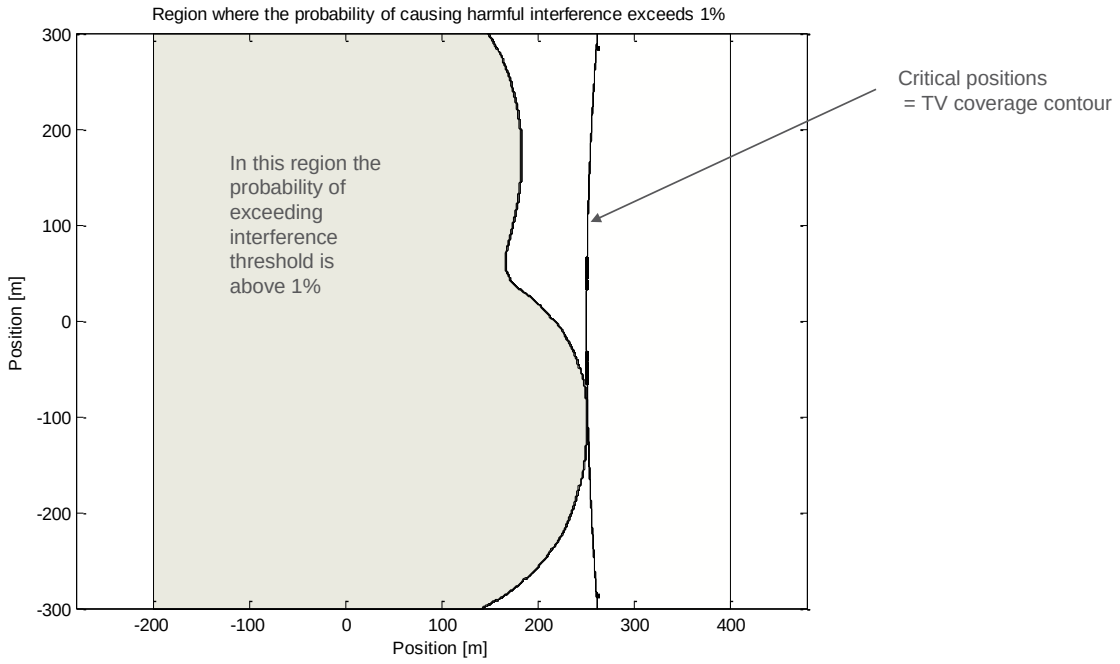

Fig. 3-9: Visualization of the region where the probability of having the aggregated interference being above the interference threshold is above 1%.

3.6 **Summary**

In this section we have introduced a power allocation strategy for secondary users operating in the TV white spaces. The goal of this strategy is to keep the probability of causing harmful interference to primary TV receivers below a threshold, possibly specified in future regulations, while maximizing the sum rate of the secondary links. It is assumed that the secondary transmitters are coordinated by a master WSD, which may be a cellular base station, and that the secondary transmissions are mutually orthogonal.

The power allocation method introduced allows dynamically taking into account the probability distribution of the aggregated interference, generated by the secondary transmissions. This is done by solving a series of convex optimization problems. This approach allows tuning of the margin of the interference threshold with the result that the margin is not needed to be set according to worst case assumptions (as done in many established literatures) and hence resulting in larger allowed secondary UL output powers which imply better secondary UL performance.

Note however that the example realization provided in this section may still be considered as a worst case scenario in that it uses positions along the TV coverage contour as the critical positions x_i, i.e., it does not use the locations of the actual receivers as that information is assumed not to be available.

If the locations of the primary receivers in the TV coverage area would be available, the strategy may be straightforwardly applied by using these locations as the critical positions x_i in the optimization. The present approach will then generate a secondary transmit power allocation for the slave WSDs that properly keeps the probability of causing excessive interference to these locations below the threshold. Further, if the actual primary receiver locations were inside the TV coverage (further away from the secondary system than the TV coverage contour) the allocation would allow higher secondary transmit powers and hence better secondary performance.

4 Cooperative Multi-band Sensing

4.1 Introduction

The process of spectrum sensing is an important functionality of cognitive radio devices enabling them to sense and inspect vacant spectrum opportunities for secondary usage. One of the cornerstones of latest secondary spectrum access development (also pointed out within the QUASAR project) is the inability of the spectrum sensing process to derive the needed reliability for practical deployments. This leads to the databases being a preferred approach by the regulatory bodies (e.g. FCC ruling on skipping the spectrum sensing requirements for TVWS devices). However, the process of spectrum sensing may prove vital for more accurate and up-to-date information on spectrum usage, complementing the database based approach. In some cases, geolocation can be inaccurate and the update period of the database query can be too rare to track all changes in the environment (e.g. indoor environments). This requires large protection zones for the primary users reducing the spectral efficiency of the secondary system. Additionally, PU systems that are not registered in the database are not taken into consideration and cannot be protected from SU's opportunistic access (e.g. Programme Making Special Events (PMSE) devices). The spectrum sensing approach enables a more frequent and local (geo-location independent) detection capable of identifying low power and "unpredictable" incumbent users like PMSEs, but lacks the capability to combat with the effect of aggregate interference. Merging the sensing with the database approach complements both processes and enables a more secure and efficient assessment. Hence, databases can be aided by sensed data (e.g. refreshing path gain calculations, detection of PMSE devices and Electronic News Gathering (ENG) equipment in TV white space scenarios [19]). The sensed data can be used in the process of updating the databases whenever there are changes in the communication conditions in the overall system (i.e. appearance of unregistered incumbent users). Additionally, sensing based approaches can be exploited for radar bands availabilities detection [20] and can be utilized for synchronizing the SU transmission with the rotational pattern of the radar antenna, or for detecting deviations from deterministic rotational patterns. Therefore, this section aims to explore the possibilities of increasing the efficiency of the spectrum sensing process with different enhancements as a complementary approach to databases.

The effects of non-cooperative single band sensing was extensively elaborated in D2.2 [21]. Applying a multi-band sensing approach where the nodes sense a wider bandwidth portion and may also incorporate high rate sampling detectors can significantly increase the efficiency of the spectrum sensing process and the corresponding probability of vacant spectrum detection. The notion of multi-band spectrum sensing refers to a chunk of the frequency spectrum that may be occupied by multiple primary signals [22] or may be interpreted as a broadband channel divided into a number of narrow sub-channels where one or more primary systems may transmit [23], [24], [25]. Effectively, the multi-band spectrum sensing can achieve higher detection performance compared to the classical (i.e. single-band) spectrum sensing approach for a given probability of harmful interference [26], which may prove vital for dynamic secondary spectrum access environments.

Providing a cooperative approach among multiple secondary nodes with sensing capabilities can further enhance the multi-band spectrum sensing. The decision (centrally or locally) for the presence of the primary users over the multiple channels is made based on the local measurement observations for all channels from all users that cooperate [25], [29], [30]. The approach may employ any of the existing data fusion models developed for the single band sensing case, but extended and adapted for multiple channels. The cooperation improves the spectrum sensing efficiency and reduces the interference caused to the primary system.

However, the benefits of cooperative multi-band sensing come in trade-off with the increase of the number of involved users needed for reliable control channel establishment and increase of the signaling overhead in the secondary network. These aspects may limit the achievable throughput of the secondary network, thus questioning the possible application of cooperative multi-band spectrum sensing in practice. Therefore, this section introduces and analyzes several cooperative multi-band spectrum sensing solutions that specifically address the above raised questions. The proposed solutions are general enough to accommodate various spectrum bands.

4.2 Examples of selected cooperative multi-band sensing solutions

Cooperative multi-band spectrum sensing essentially represents an optimization problem, where the main objective is to maximize the opportunistic throughput under certain interference limitation in the secondary (i.e. the cognitive) network [25], [27], [28]. This section introduces and analyzes several examples of cooperative multi-band spectrum sensing, i.e.:

- Distributed Multi-band Spectrum Sensing (DMSS),
- Energy efficient multi-band sensing,
- Cooperative Multi-band Spectrum Sensing (CMSS) and
- Fast Cooperative Spectrum Sensing (FCSS).

Every introduced and analyzed example in this section specifically addresses some of the raised problems associated with cooperative multi-band sensing. DMSS considers a system of multiple frequency bands where each user can measure only one band in cooperation with other secondary users. It investigates the *minimal required number of sensed bands* in multiband environment under certain constraints for the interference at the primary system and service outage probability. The energy efficient multiband spectrum sensing model stems on the DMSS scenario and, furthermore, investigates the *optimal number of users* that should be allocated for reliable measurement in each frequency band. This allows maximization of the achievable throughput and minimization of the total power spent. The CMSS investigates the *optimal sensing duration* and *optimal number of collaborating nodes* that satisfy the required spectrum sensing reliability and maximize the opportunistic throughput in the secondary cognitive network for different fusion rules. The FCSS model evaluates the multi-band spectrum sensing by taking into account the multiple access protocols including TDMA and CSMA/CA during data fusion. It examines the *most suitable sensor assignment strategy per band* and *optimal number of sensing nodes* that maximize the opportunistic throughput.

The main questions being answered in this section are the proportion of sensing vs. control signaling in the secondary network, the influence of the secondary multiple access on secondary spectrum efficiency and the justification of using adaptive strategies in secondary environments. They represent important QUASAR research pillars, but also clearly facilitate the analysis of the practical (non)feasibility of the spectrum sensing process in general.

4.2.1 Distributed Multi-band Spectrum Sensing (DMSS) considering the secondary service demand

A sensing strategy determines which spectrum band and for how long each SU should measure the spectrum. Sensing strategies have been proposed in the context of multi-channel MAC protocols for secondary networks. However, in the design of MAC protocols either perfect sensing accuracy is assumed at the PHY layer [31], [32], [33] or the secondary performance is described solely in terms of secondary network throughput [34], [35], [36]. Other metrics to quantify the secondary network performance like

blocking probability, queuing and packet transmission delay have been proposed in [37], [38], [39], [40]. However, perfect sensing accuracy is considered therein.

The DMSS approach attempts to integrate: (i) imperfect sensing at the PHY layer (ii) a sensing strategy at the MAC layer (iii) a multi-channel MAC protocol, and (iv) performance evaluation in terms of secondary service outage.

There is an interesting trade-off between the service demand of the secondary network and the demand in measured spectrum. If the SUs measure a few spectrum bands, the sensing accuracy can be improved by using cooperative spectrum measurements. However, the chance of detecting enough available bands for serving all SUs will be low. On the other hand, if the measurements are distributed over many spectrum bands, the chance of measuring available bands increases. However, due to the sensing errors, the available bands can be classified as occupied and the spectrum sharing opportunity in these bands will be lost.

We are looking to identify what grows quicker: the number of SUs utilizing the spectrum or the demand in measured spectrum. For instance, considering a secondary network running a certain service and assuming that an additional SU arrives, obviously, the capacity requirement of the overall network increases. At the same time, the sensing performance can be enhanced because there are more SU available for sensing. In this kind of scenario, we identify whether it is sufficient to rearrange the allocation of SU into the existing measured bands and modify the measurement time, or it is required to increase the number of measured bands for serving also the new user. If the number of SUs utilizing the spectrum grows much quicker compared with the number of measured bands then, there exists a potential for spectrum sharing for the secondary service under consideration.

4.2.1.1 Model description

We consider a centralized secondary network consisting of N users and K spectrum bands available for sensing. The secondary network is not aware of the bands that are available for sharing at its location. It has to identify the available bands by spectrum measurements. All the bands are assumed to offer the same transmission rate to the SUs when they are available. Different bands can be distinguished based on their prior probability $\Pr_0^{(k)}$ of being available. It is assumed that the SUs are aware of the prior probabilities $\Pr_0^{(k)}$ or the fraction of bands available for sharing at their locations.

Each SU has to initiate a call through the secondary network base station. For illustration purposes we consider a simple multi-channel MAC protocol for managing the secondary spectrum access similar to the point coordination function in IEEE 802.11. Also, due to its simplicity, we consider constant rate voice connection for the secondary network service. By using different MAC protocols or different types of services only the number of traffic channels an available TV band can support will change.

The availability of spectrum bands can change over time. For protecting the primary receivers the spectrum measurements should be carried out periodically. The secondary network base station is responsible for specifying the spectrum band and the duration of sensing to the SUs. Each SU is allowed to measure a single band at a time. As a result, the maximum number of measured bands is $N, K \leq N$. The time interval between two consecutive spectrum measurement intervals is referred to as the detection cycle. A schematic diagram of the detection cycle is depicted in the following figure.

Fig. 4-2: Detection cycle incorporating spectrum measurement time, reporting time to the secondary base station and communication time for secondary users

During the measurement interval T_m, each SU measures the spectrum band specified from the base station. During the reporting interval T_r, the SUs convey the measurement results to the base station over error-free reporting channels. The base station decides which measured bands are occupied and which are available by combining the measurement results received form the different SUs. During the communication interval T_c, the base station polls the SUs in a round robin fashion. The durations of signalling, measurement and communication intervals are assumed to be perfectly synchronous between all measured bands.

For quantifying the secondary network performance we use the service outage probability. We say that the secondary network experiences an outage when the number of bands detected to be available is not sufficient to carry all the secondary calls. Under outage, some of the secondary calls will have to be blocked. We identify the minimum required number of measured bands such that the outage probability $\Pr_b$ is maintained under a certain target value P, $\Pr_b \leq P$.

It is assumed that SUs measuring the same spectrum band collect independent spectrum measurements. Also, it is assumed that each spectrum band has the same fading statistics for all SUs. These two assumptions can be valid for short range cognitive networks where the SUs are located far from the primary transmitters.

In order to decide whether the k th measured band is available or occupied, we use a binary hypothesis test. Each user estimates the received signal energy during the measurement window and conveys the measurement result to the base station. We utilize equal gain combining among the SUs measuring the same band. If the base station decides that the primary signal level is larger than the target detection level γ_k then the k th measured band is assumed to be occupied. Otherwise, it is decided to be available for spectrum sharing. The channel between the primary transmitters and the SU is considered to incorporate both fast fading and shadowing [41]. The parameter η is used to describe the number of independent fast fading blocks within the measurement time.

4.2.1.2 Problem formulation

It is desirable to reduce the number of measured bands in order to decrease the measurement time and utilize the available bands efficiently. At the same time, the service outage probability for the secondary system must be controlled, $\Pr_b \leq P$. Also, the probability to miss the primary signal and generate unacceptable interference to the primary receivers must be maintained under certain target, $\Pr_{miss}^{(k)} \leq \Pr_{out}$, where $\Pr_{miss}^{(k)}$ stands for the misdetection probability in the k th measured band and the maximum allowable miss probability $\Pr_{out}$ is taken from the primary system's specifications.

If all the bands are characterized by the same fading distribution and the same detection level γ_k , then, the misdetection probability is simply a function of the number of cooperating users. Let us denote by n_k the group of users measuring the k th band and by $|n_k|$ the cardinality of the group. We minimize the number of measured bands by optimizing the number of SUs measuring each spectrum band and the measurement time.

Since the measurement time is common for all the measured bands which offer the same transmission rate opportunity, the available bands can carry the same number of secondary calls. The measurement time T_m can be mapped into the number of calls N_u an available band can support by dividing the communication interval with the time required to transmit one voice packet. The maximum number of supported calls $N_u^{(\max)}$ can be derived by setting the measurement and the reporting interval equal to zero. The optimization problem can be formulated as:

$$\begin{aligned} \underset{|n_k|, N_u}{\text{Minimize:}} \quad & K. \\ \text{Subject to:} \quad & \Pr_b \le P \\ & \sum_{k=1}^{K} |n_k| = N \\ & N_u \le N_u^{(\max)} \\ & \Pr_{miss}^{(k)} \le \Pr_{out} \ \forall k \end{aligned} \tag{4-1}$$

Next, we show how to compute the service outage probability $\Pr_b$. Recall this is the probability at least one SU call is not allocated during the detection cycle. Let us consider a scenario s where only ν out of the K measured bands are detected to be available. The available bands are grouped under the set Φ_s , while, the rest of the measured bands are grouped under the complementary set Φ_s^C . The occurrence probability $\Pr_s$ for the scenario s is:

$$\Pr_s = \prod_{k \in \Phi_s} g(\lambda_k) \cdot \prod_{k \in \Phi_s^C} (1 - g(\lambda_k)) \tag{4-2}$$

where $g(\lambda_k)$ stands for the probability the k th measured band is classified to be available.

Note that when a spectrum band is erroneously detected to be available, the secondary transmission rate will be lower than the expected due to the primary generated interference. In that case, the secondary base station can monitor the lower rate and stop the secondary transmissions on the occupied spectrum bands. Because of that, it is assumed that SU calls are carried only over the bands correctly identified to be available for sharing. As a result, $g(\lambda_k) = \Pr_0^{(k)} \cdot (1 - \Pr_{false}^{(k)})$ where $\Pr_{false}^{(k)}$ stands for the false alarm probability.

Since all the available bands can carry the same number N_u of SU calls, an outage occurs in the case of: $\nu \cdot N_u < N$. The maximum number of detected available bands that still results in an outage is $\nu_{\max} = \lceil N/N_u - 1 \rceil$. The outage probability $\Pr_b$ can be derived by summing over the occurrence probabilities $\Pr_s$ of all scenarios s where the number of detected available bands is smaller than or equal to $\nu_{\max}$.

$$\Pr_b = \sum_{\nu=0}^{\nu_{\max}} \sum_{s=1}^{C(K,\nu)} \Pr_s \tag{4-3}$$

where $C(K,\nu)$ is the total number of $\nu-$combinations in a $K-$element set.

4.2.1.3 Optimization algorithm

In order to solve the optimization problem (4-1), we first identify the minimum required number of measured bands K_0 under perfect sensing accuracy. In the presence of sensing errors, we increment the number of measured bands $K \to K+1$ starting from $K = K_0$ until the optimization constraints are satisfied. Given the number K of measured bands, we identify the measurement time and the SU allocation $|n_k|, k = 1,\ldots K$ minimizing the outage probability $\Pr_b$. For a fixed K, the optimization problem becomes:

$$\begin{aligned} \underset{|n_k|, N_u}{\text{Minimize:}} \quad & \Pr_b \\ \text{Subject to:} \quad & \sum_{k=1}^{K} |n_k| = N \\ & N_u \le N_u^{(\max)} \\ & \Pr_{miss}^{(k)} \le \Pr_{out} \; \forall k \end{aligned} \tag{4-4}$$

In order to solve the optimization problem (4-4), one can fix the measurement time and optimize the SU allocation $|n_k|, k = 1,\ldots K$. The optimization should be carried out for each feasible N_u. Finally, the SU allocation and measurement time minimizing the outage probability $\Pr_b$ should be selected. Given the number of measured bands and the measurement time we identify the optimal SU allocation by solving the following optimization problem:

$$\begin{aligned} \underset{|n_k|}{\text{Minimize:}} \quad & \Pr_b \\ \text{Subject to:} \quad & \sum_{k=1}^{K} |n_k| = N \\ & \Pr_{miss}^{(k)} \le \Pr_{out} \; \forall k \end{aligned} \tag{4-5}$$

It is easy to prove that the decision thresholds minimizing $\Pr_b$ satisfy the constraints $\Pr_{miss}^{(k)} \le \Pr_{out}, \forall k$ with equality. In that case the detection probability $g(\lambda_k)$ can be written as a function of the number of users measuring the k th band. As a result, the optimization problem (4-5) is degenerated to an integer programming problem. The integer optimization can be solved by exhaustive search for a small number of SU *N*. For a high number of SUs we propose to solve it by means of a greedy algorithm.

The greedy algorithm has been verified for a small number of SUs and is found to perform remarkably well. In chapter 4.2.1.4 it is used to study the relation between the number of SUs utilizing the spectrum and the demand in measured spectrum.

4.2.1.4 Results

The parameter settings for the primary and the secondary system are summarized in Table 4-1 and Table 4-2 respectively.

Table 4-1: Parameter settings for the primary system

target detection SNR	-12 dB
shadowing standard deviation	3 dB
coherence time	the case with $\eta = 5$ independent blocks within the measurement interval corresponds to fast fading channel while, the case with single block $\eta = 1$ corresponds to slowly fading channel
maximum allowable miss probability	2%
prior probability for the availability of bands	The fraction Pr_0 of available bands at the location of secondary network is assumed to be known. This is a parameter whose impact is identified in our computations
bandwidth for each measured band	6 MHz

Table 4-2: Parameter settings for the secondary system

duration of the detection cycle	120 ms
voice packetization interval	40 ms
achievable rate on available spectrum bands	3 Mbps
maximum number of calls an available band can carry	17
service outage target probability	this is a parameter whose impact is studied in our computations

In Fig. 4-3 we identify the minimum required number of measured bands with respect to the number of SUs N for different service outage probability target P. The fraction of available bands at the location of the secondary network is assumed to be equal to 50% on the left and 75% on the right. A few remarks can be drawn based on Fig. 4-3:

- When the number of SU increases, one can decrease the measurement time in order to maintain the same number of measured bands. For instance, according to Fig. 4-3 (right) 6 bands are sufficient to serve from 18 to 34 SU calls with target service outage probability 1%. The measurement time for 18 and 34 calls are 45.6 ms and 5.3 ms respectively.
- The number of measured bands does not increase monotonically with the size of secondary network. For instance, in Fig. 4-3 (left) 14 bands are required to serve 18 calls and only 8 bands to serve 22 calls. In both cases the outage probability target is 5%. The reason being that, for small-sized networks the gain through cooperative measurements is small. Because of that, it is better to distribute the SU measurements in multiple bands to increase the chance of measuring available bands.
- If the target outage probability is low and the size of secondary network is small, the optimization problem (4-1) may not have a feasible solution. When the target service outage is small, many bands should be measured to identify enough available bands. For small-sized networks only a few SU can cooperatively measure the same band. Because of that, the false alarm probability remains high and bands that are actually idle are detected to be occupied.
- The number of SUs utilizing the spectrum grows much quicker compared to the number of bands required to measure.

In Fig. 4-4 the impact of spectrum availability at the location of the secondary network is demonstrated. The comparison with perfect sensing is included in order to illustrate the impact of fading and noise in the number of measured bands. For areas with high availability, $\Pr_0 > 0.5$, the required number of measured bands is small. At the same time, the number of SU measuring cooperatively the spectrum is sufficient to average out the fading effects. The impact of imperfect sensing is distinct in areas with low spectrum availability and strict service outage probability target (see Fig. 4-4 left).

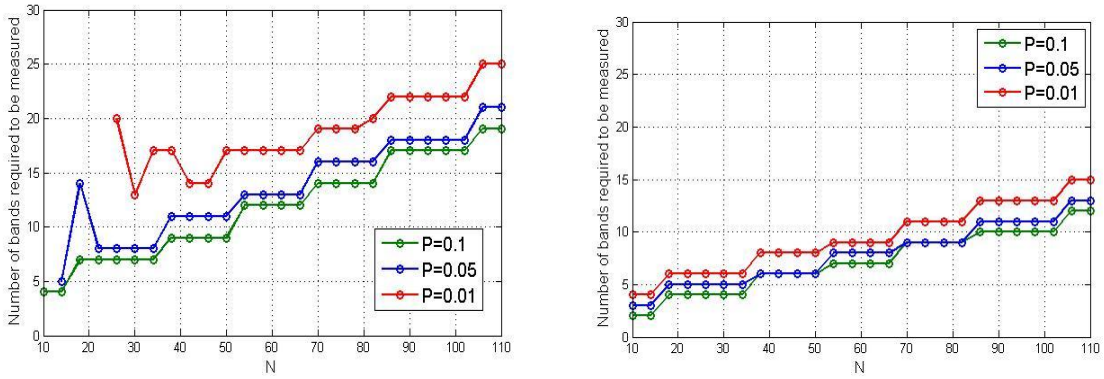

Fig. 4-3: Minimum required numer of measured bands vs number of secondary users for different blocking probabilities. The fraction of available bands at the location of the secondary system is equal to 50% (left) and 75% (right).

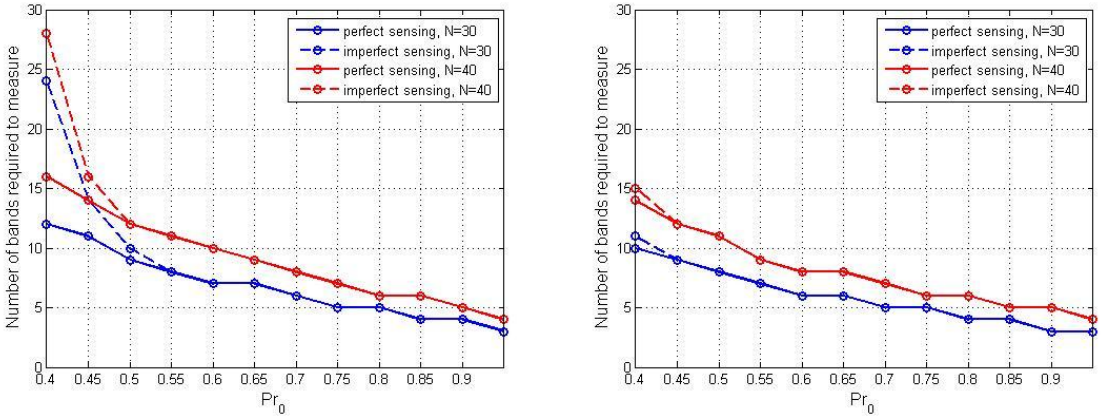

Fig. 4-4: Minimum required number of measured bands vs fraction of available bands $\Pr_0$ at the location of the secondary system. The blocking probability is equal to $P = 0.02$ (left) and $P = 0.05$ (right).

4.2.2 **Energy efficient multi-band sensing**

The existing work in multi-band spectrum sensing assumes that each SU has to measure the complete candidate bandwidth [25], [42], [43], [44], [45]. That can be inefficient in terms of time and energy resources. A sensing strategy can be used to determine the allocation of SU to multiple spectrum bands for spectrum sensing. In Section 4.2.1 we proposed a sensing strategy that takes into account the capacity requirement of the secondary network service. In this section we proposed a sensing strategy that takes into account the power spent for sensing. The service of the secondary network is not specified as in Section 4.2.1 and the secondary network performance is described in terms of achievable data rate. The distributed sensing of multiple spectrum bands can be viewed as multi-objective optimization problem. This section proposes maximization of a

cost function that considers both the SU data rate and the power spent for sensing. The optimization target is the allocation of SU to different spectrum bands for spectrum sensing.

There is an interesting trade-off between the sensing accuracy and the power spent for sensing. Allocating all SU for spectrum sensing may affect marginally the sensing performance after some point. If the energy consumption is an issue, it may be more beneficial for the secondary network to refrain some of the SU from sensing. The trade-off between energy efficiency and sensing performance has been studied so far for secondary networks seeking for transmission opportunities in a single spectrum band [46]. In order to increase the transmission opportunities, the SUs will naturally search over multiple spectrum bands. We identify how many bands it is reasonable to measure in order to balance between achievable data rate and power spent for sensing.

4.2.2.1 Model description

We consider the same model for the primary system and the secondary network as described in Section 4.2.1.

If the k th band is available, the achievable data rate of SU in this band is denoted by $r_0^{(k)}$. If the k th band is occupied but it is erroneously identified to be available, the secondary data rate is denoted by $r_1^{(k)}$. Obviously, $r_1^{(k)} < r_0^{(k)}, \forall k$ due to the presence of primary system generated interference at the location of the secondary network.

The expected data rate of the SU network over the k th spectrum band is the sum of achievable rates $r_1^{(k)}, r_0^{(k)}$ weighted with the probability to classify the measured band as available: $r_0^{(k)} \Pr_0^{(k)} \left(1 - \Pr_{false}^{(k)}\right) + r_1^{(k)} \Pr_1^{(k)} \Pr_{miss}^{(k)}$. The expected throughput over all spectrum bands is simply the sum: $O_1 = \sum_{k=1}^{K} r_0^{(k)} \Pr_0^{(k)} \left(1 - \Pr_{false}^{(k)}\right) + r_1^{(k)} \Pr_1^{(k)} \Pr_{miss}^{(k)}$. It is assumed that all SUs are identical. In that case, the total power consumption increases linearly with the number of SU involved in spectrum sensing. If the energy spent per SU is denoted by P_s, the total energy spent for sensing can be written as: $O_2 = P_s \cdot \sum_{k=1}^{K} |n_k|$.

In order to study the trade-off between expected achievable data rate and energy consumption we combine the two objectives O_1, O_2 into a single function as:

$$J = (1-\alpha) \cdot \frac{O_1}{R_{\max}} - \alpha \cdot \frac{O_2}{N \cdot P_s} \tag{4-6}$$

where $R_{\max}$ is an upper bound for O_1 $\alpha, 0 \le \alpha \le 1$ is a coefficient used to weight the trade-off between O_1 and O_2. For example, as the value of α increases, more emphasis is put on the energy consumption.

4.2.2.2 Problem formulation and optimization algorithm

In sensing-based spectrum allocation the probability to generate unacceptable interference increase to the primary receivers is controlled by keeping the miss detection probability under some target value, $\Pr_{miss}^{(k)} \le \Pr_{out}^{(k)}, \forall k$. In addition, we decided to set a target constraint $\Pr_{und}^{(k)}$ on the false alarm rate for the k th measured band

$$\begin{aligned} \underset{\lambda_k,|n_k|}{\text{Maximize:}} \quad & J \\ \text{Subject to:} \quad & \sum_{k=1}^{K}|n_k| \le N \\ & \Pr_{false}^{(k)} \le \Pr_{und}^{(k)}, \forall k \\ & \Pr_{miss}^{(k)} \le \Pr_{out}^{(k)}, \forall k \end{aligned} \tag{4-7}$$

It is easy to show that the miss probability maximizing the optimization function (4-6) satisfies the constraint with equality, $\Pr_{miss}^{(k)} = \Pr_{out}^{(k)}, \forall k$. Given the miss probability target, the false alarm constraint is satisfied when a minimum number of SU $n_{\min}^{(k)}$ cooperatively measure the k th band.

The optimization problem (4-7) can be solved by using exhaustive search for a limited number of SU and spectrum bands. When the search space becomes large, some heuristic algorithm will be required. We noticed that the distributed sensing problem (4-7) can be viewed as a multiple choice knapsack packing (MCKP) problem. Each spectrum band can be represented by a class and each possible group of SU measuring a band can be represented by an item. Let us denote by x_{ij} the binary variable describing whether the i th spectrum band (or class) is measured by j SU. Then, the optimization problem (4-7) can be also formulated as:

$$\begin{aligned} \underset{x_{ij},\forall i,j}{\text{Maximize:}} \quad & \sum_{i=1}^{K}\sum_{j=n_{\min}^{(i)}}^{N} p_{ij}\cdot x_{ij} \\ \text{Subject to:} \quad & \sum_{i=1}^{K}\sum_{j=n_{\min}^{(i)}}^{N} w_{ij}\cdot x_{ij} \le N \\ & \sum_{j=n_m^{(i)}}^{N} x_{ij} \le 1, \forall i \\ & x_{ij} \in \{0,1\}, \forall i, j \end{aligned}$$

where $x_{ij} = 1$ describes the case that j SU are allocated to measure the i th spectrum band, the weights $w_{ij} = j, \forall i$ and the profits p_{ij} can be computed based on (4-6)

$$p_{ij} = \frac{1-\alpha}{R}\cdot\left(r_0^{(i)}\cdot \Pr_0^{(i)}\cdot\left(1-\Pr_{false}^{(i)}\left(\lambda_{ij}\right)\right)+ r_1^{(i)}\cdot \Pr_1^{(i)}\cdot \Pr_{out}^{(i)}\right)-\frac{\alpha}{N}\cdot j + C_0 \tag{4-8}$$

4.2.2.3 Results

There are many available algorithms for the solution of MCKP problems [47]. Among them we select the greedy optimization algorithm due to its low complexity. First, we compare the results obtained by using exhaustive search and by the MCKP algorithm for a small number of SU and spectrum bands. Then, we use the MCKP algorithm for studying distributed spectrum sensing over very wide bandwidth.

We consider a case with $K = 6$ bands available for sensing. The spectral efficiency for secondary transmissions over available and occupied bands is taken equal to 0.5 b/s/Hz and 0.1 b/s/Hz respectively. For 6 MHz transmission bandwidth the achievable data rate is equal to 3 Mbps and 0.6 Mbps respectively. The number of collected samples is set to 1000. The shadowing standard deviation is 3 dB and the target detection level 12 dB under the noise level. The availability of six bands is selected randomly between 0.4 and 0.6. The algorithm performance is verified in different fading environments. The fading impact is introduced through the parameter η that describes the number of independent fast fading blocks within the measurement time. When $\eta = 1$ the channel coherence time

is larger than the measurement time. In that case the fast fading is not averaged out at a single SU and its impact on the detection performance is severe. On the other hand, when $\eta = 5$ there are five independent fast fading realizations within the collected block of measured samples.

In Fig. 4-5 we obtain the optimal SU allocation by using exhaustive search and also by the MCKP algorithm. For the derived allocations the expected data rate is computed.

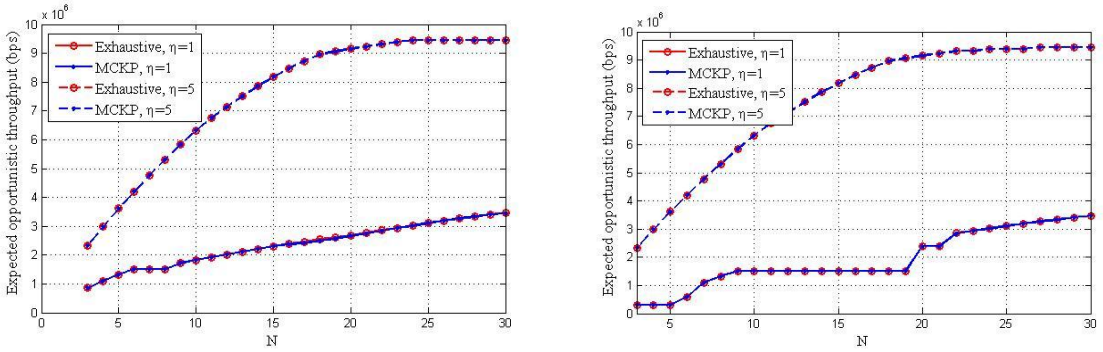

Fig. 4-5: Expected throughput over six spectrum bands by using exhaustive search and the knapsack algorithm for different size of secondary network. Weighting coefficient is taken equal to $\alpha = 0.05$ (left) and $\alpha = 0.15$ (right).

Having verified in Fig. 4-5 that the MCKP algorithm performs remarkably well in small-sized SU networks we use it to study the distributed sensing problem under wide TV bandwidth. The derived allocation of SU over 20 spectrum bands is depicted in Fig. 4-6 – Fig. 4-8. It is assumed that only the fraction of available bands Pr_0 at the location of the SU network is known. Based on these figures, the following remarks can be drawn

- When the fading can be averaged out at a single SU, $\eta = 5$, the SUs are allocated to the bands in a round robin fashion. We stop adding SU to a measured band when the gain in sensing accuracy by allocating more SU becomes marginal (see Fig. 4-7). When a target false alarm rate is also set, the SUs are still allocated in a round robin fashion after the required number of users is allocated in each band (see Fig. 4-6).
- When the fading is severe $\eta = 1$, we initially allocate one SU per band to increase the chance of measuring available bands. Many SUs are required to collect cooperative spectrum measurements for mitigating the fading effects and enhance the sensing accuracy. Because of that, the energy consumption outweighs the achievable data rate in the cost function unless there are enough SUs to cooperate (see Fig. 4-8).

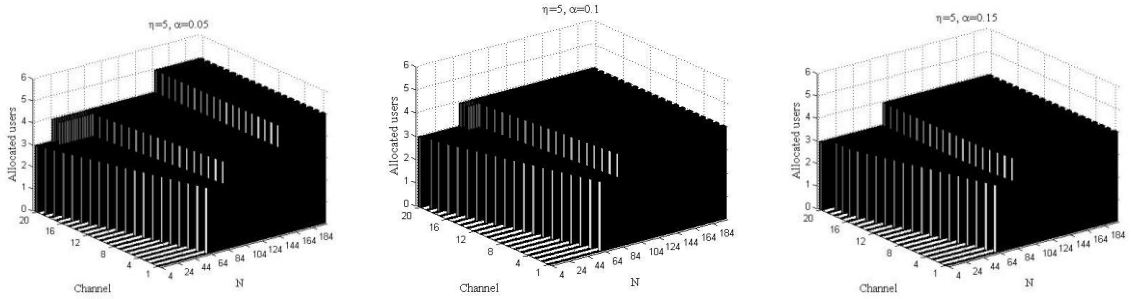

Fig. 4-6: Allocation of users in multiple spectrum bands for spectrum sensing by using the knapsack algorithm. Fraction of available bands at the location of secondary network $\Pr_0 = 0.5$ and $\eta = 5$ independent fast fading realization within the measured time. In each measured band there should be allocated at least three secondary users to meet the false alarm target; equal to 10%.

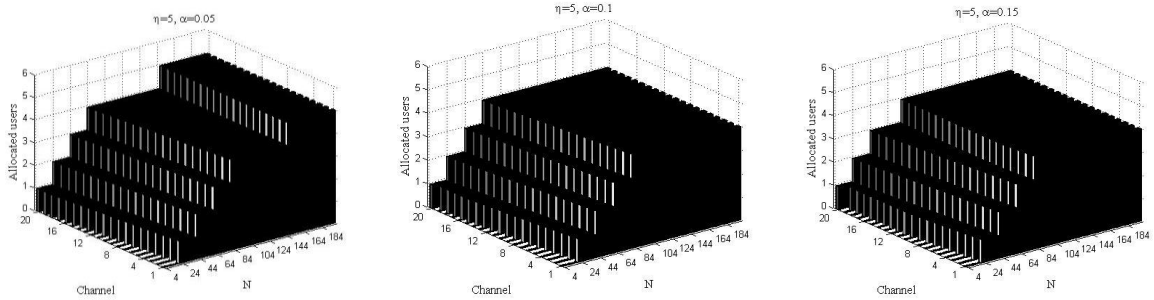

Fig. 4-7: Allocation of users in multiple spectrum bands for spectrum sensing by using the knapsack algorithm. Fraction of available bands at the location of secondary network $\Pr_0 = 0.5$ and independent fast fading realization within the measured time $\eta = 5$. No false alarm target is specified.

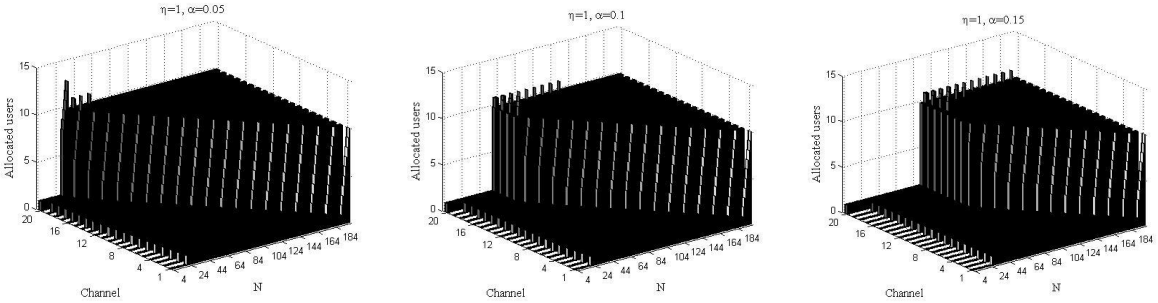

Fig. 4-8: Allocation of users in multiple spectrum bands for spectrum sensing by using the knapsack algorithm. Fraction of available bands at the location of secondary network $\Pr_0 = 0.5$ and independent fast fading realization within the measured time $\eta = 1$. No false alarm target is specified.

4.2.3 **Cooperative Multi-band Spectrum Sensing (CMSS)**

The spectrum sensing reliability depends on the type of used detector and can be mainly improved by either *increasing the sensing time* [48] or *cooperation among the involved secondary users*. However, both solutions decrease the throughput in the secondary network since the time resources are spent either for spectrum sensing or for control information exchange. This subsection elaborates the CMSS model that overcomes this problem.

4.2.3.1 Model description

The CMSS model assumes a centralized and cooperative secondary cognitive network with a Fusion Centre (FC) and *N* secondary users that sense *K* channels. Each secondary user employs energy detection to sense all *K* channels and send its sensing report to the FC through a common control channel. The FC fuses the sensing reports and decides about the primary users' presence/absence over the multiple channels. The main goal of the CMSS model is to find the *optimal number of cooperative nodes* and *sensing duration* that *maximizes the throughput* in the cognitive network.

The channel access is assumed to be in a time division mode, Fig. 4-9. Each node senses all *K* channels for τ_s seconds and spends τ_c seconds for sensing report exchange. The estimated sensing time and control channel duration are given with eq. (4-9) and eq. (4-10), respectively.

$$\tau_s = K \cdot \tau_i \tag{4-9}$$

$$\tau_c = \frac{K \cdot N \cdot b}{R_c} + \tau_c^{'} \tag{4-10}$$

where τ_i is the needed sensing time for a single channel (i.e. the i^{th} channel), *b* is the number of bits per sensing report, R_c is the control channel bit rate and τ_c' is a time interval dedicated for either an additional control channel information exchange or synchronization purposes. As a result, a node has *T* - τ_s - τ_c seconds for data transmission, where *T* is the frame duration.

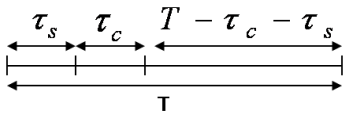

Fig.4-9: TDM channel access

The potential throughput from the Shannon capacity theorem [49] for the i^{th} channel with a bandwidth *B*(*i*) can be calculated as:

$$r(i) = B(i) \cdot \log(1 + SNR(i)) \tag{4-11}$$

The secondary users can use the *K* channels only if being vacant (i.e. not occupied by a primary one) and correctly detected (i.e. the sensing does not produce a false alarm event). Therefore, the aggregate opportunistic throughput in the cognitive network is the sum of the estimated throughputs per all channels:

$$R = \sum_{i=1}^{K} \frac{T - \tau_s - \tau_c}{T} \cdot r(i) \cdot P_{H_0}(i) \cdot (1 - P_{fa}(i)) \tag{4-12}$$

where $P_{H0}(i)$ is the probability that the i^{th} channel is available for secondary usage and $P_{fa}(i)$ is the probability that the i^{th} channel is not correctly detected as vacant.

4.2.3.2 Problem formulation

Eq. (4-13) formally describes the initial problem of the CMSS model:

$$\begin{aligned} &\max_{\tau_i \; N} \sum_{i=1}^{K} \frac{T - \tau_s - \tau_c}{T} \cdot r(i) \cdot P_{H_0}(i) \cdot (1 - P_{fa}(i)) \\ &s.t. \quad I_i = P_{H_1}(i) \cdot P_{miss}(i) \le \alpha \quad \Rightarrow \quad P_d(i) \ge \alpha^{'} \qquad \forall i \in \{1,..,K\} \end{aligned} \tag{4-13}$$

where I_i is the interference at the i^{th} channel (caused by a primary user presence), $P_{H1}(i)$ is the probability that the i^{th} channel is occupied by a primary user and $P_{miss}(i)$ is the misdetection probability for the i^{th} channel. The objective function is to maximize the aggregate (i.e. cumulative) throughput in the cognitive network by choosing the appropriate sensing time and the number of cooperating nodes. The constraint function states that interference per channel caused by the secondary users should not exceed a certain value α. CMSS envisions that $P_{H1}(i)$ is a constant and $P_{miss}(i) = 1 - P_d(i)$, where $P_d(i)$ is the detection probability for the i^{th} channel, reducing the interference constraint function to a detection probability constraint (eq. (4-13)).

Further analysis requires an adoption of a data fusion technique. As already stated, CMSS can either use EGC or MV.

CMSS with EGC. The false alarm probability and the detection probability for the i^{th} channel in this case are given with:

$$P_{fa}(i) = \frac{\Gamma(N \cdot m, \lambda_i / 2)}{\Gamma(N \cdot m)} \tag{4-14}$$

$$P_d(i) = Q_{N \cdot m}\left(\sqrt{2m\sum_{j=1}^{N}\gamma_j}, \sqrt{\lambda_i}\right) \tag{4-15}$$

where m is the time-bandwidth product, thus the number of sampling points is $u = 2m$, λ_i is the detection threshold for the i^{th} channel chosen for a specific target false alarm probability, γ_j is the received SNR at the j^{th} user, $\Gamma(.,.)$ and $\Gamma(.)$ are the incomplete and the complete gamma functions, respectively, and $Q_{Nm}(.,.)$ is the generalized Marqum Q function. Additionally, eq. (4-16) expresses the time-bandwidth product as a function of the sensing time:

$$\tau_i = \frac{u}{f_s} = \frac{2 \cdot m}{f_s} \quad \Rightarrow \quad m = \frac{\tau_i \cdot f_s}{2} \tag{4-16}$$

Finally, the optimization problem from eq. (4-13) specified for the EGC case is formulated as:

$$\begin{aligned} &\max_{\tau_i\ N} \sum_{i=1}^{K} \frac{T - K \cdot \tau_i - \dfrac{K \cdot N \cdot b_{egc}}{R_c} - \tau_c^{'}}{T} \cdot r(i) \cdot P_{H_0}(i) \cdot (1 - P_{fa}(i)) \\ &s.t. \quad P_d(i) = Q_{N \cdot m}\left(\sqrt{\tau_i \cdot f_s \cdot \sum_{i=1}^{N}\gamma_i}, \sqrt{\lambda_i}\right) \geq \alpha^{'} \quad \forall i \in \{1,..,K\} \end{aligned} \tag{4-17}$$

$$s.t. \quad P_{fa}(i) = \frac{\Gamma\left(N \cdot \tau_i \cdot \frac{f_s}{2}, \frac{\lambda_i}{2}\right)}{\Gamma\left(N \cdot \tau_i \cdot \frac{f_s}{2}\right)} \leq \beta \quad \Rightarrow \quad \lambda_i = 2 \cdot \Gamma^{-1}\left(N \cdot \tau_i \cdot \frac{f_s}{2}, \beta\right) \quad \forall i \in \{1,..,K\}$$

The objective function and the first constraint function follow the same form as in eq. (4-13). The second constraint function in eq. (4-17) refers to the false alarm probability and the subsequent choice of an appropriate detection threshold.

The optimization problem (4-17) represents mixed integer problem. However, the minimal number of cooperating nodes and the minimal sensing time that satisfy the second constraint function maximizes the objective function in eq. (4-17) (proof is presented in Appendix A.2: Proof of Lemma 4-1). The second constraint function

maximizes the detection probability (i.e. the first constraint function) when equality is achieved (proof is presented in Appendix A: Proof of Lemma 4-2). An exhaustive search algorithm can be applied for finding the minimal τ_i and N that satisfy the constraint functions in eq. (4-17) and maximize the objective function. The algorithm makes following: for every N, it finds the minimal sensing time, so that the second constraint function is satisfied.

CMSS with MV. The false alarm probability and the detection probability for the i^{th} channel in this case are given with:

$$P_{fa}(i) = \sum_{j=N/2}^{N} \binom{N}{j} {P_{fa}}^{j} (1-P_{fa})^{N-j}, \quad P_{fa} = \frac{\Gamma(m, \lambda/2)}{\Gamma(m)} \tag{4-18}$$

$$P_d(i) = \sum_{j=N/2}^{N} \binom{N}{j} {P_d}^{j} (1-P_d)^{N-j}, \quad P_d = Q_m\left(\sqrt{2m\gamma}, \sqrt{\lambda}\right) \tag{4-19}$$

where the values of P_{fa} and P_d refer to the false alarm probability and detection probability of a single node, respectively. The initial optimization problem in eq. (4-13) can then be reduced to an optimization problem formulated as:

$$\max_{\tau_i\, N} \sum_{i=1}^{K} \frac{T - K\cdot\tau_i - \frac{K\cdot N\cdot b_{mv}}{R_c} - \tau_c'}{T} \cdot r(i) \cdot P_{H_0}(i) \cdot (1 - P_{fa}(i))$$

$$s.t. \quad P_d(i) = \sum_{j=N/2}^{N} \binom{N}{j} {P_d}^{j} (1-P_d)^{N-j} \geq \alpha' \quad | \quad P_d = Q_m(\sqrt{\tau_i \cdot f_s \cdot \gamma_i}, \sqrt{\lambda_i}) \quad \forall i \in \{1,..,K\} \tag{4-20}$$

$$s.t. \quad P_{fa}(i) = \sum_{j=N/2}^{N} \binom{N}{j} {P_{fa}}^{j} (1-P_{fa})^{N-j} \leq \beta \quad \Rightarrow \quad P_{fa} = \frac{\Gamma(\tau_i \cdot \frac{f_s}{2}, \frac{\lambda_i}{2})}{\Gamma(\tau_i \cdot \frac{f_s}{2})} \leq \beta_n'$$

$$\forall i \in \{1,..,K\} \wedge \forall n \in \{1,..,N\} \quad \Rightarrow \quad \lambda_i = 2 \cdot \Gamma^{-1}(\tau_i \cdot \frac{f_s}{2}, \beta_n')$$

As in the EGC case, the second constraint function helps to find the detection thresholds needed in the first constraint. The detection threshold that maximizes the objective function is obtained for $P_{fa} = \beta_n'$, where β_n' should be chosen for each number of collaborating nodes n $\in$ {1..N} so that $P_{fa} \leq \beta$. The first constraint function limits the interference caused to the primary users by controlling the detection probability. Thus, similarly to the EGC case, the minimal sensing time and the number of cooperating nodes that satisfy the first constraint function maximizes the objective function (see the proof in Appendix A.2, same as in the EGC case).

4.2.3.3 Results

This subsection gives a performance evaluation based on the analytical approach elaborated before. The number of cooperative nodes and the optimal sensing time are determined using an exhaustive search algorithm according to the parameters shown in Table 4-3.

Table 4-3: Parameters for the performance evaluations

Frame duration	T	2s
Number of collaborating nodes	N	1,…,10
Sensing time	τ_i	{0.01,…,1} s
Number of channels	K	6
Bandwidth per channel	B	6 MHz
Sampling frequency	f_s	2000 Hz
Average level of channel SNR	γ	2dB
Probability for primary user absence	P_{H0}	0.5
Control channel overhead duration	τ_c	0.01s
Control channel bit rate	R_c	100Kbps
Bits per sensing report, EGC	b_{EGC}	4byte=32 bits
Bits per sensing report, MV	b_{MV}	1 byte=8 bits
Detection probability constraint	α'	0.99
False alarm probability constraint	β	0.01
False alarm probability constraints MV	β_n'	{0.01,0.005,0.06,0.04,0.105,0.085,0.143, 0.12,0.17,0.15}, for n = 1, 2, 3, 4, 5, 6, 7, 8, 9, 10

Fig. 4-10 depicts the optimal pairs (number of cooperating nodes, sensing time) for which the required constraints in eq. (4-17) and eq. (4-20) are satisfied. Fig. 4-11 depicts the achieved throughput for the optimal pairs as a function of the sensing time.

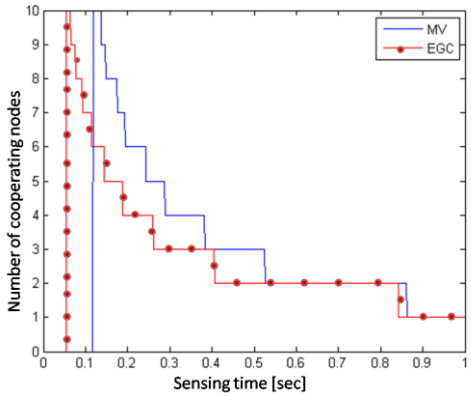

Fig. 4-10: Optimal pairs (number of cooperative nodes, sensing time)

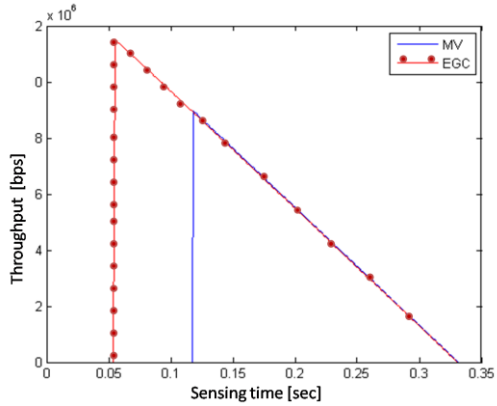

Fig. 4-11: Throughput vs. sensing time

It is evident that minimal sensing time for both techniques (EGC and MV) is achieved for the maximal available number of cooperating nodes, Fig. 4-10. This suggests that if a higher number of cooperating nodes is used, then the sensing duration per channel will reduce more. Also, the EGC fusion technique meets the imposed constraints with lower amount of resources than MV, Fig. 4-10, and outperforms MV for lower sensing time

duration, Fig. 4-11. Longer sensing durations yield comparable results for both fusion techniques, Fig. 4-11.

Fig. 4-10 and 4-11 demonstrate that maximal throughput is achieved with certain small sensing time in combination with the highest number of cooperative nodes (i.e. 10 in this case). However, the sensing time is determined by the device capabilities reflected through the sampling rate. Fig. 4-12 depicts the optimal sensing time (that maximizes the throughput with 10 cooperative nodes) for both EGC and MV fusion techniques as a function of the sampling rate. Fig. 4-13 gives the maximal achievable throughput for any sampling rate for both EGC and MV. It is obvious that as the sampling rate increases, the optimal sensing time (for 10 cooperative nodes) that satisfies the constraints decreases, Fig. 4-12. This results in higher maximal throughput for higher sampling rates, Fig. 4-13. Also, faster sampling devices yield higher throughput performances, Fig. 4-13. Finally, EGC achieves higher maximal throughput than MV for a same sampling frequency, Fig. 4-13.

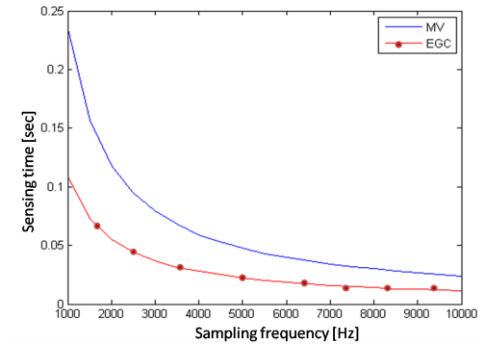

Fig. 4-12: Sensing time vs. sampling rate

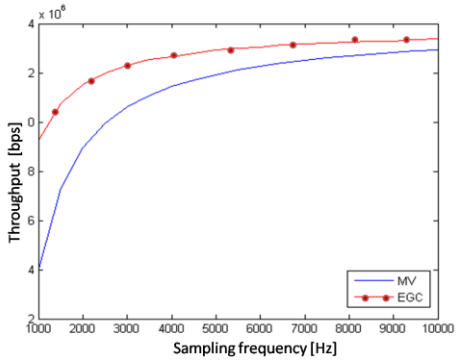

Fig. 4-13: Maximal achievable throughput vs. sampling frequency

Finally, Fig. 4-14, 4-15 and 4-16 depict the SNR influence on both EGC and MV techniques in the CMSS model. Fig. 4-14 represents the minimal number of cooperating nodes that satisfy the target constraints under different SNR values. Fig. 4-15 depicts the minimal required sensing time duration that meets the constraints under different SNR values. Fig. 4-16 shows the calculated throughput for the number of cooperating nodes and sensing time at Fig. 4-13 and Fig. 4-14, respectively. It is clear that, for lower SNR values, the EGC outperforms MV, whereas for higher SNR values, EGC and MV achieve similar throughput performances.

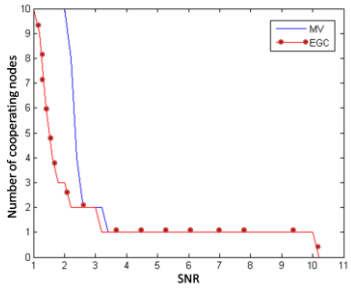

Fig. 4-14: SNR vs. number of collaborating nodes

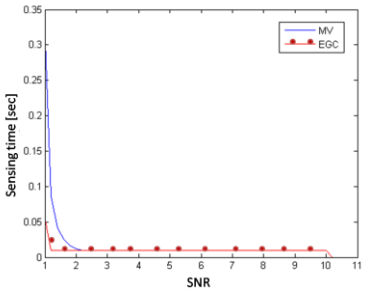

Fig. 4-15: SNR vs. sensing time

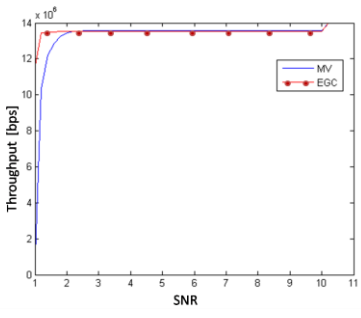

Fig. 4-16: SNR vs. throughput

The CMSS scheme proves that cooperation with under-sampling can lead to higher throughput in secondary networks as compared to the single sensing case.

4.2.4 **Cooperative Multi-band Sensing with Reporting MAC Considered**

Cooperative spectrum sensing generally consists of two stages: sensing and reporting, where sensors measure channels at the sensing stage and then uses a multiple access protocol to report their local measurement results. Both operations are time critical and required for efficient spectrum opportunity exploitation by the secondary system. However, almost all the cooperative sensing strategies have ignored the reporting process or greatly simplified it by assuming a perfect time-slotted multiple access ([50], [51], [52], [53]). In this work, we examine the impact of reporting MAC protocols on centralized cooperative spectrum sensing in multiband cognitive networks. Specifically, we study the applicability of TDMA and IEEE 802.11 CSMS/CA protocols for cooperative spectrum sensing reporting. The results show that the reporting overhead caused by multiple access is non-negligible, especially for the contention based MAC protocols. Moreover, we find out that, since each cooperating sensor has only one data packet to send, the main role of the reporting MAC is different from traditional wireless MAC protocols which are employed to regulate and balance network resources among nodes. The fairness issue no longer plays a role. The dominant measure for the reporting MAC protocol is how fast the local observations can be reliably transmitted to the fusion center. We then propose a Fast Cooperative Spectrum Sensing strategy (FCSS) by exploiting concurrent occurrence of the spectrum sensing activities and the reporting process with an improved IEEE 802.11 MAC protocol. The proposed reporting MAC is a simple modification to the IEEE 802, and can significantly reduce the complexity of contention resolution algorithm and shorten the reporting duration.

In addition, our work has also considered two sensor assignment strategies over multiple channels: static assignment and random selection. A general mathematical model has been developed to quantify the achievable bandwidth utilization within a secondary systems, which takes into account different combinations of sensor assignment strategies, reporting MAC protocols, fusion rules and regulatory constraint. The model can be used to optimize the network parameters including number of sensors and sensor assignment settings to shorten the total sensing and reporting time, and hence maximize the secondary spectrum efficiency under regulatory constraints.

4.2.4.1 System model and problem formulation

We consider a multiband cognitive network consisting of M licensed channels indexed from 1 to M and one common control channel (CCC) dedicated to the fusion process of multiple secondary users. Let N denote the number of cooperative secondary sensors distributed over M channels and each sensor has a single half-duplex transceiver. In centralized cooperation, a quiet period T_q is usually defined and consists of two phases: sensing and reporting. The sensors measure one or a number of channels during the sensing phase T_s and report their observations to a fusion center through CCC in the reporting phase T_r.

From the secondary system's perspective, a long quiet period could result in significant inefficiency in licensed bandwidth utilization especially when there are a large number of licensed channels, since all the M channels cannot be utilized by secondaries during T_q. Considering a periodic sensing strategy where the sensing operation is performed every T period of time, the achievable normalized throughput of the secondary system can be expressed as:

$$\eta = \frac{T - T_q}{T} \frac{1}{M} \sum_{i=1}^{M} P_i(H_0)(1 - P_{fi}) \tag{4-21}$$

where $P_i(H_0)$ is the probability that the i^{th} channel is free from primary transmissions, and P_{fi} is the false alarm probability of the i^{th} channel. It should be noted that eq. (4-21) is a simplified expression of the achievable secondary throughput. In practice, the secondary users also transmit when a missed detection takes place. In our model, we suppose that eq. (4-21) dominates the achievable throughput and ignore the other

aspect, since numerous spectrum measurement campaigns have shown that the primary activity probability $P_i(H_1)$ is very small in reality (less than 0.3), which is also a key factor in making the exploration of secondary usage economically feasible.

We start from a base scenario and assume that $P(H_0)$ of each channel is identical for the sake of simplicity. Mathematically, the problem can be formulated as an optimization problem as follows:

$$\max \frac{T-T_q}{T}(1-\frac{1}{M}\sum_{i=1}^{M}P_{fi}) \tag{4-22}$$

$$\text{subject to} \min_{0\le i\le M} P_{di} \ge P_d^* \tag{4-23}$$

$$\text{or subject to} \frac{1}{M}\sum_{i=1}^{M}P_{di} \ge P_d^* \tag{4-24}$$

where P_{di} is the detection probability of the i^{th} channel and P_d^* is the target detection probability with which the primary system is defined as being sufficiently protected. We have considered two types of protection constraints for a multiband primary system as indicated by eq. (4-23) and (4-24) where the protection constraints of multiple channels are defined from single and average points of view, respectively. These two constraints can be considered either jointly or separately. Note that P_d^* in eq. (4-23) and (4-24) can be different. By observing eq. (4-22)-(4-24), our target is transformed to derive the quantities of P_χ and T_q , where P_χ stands for the average detection (` $\chi$ ' is `D ') or false alarm (` $\chi$ ' is `F') probabilities over M channels.

We apply this optimization model in the following two subsections to analyze the impact of reporting MAC on cooperative spectrum sensing and our proposed FCSS scheme.

4.2.4.2 The Impact of Reporting MAC on Cooperative Sensing

We consider that the spectrum sensing and reporting are performed in a time division manner. The reporting phase is started only when all the sensors finish their channel measurements, i.e. $T_q=T_s+T_r$.

A. Sensing phase

In T_s, each sensor has to determine which channels should be sensed among the M channels. We consider two sensor assignment schemes as follows.

A.1 Static assignment

In this scheme, N sensors are evenly distributed on M channels. Each sensor is assigned a fixed number of channels m and senses these channels in a sequential order. The number of sensors allocated per channel is kept the same and the number of measurements per channel is then given by Nm/M , on average. The detection performance of each channel is identical and we have:

$$P_\chi = \frac{1}{M}\sum_{i=1}^{M}P_{\kappa i}(\frac{Nm}{M}) = P_\kappa(\frac{Nm}{M}) \tag{4-25}$$

where P_κ stands for the detection (κ is d) and false alarm (κ is f) probabilities.

The sensing duration T_s is given by:

$$T_s = \min(m, M)(\tau_s + t_{sw}) \tag{4-26}$$

where t_{sw} is the channel switching time, and τ_s is the amount of time employed for the primary signal collection on one channel by each sensor. We assume τ_s of each sensor is identical and is a fixed value.

A.2 Random selection

In this scheme, each sensor can randomly select *m* number of channels to perform sensing. However, it should be noted that, with random selection, there exists the possibility that the number of sensors on some channel is zero, which makes this channel inaccessible to the secondary users. To avoid this possibility, we assume that *N* sensors are initially evenly distributed on *M* channels to conduct channel measurements according to the static assignment rule. Each sensor sequentially measures m_{sa} number of channels to ensure that each channel is measured at least once. Afterwards, all the sensors perform random selection. As a result, the average number of measurements $\mathbf{n}=\{n_1,n_2,\cdots,n_M\}$ over *M* channels meets the condition:

$$m_s=\sum_M n_i=N(m_{sr}+m_{sa}),\forall n_i\in[\frac{Nm_{sa}}{M},N] \tag{4-27}$$

The channel selection problem can be thought of as distributing m_s nodes into *M* channels with equal probability *1/M*. Thus, without considering the condition defined by eq.(4-27), the probability that channels $1,2,\cdots,M$ get $n_1,n_2,\cdots,n_M$ number of measurements, respectively, is given by a multinomial distribution:

$$\frac{m_s!}{(n_1!n_2!\cdots n_M!)}(\frac{1}{M})^{m_s} \tag{4-28}$$

This probability should be normalized over the space defined by eq. (4-27) to ensure a valid probability distribution between [0,1]. Hence, the probability that channels $1,2,\cdots,M$ get $n_1,n_2,\cdots,n_M$ number of measurements, respectively, is given by:

$$f(\mathbf{n})=\frac{\frac{m_s!}{(n_1!n_2!\cdots n_M!)}(\frac{1}{M})^{m_s}}{\sum_{\mathbf{n}}\frac{m_s!}{(n_1!n_2!\cdots n_M!)}(\frac{1}{M})^{m_s}}=\frac{\frac{1}{(n_1!n_2!\cdots n_M!)}}{\sum_{\mathbf{n}}\frac{1}{(n_1!n_2!\cdots n_M!)}} \tag{4-29}$$

where the denominator is the sum of all combinations of **n** satisfying eq. (4-27).

The average of detection performance over *M* channels is given by:

$$P_\chi=\frac{1}{M}\sum_{\mathbf{n}}\left(f(\mathbf{n})\sum_{i=1}^{M}P_{\kappa i}(n_i)\right) \tag{4-30}$$

The sensing duration T_s is given by:

$$T_s=\min(m_{sr}+m_{sa},M)(\tau_s+t_{sw}) \tag{4-31}$$

B. Reporting phase

The length of reporting phase T_r mainly depends on two aspects: the amount of data sent by sensors and the transmission strategies of the local observations. We consider TDMA and CSMA/CA multiple access mechanisms. For the latter, we study IEEE 802.11 DCF due to its wide deployment. The details on deriving T_r for each multiple access scheme are as follows.

B.1 TDMA

TDMA is a static multiple access scheme for which each slot is designated to one sensor, and hence provides a clear guarantee on the completion time of data collection as follows:

$$T_r=Nt_{data} \tag{4-32}$$

where t_{data} is one time slot taken to transmit the data from one sensor to the center.

B.2 CSMA/CA

In this case, as long as a sensor has a packet to send, it waits until the channel is sensed idle for a DIFS period denoted by t_{difs}. Then, all nodes contend to access the channel through random backoff. Once the fusion center receives a data from one sensor, it responds with an acknowledge. If no acknowledge is received by the sensor within the expected time, the data is assumed to be corrupted during the packet collisions and will be retransmitted. Each collision causes the contention window size to be exponentially increased. The reporting period T_r is highly dependent on the number of collisions. For two operation modes of CSMA/CA, T_r is given as follows.

$$\textbf{Two Way :} \quad T_r = (N + \aleph_c)(t_{difs} + t_{data} + t_{ack} + t_{sifs}) + t_{bo} \tag{4-33}$$

$$\textbf{Four Way :} \quad T_r = N(t_{difs} + t_{rts} + t_{cts} + t_{data} + t_{ack} + 2t_{sifs}) + \aleph_c(t_{difs} + t_{rts} + t_{cts} + t_{sifs}) + t_{bo} \tag{4-34}$$

where $\aleph_c$ is the total number of collisions with which the packets need to be retransmitted, and t_{bo} is the time spent on backoff counting by all the sensors. The parameter t_{bo} is equal to the total backoff time experienced by the last reporting node, since the backoff processes of all the nodes take place concurrently.

To derive $\aleph_c$ and t_{bo}, we begin by estimating the collision probability and contention window evolution experienced by sensors. We adopt a simplified approach to estimate all the backoff activities and collisions seen by the last node. We use the average value for a variable wherever possible. Let *W* stand for the initial contention window of each node. The backoff window of each node is then uniformly distributed over *[1,W]* with the average value of *W/2*; for simplicity, we use *W/2* instead of *(W+1)/2*. If a node fails to send its data, its contention window size is doubled. This doubling continues in the case of each collision until the contention window reaches its maximum limit W_{max}. As a result, the contention window before the i^{th} collision is $W_i^c = \min(2^{i-1}W, W_{\max})$. From average point of view, the probability that a node attempts to transmit in an arbitrary slot before the i^{th} collision is determined by its average backoff window $W_i^c/2$ and given by $2/W_i^c$. If one node begins transmission, the probability that other nodes do not transmit in the same slot is $(1-2/W_i^c)^{n_i-1}$, where n_i denotes the average number of contending nodes during the i^{th} collision. The collision probability p_i is given by:

$$p_i = 1-(1-2/W_i^c)^{n_i-1}, i \geq 1 \tag{4-35}$$

During the i^{th} collision, $n_i(1-p_i)$ number of nodes transmit successfully and quit from the reporting stage. The rest $n_i p_i$ number of nodes suffer from the collision and continue accessing the shared channel with a larger contention window. Therefore, the number of contending nodes in the *(i+1)*th contention becomes $n_{i+1} = n_i p_i$. n_i is given by:

$$n_i = \begin{cases} N & \text{if } i = 1 \\ n_{i-1}p_{i-1} & \text{if } i > 1 \end{cases} \tag{4-36}$$

The quantity n_i can then be easily solved based on the two equations above. As the number of collisions *i* increases, the number of contending nodes n_i during each collision decreases and can eventually reach a positive value n_{i_L} no more than one after certain number of collisions i_L. This node can be thought of as the last reporting node. It experiences the $(i_L-1)^{th}$ and $i_L{}^{th}$ collisions with the probabilities $1-n_{i_L}$ and

n_{i_L} respectively. The total average backoff window of the last reporting node is then approximated by:

$$W_{bo} = n_{i_L} \sum_{i=1}^{i_L} \frac{W_i^c}{2} + (1 - n_{i_L}) \sum_{i=1}^{i_L - 1} \frac{W_i^c}{2} \tag{4-37}$$

Hence, t_{bo} can be solved by $t_{bo} = W_{bo} t_{slot}$

In general, a collision is attributed to more than one node having the same backoff window. We compute the probability that k nodes among n_i nodes select the same window slot as:

$$P_{col}(k) = \binom{n_i}{k} \left(\frac{1}{W_i^c}\right)^k \left(1 - \frac{1}{W_i^c}\right)^{n_i - k} \tag{4-38}$$

where n_i is assumed to be an integer. The collision probability due to k nodes among n_i nodes is then given by:

$$\Pr(k) = \frac{P_{col}(k)}{1 - P_{col}(0) - P_{col}(1)}, \quad k \geq 2 \tag{4-39}$$

where the denominator is a normalization term. Therefore, the total number of collisions $\aleph_c$ is given by:

$$\aleph_c = \sum_{i=1}^{i, n_i > 1} \aleph_c(i) = \sum_{i=1}^{i, n_i > 1} \sum_{k=2}^{n_{i+1}} n_{i+1} \Pr(k), \tag{4-40}$$

where $\aleph_c(i)$ denotes the average number of collisions at the i^{th} average collision.

4.2.4.3 Fast Cooperative Spectrum Sensing (FCSS)

In this section, we propose a cooperative strategy for multiband cognitive networks, which we call Fast Cooperative Spectrum Sensing (FCSS), by exploiting concurrent occurrence of the sensing process and an improved MAC protocol to reduce the total sensing and reporting time. In the scheme, the sensing phase overlaps with the reporting phase as shown in Fig. 4-17, where all the sensors firstly perform sensing during T_{sa} and then enter the reporting phase T_r during which part of the sensors continue to conduct the channel measurement. Note that the sensing phase T_S ends earlier than T_r because all the sensors become inactive during the transmission of the last reporting node. The overlapped duration is denoted by the symbol T_{sr}.

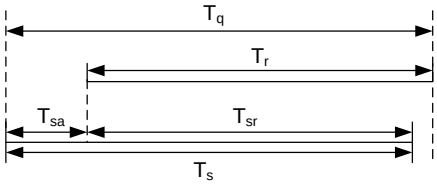

Fig. 4-17: A quiet period with overlapped sensing and reporting phases

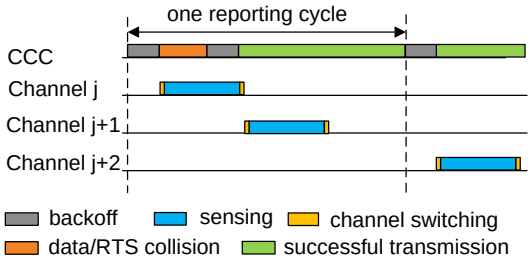

Fig. 4-18: An illustration of implementation details during T_{sr}.

On the other hand, we consider contention based MAC protocols for the reporting process. The traditional wireless CSMA/CA MAC protocols were originally designed to

serve data networks with long haul traffic where each node has a queue of data to transmit. They use complex contention resolution mechanisms (e.g., exponential backoff) to avoid bandwidth loss due to transmission collisions and hence regulate the network resources among nodes to meet the throughput and fairness requirement. Such mechanisms usually incur high contention overhead. Different from the long-haul traffic network, each node in the data fusion process has to transmit only one data packet through a multiple access process. It does not matter whether one packet arrives earlier than the others or consumes more bandwidth. The fairness is no longer a desirable quality to be sought. Thus, a node experiencing collisions does not mean that it has to back off with a larger contention window and spare resources to maintain a fair usage. On the contrary, more attention should be paid to transmitting local measurements as fast as possible. We propose an enhancement to IEEE 802.11 DCF MAC protocol in which the contending nodes reduce or keep their contention window instead of doing costly exponential backoff in the case of collisions.

Similar to the non-overlapping scheme, we are interested in estimating of P_χ and T_q, where $T_q=T_{sa}+T_r$ and the value of P_χ depends on the number of measurements n_i executed on each channel during T_s. We analyze T_s and T_r as follows.

A. Reporting phase T_r

Since the value of T_s is significantly dependent on the length of T_r, we first derive T_r. Fig. 4-18 presents the implementation details for the overlapped duration $T_{sr.}$ The reporting phase can be modeled as a cyclic process where one cycle is defined as the interval between the start of a new packet transmission attempt and the start of the next packet transmission attempt. During each cycle, when the CCC is sensed idle, all the sensors compete to report their data through the backoff mechanism. Once a transmission (including collision) begins, the others proceed to implement the measurement tasks. after completing the measurement of one channel, each sensor switches to the CCC again to check its availability instead of continuing to sense more number of channels. If the CCC is still detected busy, the sensor will jump to measure another licensed channel. This process is repeated until the CCC is found idle. The operation of switching to the CCC after every channel measurement comes at the cost of increased channel switching time, but in return for much lower computation complexity and broader generality for more situations. Those who have completed reporting the data stop their sensing activities.

In the case of a collision, the colliding sensors reduce their contention windows and compete for the CCC through a second backoff contention. Those nodes who fail in the second contention restore their contention window size and proceed to measure the primary channels. Here, the colliding sensors do not double their contention windows in the case of collisions. This is because most of the sensors are remaining on measuring the primary channels. The number of colliding nodes on the CCC is fairly small, which indicates a rather low probability of collisions on the second contention with a certain contention window. We derive the number of colliding nodes in one collision and provide the proof as follows.

Assume that k nodes are contending to make reports at the beginning of one reporting cycle. Given the contention window W, the probability that i contending nodes select the same backoff window follows a binomial distribution and is given by $\binom{k}{i}\left(\frac{1}{W}\right)^i\left(1-\frac{1}{W}\right)^{k-i}$.

This is is a monotonically decreasing function of i for $i>0$ and a monotonically increasing function of k. In the case of $W_1=32$ and $k=30$, the probability that there are 4 contending nodes in one arbitrary slot is as low as 0.01%, which indicates that the number of colliding nodes in one collision is hardly greater than 4. For such a small number of nodes in the second contention, a relatively small value of W_c can be selected so that collisions hardly occur. We select $W_c=16$ in our study.

The reporting duration T_r can be expressed as:

$$T_r = \sum_{k=1}^{N} T_{rk} + t_{bo} \tag{4-41}$$

where T_{rk} is the duration of the k^{th} reporting cycle without taking into account the backoff time in the first contention. T_{rk} is given by:

$$T_{rk} = \begin{cases} t_{difs} + p_k t_{col} + t_{dk} & k < N \\ t_{difs} + t_{dk} & k = N \end{cases} \tag{4-42}$$

where p_k denotes the collision probability and is given by p_k=1-(1-1/W)$^{N-k}$, t_{col} and t_{dk} are the durations for one collision and one successful data transmission, respectively. For the two-way and four-way handshaking mechanisms, they are given by:

$$\text{Two Way}: \quad \begin{aligned} t_{col} &= \frac{W_c}{2} t_{slot} + t_{difs} + t_{data} + t_{ack} + t_{sifs} \\ t_{dk} &= t_{data} + t_{ack} + t_{sifs} \end{aligned} \tag{4-43}$$

$$\text{Four Way}: \quad \begin{aligned} t_{col} &= \frac{W_c}{2} t_{slot} + t_{difs} + t_{rts} + t_{cts} + t_{sifs} \\ t_{dk} &= t_{rts} + t_{cts} + t_{data} + t_{ack} + 2t_{sifs} \end{aligned} \tag{4-44}$$

Note that t_{data} of each reporting cycle may vary since each sensor could measure a different number of channels. The time t_{bo} can be derived using the same approach in Section 4.2.4.2.

B. Sensing phase T_s

As illustrated in Fig. 4-21, T_s is comprised of two parts: T_{sa} and T_{sr}. During T_{sr}, without tuning into the CCC to listen to each other's transmission, one has no means to know which sensors have made reports and which channels the others have measured. This makes an equal assignment of measurements over all the channels infeasible. Hence, we employ the random channel selection algorithm. All the sensors measure the channels according to the static assignment rule during T_{sa}, and then performs random selection during T_{sr}. Therefore, the detection performance P_χ has the same formula expressions as (4-29) and (4-30). The sensing duration T_{sa} is given by:

$$T_{sa} = m_{sa}\tau_s + m_{sa}t_{sw} \tag{4-45}$$

4.2.4.4 Numerical results

This section presents a performance evaluation based on the analytical approach elaborated above. We have studied a variety of network setups with the number of channels M ranging from 1 to 10. We only present the case of M=6 due to the same results observed.

A. Parameter Settings

For the sake of simplicity, we only consider the energy detection and an equal weight data fusion rule in the numerical evaluation. However, this does not exclude our model from being used for other detection and data fusion techniques. For the measurement of the ith channel by n_i number of sensors, we use the test statistic:

$$T(y) = \frac{1}{n_i \tau_s f_s} \sum_{k=1}^{n_i} \sum_{j=1}^{\tau_s f_s} |y(j)|^2 \tag{4-46}$$

where f_s is the sampling rate and $\tau_s \cdot f_s$ is the number of samples. For a high number of samples, according to central limit theorem, *T(y)* can be approximated by Gaussian distributions. The detection and false alarm probabilities of n_i cooperating sensors are obtained as follows:

$$P_f(n_i) = Q\left((\frac{\varepsilon}{\sigma_u^2} - 1)\sqrt{\frac{n_i \tau_s f_s}{2}} \right) \quad (4\text{-}47)$$

$$P_d(n_i) = Q\left((\frac{\varepsilon}{(\gamma+1)\sigma_u^2} - 1)\sqrt{\frac{n_i \tau_s f_s}{2}} \right) \quad (4\text{-}48)$$

where *Q(.)* is the complementary distribution function of a standard Gaussian variable and is given by $\frac{1}{\sqrt{2\pi}}\int_x^\infty e^{-\frac{t^2}{2}} dt$, σ_u^2 is the variance of *u*; γ denotes the received SNR of the primary signal measured at the secondary receiver under the hypothesis H_1; ε is the detection threshold.

In our study, the sensing sampling rate is assumed to be f_s=*6*MH$_z$. We set the target values of P_d *(1)=0.9* and P_f*(1)=0.1* with $\gamma = -20dB$, and derive a fixed value of ε / σ_u^2 which is further used in eq. (4-47) and (4-48) to compute the relationship between P_d *(1),* P_f *(1)* and τ_s. We adopt IEEE 802.11a (6Mbps) and 802.11b DSSS (1Mbps) as the CSMA/CA reporting MAC protocols. The reported data size of one sensor is 128 bytes. We use 80μs of channel switching time.

B. Results

Fig. 4-19 depicts a comparison of throughput performance between three MAC protocols. IEEE 802.11a with 6Mbps is used for the reporting process. The single detection capability is set to P_d*(1)=0.8*. Correspondingly, the channel measurement time τ_s approximates 1 ms. Each sensor measures *m=6* channels. It can be seen that there exists an optimal number of sensors with which the secondary bandwidth utilization can be maximized under the imposed constraint of the average detection probability. It is observed that, given a regulatory requirement of 95% detection probability, around 7% and 13~15% of the potential capacity is lost for TDMA and CSMA/CA respectively due to the sensing and reporting overhead. Of this overhead, 58% (TDMA) and 77~80% (CSMA/CA) are attributed to control signalling and the rest to sensing. One can increase the CCC transmission rate or the sensing period to minimize the overhead. However, the former is not always feasible. A long sensing period may increase the danger of missed detection of primary system activities. Therefore, it is necessary to use an efficient reporting MAC in cooperative sensing.

Fig. 4-20 explores the relationship between the achievable bandwidth utilization and the single detection capability. It can be seen that a high single detection probability does not always lead to optimal throughput capacity. A high single detection capability comes at the cost of long measure time which decreases the bandwidth for secondary transmission. For example, in the figure, given a target average detection probability of 0.95, the achievable bandwidth for P_d*(1)=0.9* is maximized when *N=3*. However, a better utilization can be reached just through simply adjusting the number of sensors to *N=5* with a reduced P_d(1)=0.8. In general, the adjustment of the number of sensors is much preferable in many deployment scenarios, since the good detection precision of a single sensor is sometimes hard to achieve due to the harsh radio transmission environment even though the hardware capability is there.

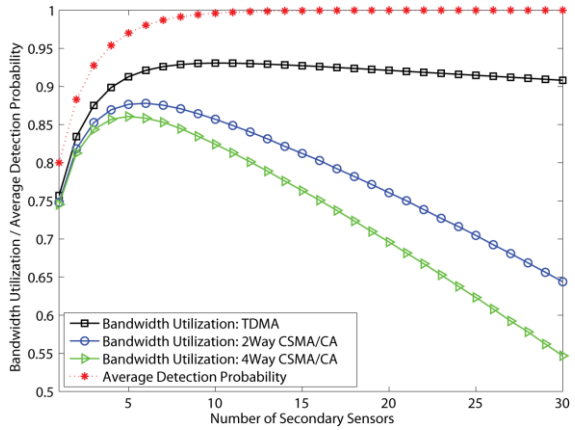

Fig. 4-19: A comparison between three MAC protocols, static assignment, *802.11a, m=6, $P_d(1)=0.8$, T=200ms*

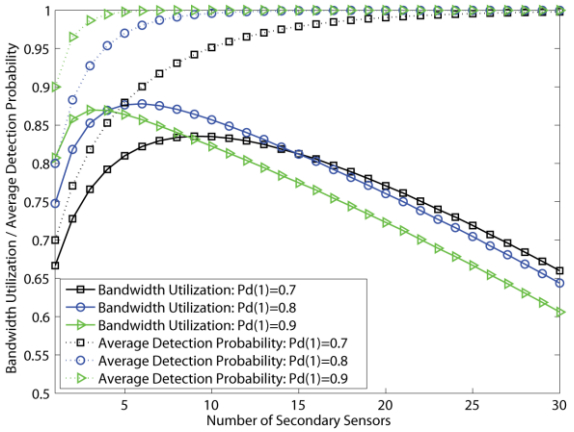

Fig. 4-20: A study on the impact of single detection capability, static assignment, *802.11a,* two-way access, *T=200ms*

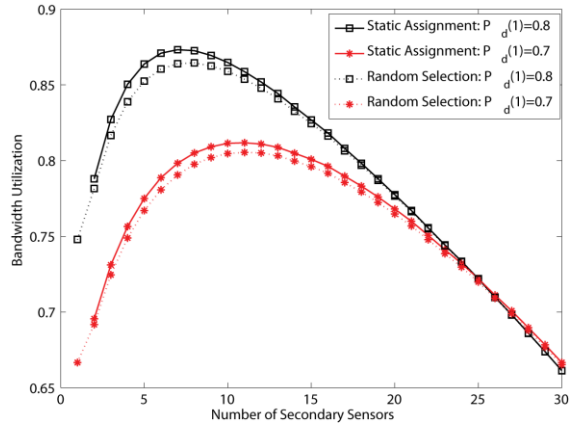

Fig. 4-21: A comparison between two sensor assignment schemes, two-way access, $m = m_{sr} + m_{sa} = 4$, *T=200ms*

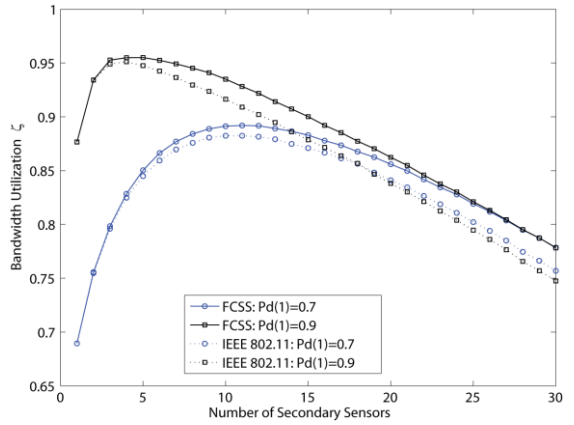

Fig. 4-22: A comparison between IEEE 802.11b and FCSS scheme, two-way access, $m = m_{sr} + m_{sa} = 6$, *T=1s*

Fig. 4-21 depicts the comparison between the static assignment and random selection sensing distribution schemes. The static assignment slightly outperforms the random selection. This is because the random selection scheme causes an uneven distribution of number of measurements over channels, which could result in a shortage of sensors on some channels. On the other hand, many sensors on one channel could contain significant spatial redundancy and have a very limited contribution to the spectrum detection performance.

Fig. 4-22 depicts that our proposed FCSS scheme has better throughput performance than the IEEE 802.11, especially as the number of cooperating sensors increases. This is explained by the fact that larger number of sensors result in more collisions which prolong the contention time. The FCSS scheme is designed to alleviate the contention overhead through avoiding the exponential backoff of contention window as in 802.11. Note that we consider an error-free control channel in the study. If an error-prone channel is considered, the exponential backoff in IEEE 802.11 scheme will frequently occur and result in significant contention overhead. Thus FCSS will exhibit much superior performance.

4.3 **Concluding remarks**

Spectrum sensing represents an essential part of cognitive radio systems and it is tightly related to the process of dynamic spectrum access. One of its major weaknesses is its inability to obtain the required reliability for practical deployments. The nature of the spectrum sensing implies that it is almost impossible to estimate the actual aggregate interference in an arbitrary point of interest making its usability limited to mostly being a complementary approach to database spectrum opportunity detection. The cooperative multi-band spectrum sensing signifies a viable solution for increased efficiency of the spectrum sensing process. However, the drawbacks of the approach lie in the increased sensing time (lower opportunistic throughput) and the higher energy consumption for sensing the multiple bands, which must be carefully scrutinized when applying the cooperative multi-band sensing schemes in practice.

This section has introduced and analysed several cooperative multi-band spectrum sensing solutions focusing on specific problems associated with cooperative multi-band spectrum sensing such as sensing time, signaling overhead, number of cooperative users etc. Their mutual cross-analysis is not possible as they target and deal with different aspects of the cooperative multi-band sensing problem, varying from the proportion of sensing vs. control signaling in the secondary network, to the influence of the secondary multiple access method on secondary spectrum efficiency.

The DMSS framework studies the interdependencies among the primary and secondary service outage probabilities (i.e. the outage when the number of available bands detected is not sufficient to serve all secondary calls), the number of the sensed bands and the number of secondary nodes. The results show that lower outage probability yields higher number of cooperating nodes and that the number of cooperating nodes increases much quicker than the number of bands subject to sensing. The energy efficient multiband spectrum sensing model focuses on the minimization of the total spent power, while maximizing the secondary network throughput. It defines a cost function between the energy consumption and the achievable secondary network throughput and concludes that the number of cooperating nodes is highly dependent on the fading effects, i.e., severe fading requires many cooperating nodes for sufficient sensing performance, which may seriously affect the energy consumption in the entire system. The CMSS investigates the optimal sensing duration and optimal number of collaborating nodes that satisfy a pre-required spectrum sensing reliability (in terms of detection probability) in order to maximize the opportunistic throughput in the secondary cognitive network. The analysis shows that for a detection probability of 99% and EGC fusion rule, when increasing the number of cooperating nodes from 3 to 10 (i.e. increasing the signaling overhead from 17% to 38%) the CMSS achieves more than an order of magnitude higher throughput. The FCSS model further introduces a MAC protocol to analyse a similar problem. The results show that the signaling overhead may go up to 7% for a 95% of detection probability, and that the proposed model always outperforms the single sensing node strategy in terms of the achieved throughput.

From the results presented in this section it is evident that cooperative multi-band sensing can increase the system efficiency (in terms of the opportunistic throughput, the energy consumption, etc.) compared to the single-node single-band sensing case with certain trade-offs, like the increased signaling overhead and increased number of sensing nodes.

5 Strategies for Cooperative Spectrum Sharing among Secondary Systems

5.1 Introduction

The spectrum sharing process refers to the techniques how one or multiple secondary users access and coexist in vacant spectrum holes. Reliable spectrum availability discovery methods and efficient sharing strategies enable coexistence of secondary devices in the vacant spectrum and, in the same time, foster efficient and increased spectrum utilization. Different spectrum sharing strategies can be classified according to different criteria such as the *secondary network architecture*, the *spectrum allocation approach*, the *secondary spectrum access method*, the *method used for spectrum availability retrieval* and other secondary scenario specific parameters [54].

Efficient and reliable spectrum sharing schemes yield accurate and reliable spectrum opportunity detection and its subsequent usage without violating primary users' protection criteria. The primary users' interference tolerance is a cornerstone aspect of every secondary spectrum sharing problem. The previous section in this deliverable targeted upgrades of a single-node sensing based spectrum opportunity detection in order to increase the reliability of the overall detection process towards more efficient spectrum sharing. The major drawback of the sensing based approach is its inability to cope with aggregate interference making its usability limited mostly to dynamic environments where there are rapid changes in the spectrum usage by different systems or for populating centralized databases. Therefore, databases become a preferred approach for practical deployments of secondary spectrum access, especially in static and life-critical scenarios such as TV white space and radar bands, fostering reliable and efficient spectrum sharing among multiple secondary systems. Databases also enable licence holders, regulatory bodies and operators to have more transparent and effective access to the underutilized spectrum. They foster efficient and reliable interference management and primary users' protection.

The focal point of this section is to explore the possibilities to deploy spectrum sharing among multiple secondary systems. The spectrum sharing strategies can be broadly categorized as *cooperative* or *non-cooperative* ones. Deliverable D4.1 defined that *a secondary system is "cooperative" if it restrains from exploiting available spectrum resources though it requires them for its current communication in order to allow other secondary systems to use them* [1]*.* This deliverable exploits the possibilities for creating and evaluating *cooperative sharing strategies*.

Cooperative sharing can refer to two different general approaches, i.e.

- ***sharing with cooperative relays*** [55] [56] and
- ***cooperation among secondary (or secondary - primary) entities in order to achieve increased sharing performances***.

The former approaches assume that relay nodes with sufficient available spectrum bands act as a bridge for communication between a source and a destination secondary node. The latter approaches assume that nodes exchange data on interference measurements or other relevant parameters, which is then used in the sharing process. In any case, the cooperation in secondary spectrum sharing scenarios yields improved system performances in terms of higher resources utilization, but also causes excessive signalling information in the network [54].

This section targets spectrum sharing strategies that use database based spectrum opportunity detection and exploit the effectiveness of the possible cooperation among the secondary systems. The cooperation among the secondary systems fosters more efficient resources utilization and in the same time reliable primary users' protection. The

scenarios are chosen to accommodate the QUASAR's general objectives and provide valuable insight for possible subsequent practical investigation.

5.2 **Sharing strategies**

Implementing cooperative sharing schemes can result in high computational complexity and excessive signalization among the cooperative entities. Performance evaluation on different parameters is needed to justify their usage in secondary spectrum access scenarios.

The cooperative spectrum sharing strategies of interest in this deliverable are:

- Network Coordinated Beamforming with user Clustering (NCBC)
- Joint power and channel allocation in a spectrum sharing scenario for WiFi-like secondary users in TV white spaces

The first one is based on a novel cooperative technique for spectrum sharing between multiple secondary CR systems. It uses Network MIMO and utilizes a combination of Network Coordinated Beamforming (NCBF) and User Clustering (UC). The second strategy proposes a suboptimal algorithm combining power and channel allocation using the Nash Bargaining Solution (NBS) cooperative game theoretic approach, while still achieving fair spectrum utilization. Both schemes aim at maximizing the number of secondary entities that can successfully coexist and efficiently share the available spectrum.

The cooperative sharing strategies in this section are envisioned as database based meaning that the secondary entities retrieve information on spectrum availability from a predefined database. The following subsections provide detailed description and performance evaluation of both of them.

5.2.1 **Network coordinated beamforming with user clustering for cooperative spectrum sharing of multiple secondary systems**

The spectrum sharing concept is very similar to the multiple access techniques in multichannel wireless networks and can be derived from conventional protocols [34]. Cooperation between the secondary CR systems can additionally increase the spectrum sharing efficiency. One possible approach that is based on cooperation and can provide high spectrum utilization is Network MIMO. MIMO systems have great potential to enhance the capacity of wireless networks [57], [58]. The spatial degrees of freedom offered by multiple antennas in multiuser MIMO networks can be exploited by scheduling multiple users to simultaneously share the same communication channel. This entails a novel and fundamental approach in multiuser communications [59].

Several practical multiuser MIMO transmission strategies have been proposed that offer different tradeoffs between performance (spectral efficiency) and computational complexity, mostly in single cell environments [60], [61], [62]. A relatively small number of strategies have been proposed for multi-cell MIMO or network MIMO, where multiple BSs cooperate with each other for enhancing the system performance [63], [64]. Network Coordinated Beamforming (NCBF) is one possible strategy that enables network MIMO by introducing BS cooperation and allows multiple receive antennas on the user side [65]. Due to the capabilities of network MIMO, the technique can be used as a very efficient method for cooperative spectrum sharing in cognitive radio systems.

This section proposes a novel cooperative spectrum sharing method denoted as Network Coordinated Beamforming with user Clustering (NCBC) [66]. It is based on the concept of Network MIMO via Network Coordinated Beamforming (NCBF). The NCBC method decreases the computational complexity of NCBF while providing high spectrum utilization making it efficient and suitable for real time spectrum sharing in CR systems.

5.2.1.1 Model description

This sub-section explains the notation used in the work as well as the concepts of the system model. Throughout the text, uppercase and lower case boldface denote a matrix **A** and a vector **a**, while the $\mathbf{A}^T$, $\mathbf{A}^H$, $\mathbf{A}^{-1}$ denote the transpose, Hermitian, and inverse matrix of **A**, respectively.

Consider the case where *K* secondary CR systems coexist and share the same spectrum hole (frequency band). It is assumed that their coverage area overlaps totally or in some parts and that every user has only one data stream. Additionally, every system has one BS and multiple users, but it serves only one user at a time, as shown on Fig. 5-1. This definition of the system model can be easily mapped onto an indoor scenario where multiple secondary CR systems, spatially collocated, use the same spectrum hole. An example scenario can be the event where a given TVWS is opportunistically shared by multiple LTE femto cells and IEEE 802.11af APs located in the same residential facility.

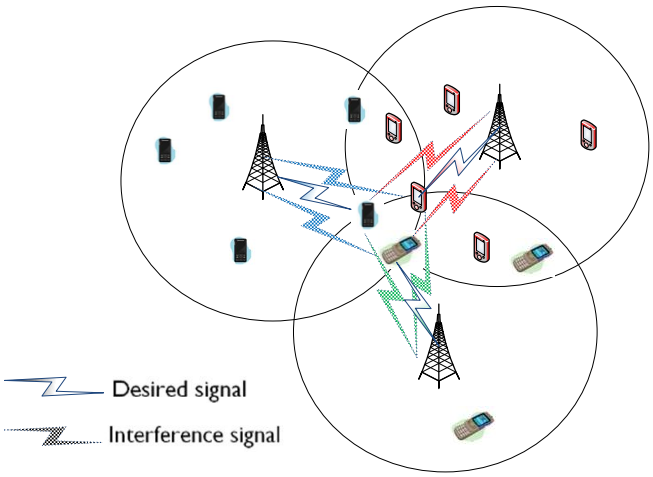

Fig. 5-1: System model

Due to the overlapping, the users from different systems will encounter high inter-system interference. A possible solution for mitigating the interference, thus enabling efficient spectrum sharing is network MIMO i.e. NCBF.

5.2.1.2 Problem formulation

Consider a multi-user MIMO channel where all BSs are equipped with one transmit antenna and all users have N_r receive antennas. As elaborated in the previous section, only one user per system is served at a given time, hence the total number of served users at any given moment is equal to *K.* It is assumed that all BSs cooperate ideally to compute the transmit beamforming and receive combining vectors. This assumption has also been made in previous work related to BS cooperation and Network MIMO [63], [64], [65]. The channel between all BSs and the *k*-th user is represented by the channel matrix $\mathbf{H}_k$ of size $N_r \times K$ and has complex entries for the channel gains. Thus, every column of $\mathbf{H}_k$ represents the single-input multiple-output (SIMO) channel between each BS and the *k*-th user.

Figure 5-2 depicts the block diagram of the NCBF scheme. It is assumed that the systems operate in TDD mode in which the temporal variations of the channels are slow compared to the duration of the data frame [60]. Let x_k and $\mathbf{n}_k$ denote the transmit symbol and the noise vector with variance σ_k^2 of the *k*-th user, respectively. Let $\mathbf{m}_k$

denote the transmit beamformer and $\mathbf{w}_k$ the receive combining vector at the *k*-th user. Then, the received signal at the *k*-th user can be expressed as:

$$y_k = \mathbf{w}_k^H \mathbf{H}_k \mathbf{m}_k \sqrt{p_k} x_k + \mathbf{w}_k^H \mathbf{H}_k \sum_{l=1, l\neq k}^{K} \mathbf{m}_l \sqrt{p_l} x_l + \mathbf{w}_k^H \mathbf{n}_k \quad (5\text{-}1)$$

where p_k is the allocated transmit power of the BS for the *k*-th user. In the case of coordinated beamforming strategies, the transmitter chooses $\mathbf{m}_k$ such that the subspace spanned by its columns lies in the null space of $\mathbf{w}_k^H \mathbf{H}_k$ $(\forall l \neq k)$, i.e. $\mathbf{w}_k^H \mathbf{H}_k \mathbf{m}_l = 0$ $(\forall l \neq k)$ and $k = \overline{1, K}$. If the number of served users in every system is higher than one, then the computational complexity of the NCBF rapidly increases making the actual approach not suitable for real time communication.

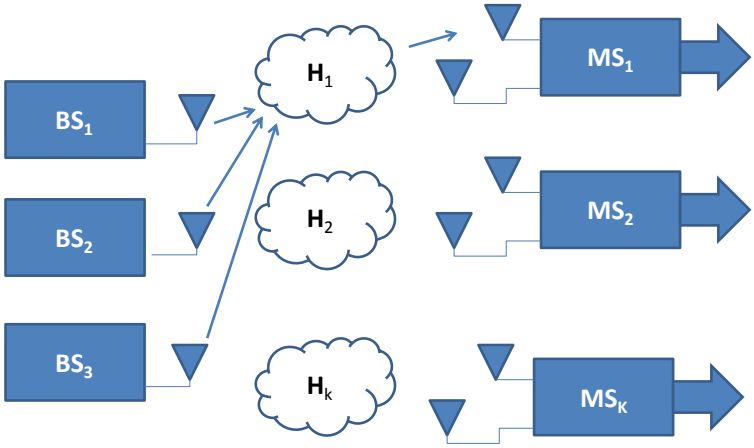

Figure 5-2: Block diagram of NCBF

The newly proposed NCBC scheme [66] represents a novel spectrum sharing method that decreases the complexity of NCBF by *grouping* the users in the given system based on the *correlation of their channel matrices*. This makes the NCBC scheme feasible for real time operation. According to NCBC, every BS has to calculate the correlation of the channel matrices among all of its users. If the correlation between them is higher than a predefined correlation threshold, then the users can be served with the same beamforming and receive combining coefficients, hence decreasing the computational complexity of NCBF. The correlation between two users can be computed as:

$$\gamma_{corr} = 1 - \left\| \lambda_k - \lambda_l \right\|_F \quad (5\text{-}2)$$

where λ_k denotes the diagonal matrix whose elements on the main diagonal are eigenvalues of the *k*-th user's channel matrix $\mathbf{H}_k$, λ_l denotes the diagonal matrix whose elements on the main diagonal are eigenvalues of the *l*-th user's channel matrix $\mathbf{H}_l$ and $\|\cdot\|_F$ denotes the Frobenius norm. If $\gamma_{corr} = 1$, the users will be completely correlated, while for $\gamma_{corr} = 0$, the users will be completely uncorrelated. Lower γ_{corr} value will result in lower system performance and higher inter-system interference.

5.2.1.3 Results

This sub-section gives an insight into the performance of NCBC in terms of Signal to Interference Ratio (SIR) and sum-rate vs. γ_{corr} and SNR, respectively. Additionally, it compares the performance of NCBC with a Frequency Division Spectrum Sharing (FDSS) technique that divides the available spectrum in equal frequency chunks between all

coexisting secondary CR systems. The performance comparison is conducted in terms of spectral efficiency (i.e. sum rate) and aggregate system capacity. To obtain relevant results, Monte Carlo simulations are carried out for all performance metrics. The channel model used in the simulation analysis is based on the Kronecker MIMO channel model for indoor environments [67] and its parameters are given in Table 5-1. For simplification of the simulation, it is assumed that all BSs use equal allocation of the transmit power for every user, hence denoting $p_k = p$.

Table 5-1: Channel model parameters

Channel Parameters	
Channel Type	NLOS indoor
Delay spread	<100 ns
Number of Paths	8
Bandwidth	10MHz

As previously elaborated, the correlation between the channel matrices of two users plays a crucial role of the NCBC performance. Fig. 5-3 depicts the SIR in dependence of γ_{corr} for different number of coexisting secondary CR systems. It is evident that the SIR ratio decreases as γ_{corr} decreases, but even for low channel correlation the SIR level does not fall below – 5dB which is above the limits for modern day systems [68]. Based on the SIR behaviour of NCBC, it is obvious that multiple users can use the same beamforming coefficient even for low channel correlation.

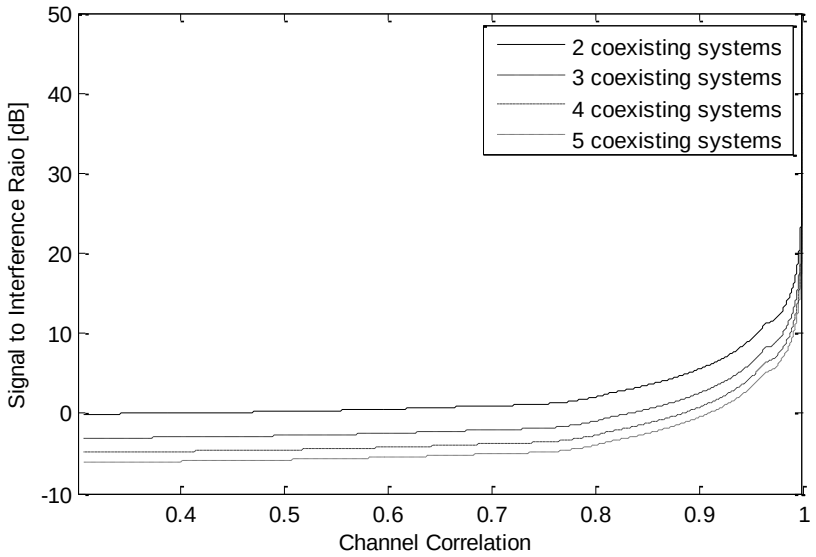

Fig. 5-3: Signal to interference ratio in dependence of the channel correlation

Another metric that depicts the performance of the NCBC in terms of the signal to interference noise ratio (SINR) is the sum-rate defined as:

$$R_s = \sum_k \log_2\left(1 + \frac{p\left|\mathbf{w}_k^H \mathbf{H}_k \mathbf{m}_k\right|^2}{1 + \sum_{l=1, l\neq k}^{K} p\left|\mathbf{w}_k^H \mathbf{H}_l \mathbf{m}_l\right|^2}\right) \quad (5\text{-}3)$$

It is clear from eq. (5-3) that the sum-rate mainly depends on the SINR value. For the case of high values of the SINR the achievable sum-rate will be higher in comparison to

the case of low SINR values. Fig. 5-4 depicts the sum-rate vs. SNR dependence for different channel correlations of the users and two coexisting secondary CR systems. It is evident that users with low channel correlation will experience lower system performance. The increment of the SNR affects only the sum-rate of the highly correlated users because of the low intra-system interference. For low channel correlation, the interference is higher than the noise power, thus the increase of the SNR does not affect the sum-rate performance.

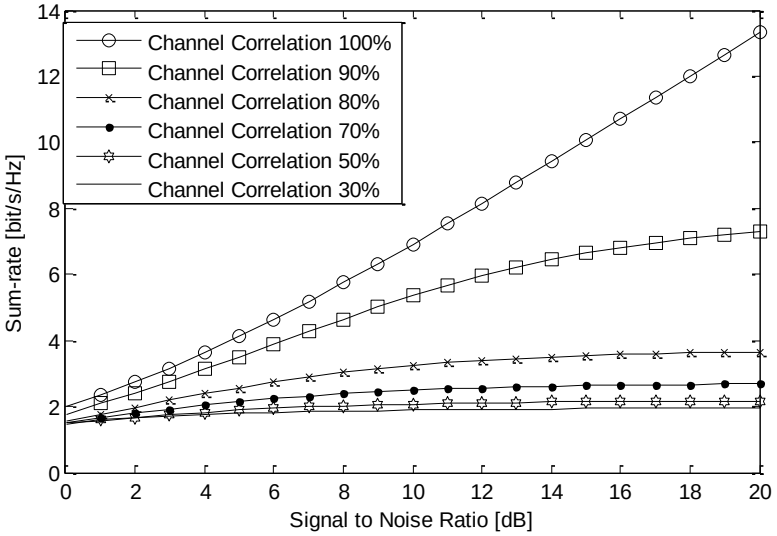

Fig. 5-4: Sum-rate in dependence of the SNR (K = 2)

Fig. 5-5 shows the sum-rate in dependence on SNR for different channel correlations of the users and five coexisting secondary CR systems. Compared to the case in Fig. 5-4, the increased number of coexisting secondary CR system results in an increase of the sum-rate, due to the higher spatial diversity gain, but also increases the computational complexity of the method.

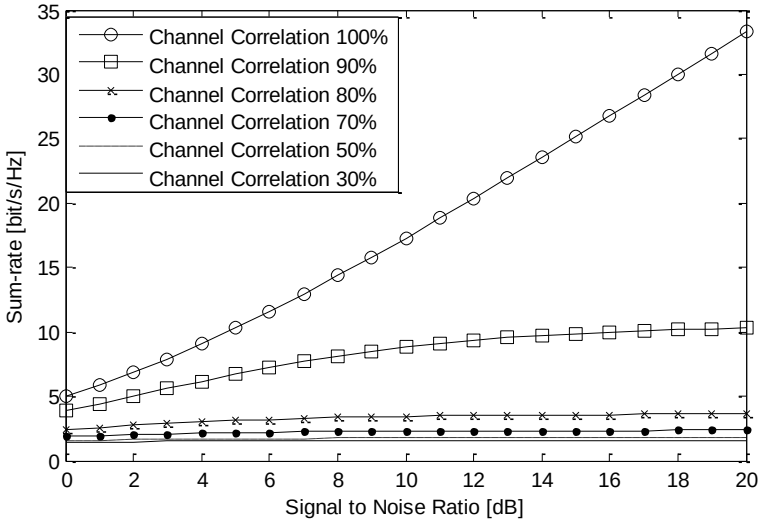

Fig. 5-5: Sum-rate in dependence of the SNR (K = 5)

The proposed NCBC method is also compared to a simple and common FDSS method that divides the vacant spectrum to equal chunks of bandwidth between the coexisting secondary CR systems. In this manner, FDSS guarantees equal sharing between all

coexisting systems. Fig. 5-6 depicts the achieved aggregate system capacity vs. the SNR for both methods and two coexisting systems. It can be seen that NCBC outperforms FDSS even for low channel correlation if the SNR level is low. This is due to the fact that for low SNR level the interference does not play the key role in terms of the system performance. For high SNR, the main degradation in terms of the performance is due to the interference, thus the NCBC only outperforms FDSS for high channel correlation where the interference level is low.

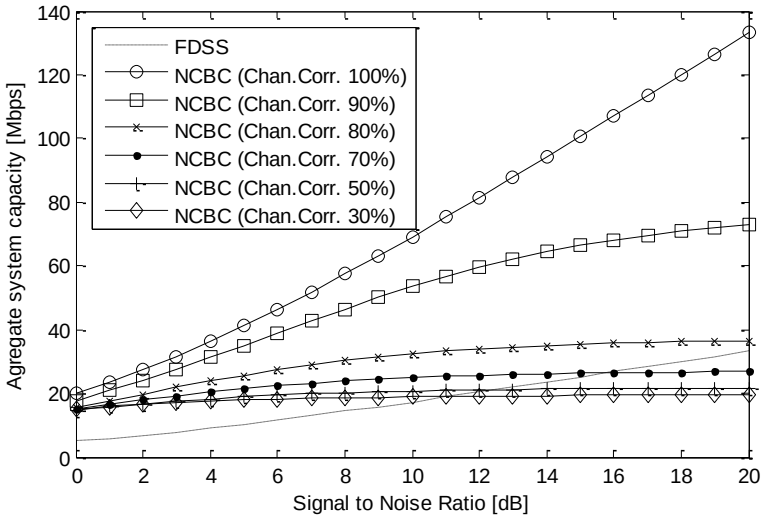

Fig. 5-6: Aggregate system capacity in dependence of the SNR (K = 2)

Fig. 5-7 depicts the aggregate system capacity of both methods in dependence on the SNR for five coexisting systems. In this case NCBC outperforms FDSS in every case due to its more efficient spectrum sharing approach.

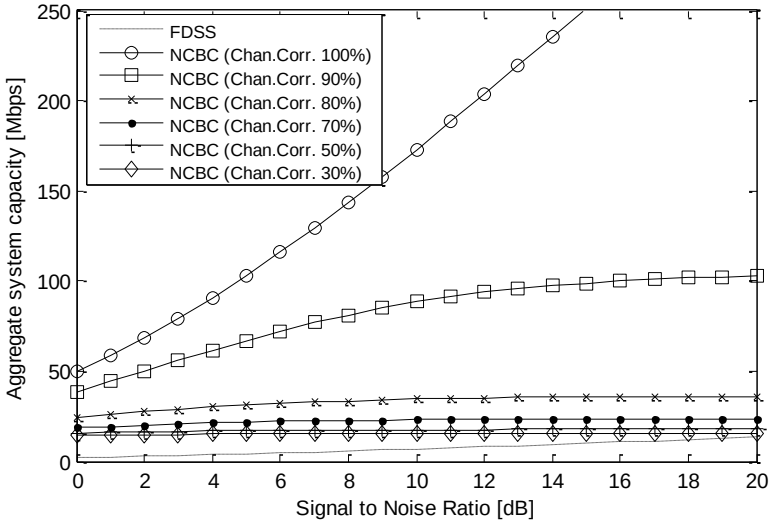

Fig. 5-7: Aggregate system capacity in dependence of the SNR (K = 5)

Fig. 5-8 shows the performance of both methods for the sum-rate in dependence on the number of coexisting secondary CR systems for SNR of 10dB. NCBC outperforms FDSS for any case and the performance gain increases as the number of coexisting system increases. This stems from the fact that the spectral efficiency of every coordinated beamforming scheme depends on the number of transmit and receive antennas. In the

case of NCBC, the number of antennas is mapped onto the number of BSs, i.e. number of coexisting systems *K*.

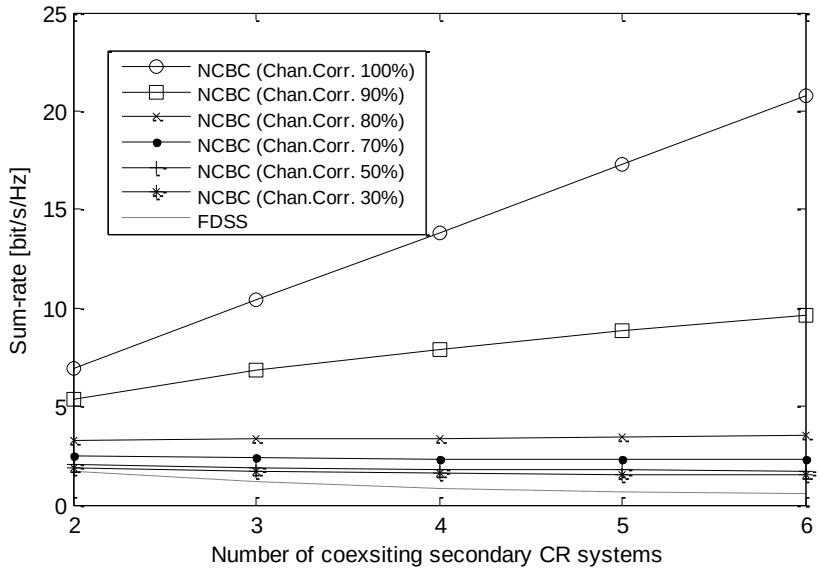

Fig. 5-8: Sum-rate in dependence of the number of coexisting secondary CR systems

Fig. 5-9 depicts the aggregate system capacity in dependence on the number of coexisting secondary CR systems for both methods (i.e. NCBC and FDSS). The results are obtained for SNR of 10dB. It is obvious again that NCBC is more efficient than FDSS for any channel correlation and number of coexisting CR systems. When using NCBC, the aggregate system capacity increases as the number of the coexisting systems increases, because of its efficient spectrum sharing capabilities. For FDSS, the system capacity decreases because the method splits the available band to every coexisting system resulting in decreased system capacity.

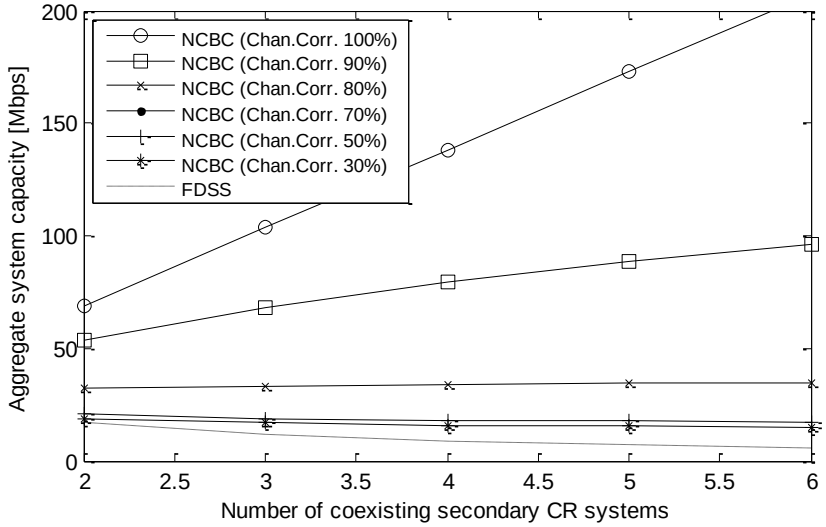

Fig. 5-9: Aggregate system capacity in dependence of the number of coexisting secondary CR systems

The NCBC method is purely theoretical, interweave based, cooperative spectrum sharing strategy that is not using any primary users' protection criteria. Instead, it tries to analyze the potential benefits of lower complexity NCBF for practical deployments without looking into the possible aggregate interference problem for the primary users. This limits its practical deployment and further analysis would be needed to accommodate the strategy to a real-world secondary access problem incorporating the primary users' protection criteria in more specific details. Nevertheless, the NCBC method clearly shows that the combination of NCBF with UC may provide increased benefits for multiple cooperating secondary systems (increased sum-rate and aggregate system capacity). The degree of the increase for practical deployments depends on the primary users' protection criteria.

5.2.2 **Combined power/channel allocation method for efficient spectrum sharing in TV white space scenario**

One of the possible scenarios for secondary spectrum access is the usage of TV white spaces for WiFi-like secondary transmissions. The traditional approach of uncoordinated user/APs deployment in classical WiFi scenarios would pose some additional interference mitigation challenges in a secondary WiFi-like sharing scenario within TV white spaces. Therefore, the solution would necessitate efficient spectrum sharing strategies in order to provide protection from excessive interference and simultaneously enable efficient coexistence for the secondary systems/users.

This section addresses the problem of joint power and channel allocation in a spectrum sharing scenario for WiFi-like secondary users in TV white spaces in order to increase the performance of the spectrum sharing. The goal is to maximize the number of supported secondary users while jointly optimizing the power and channel allocation and enabling protection for the primary system [69]. Due to the high complexity in obtaining optimal power/channel allocation strategies, the problem is solved utilizing a suboptimal algorithm based on the NBS game theoretic approach.

5.2.2.1 Scenario description

The targeted scenario for the spectrum sharing strategy of interest here envisions multiple uniformly distributed Secondary Access Points (SAPs) and multiple Secondary Users (SUs) connected to the SAPs operating in TV white spaces (Fig. 5-10). Every SAP obtains channel availability information from a predefined database by querying it with its location coordinates. SAPs are assumed to be equipped with geo-location devices that enable them to retrieve information on spectrum availability from a centralized database hosting information on spectrum opportunity.

The subsequent performance analysis assumes that the database contains data on the available TV channels in Macedonia [70] applying ECC rules for primary TV system protection. This approach is taken from QUASAR's WP5 clearly showing the potentials for practical deployment of the targeted scenario. The targeted area is 20 x 20 pixels, where each pixel represents 120 x 120 m of the real terrain. The location is chosen near the capital of Skopje for a suburban area. The database, based on the the coordinates of the uniformly distributed generated SAPs, supplies information on the available 8 MHz TV channels and a map of permitted secondary systems' transmitting power at every pixel. The sharing strategy then implements transmitting power optimization for every SAP based on the conditions for SUs maximization.

Uncoordinated user deployment of SAPs in a WiFi-like scenario would result in multiple secondary systems transmission areas and frequencies overlap. Moreover, the joint optimization of every SAP’s transmitting power and channel resources in the same time can be a highly complex problem. A proposed solution would have to introduce a rational balancing between the power and the channel allocation methods for the SUs, which is the target for the subsequently formulated problem.

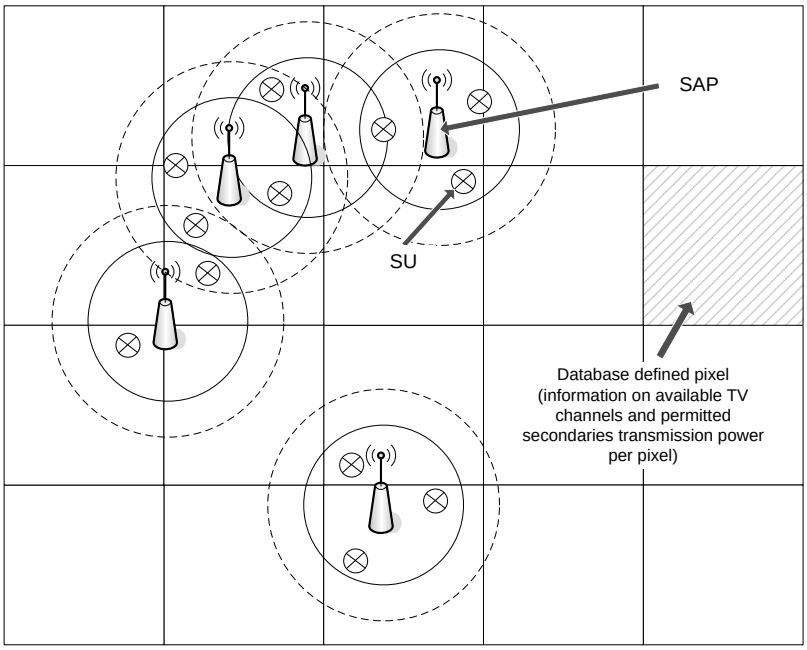

Fig. 5-10: WiFi-like in TV white spaces scenario description

5.2.2.2 Problem formulation

Because of the overlapping transmission areas, some SUs can be highly interfered by neighbouring SAPs. The fact that certain SUs will be able to "hear" different SAPs will be used to introduce cooperation between SAPs. These SUs are chosen as relay SUs that will be used from neighbouring/overlapping SAPs for exchanging information on transmission power, available spectrum TV channels and number of connected SUs at every SAP.

The power received by every user is calculated using the Hata model, i.e.:

$$PL_{ij} = 69.55 + 26.16\log_{10}(f) - 13.82\log_{10}(h_b) - 3.2((\log_{10}(11.75h_m))^2) - 4.97 + (44.9 - \log_{10}(h_b))\log_{10}(d_{ij}) \quad (5\text{-}4)$$

where f is the central transmitting frequency, d_{ij} is the distance between SU_i and SAP_j, h_b is the SAP height and h_m is the SU height. SAPs are characterized with transmission and interference area. Suppose SAP_j transmits with a power of p_j and its transmission range is $R_{Tj}(p)$. The condition for successful transmission would be $PL_{ij}\, p_j > a$, where a is the receiver sensitivity threshold. The received signal should be above the receiver sensitivity threshold in order to allow the SU and the SAP to establish a successful connection. Therefore, the transmission range of transmitting SAP_j is:

$$R_{Tj}(p) = \frac{PL_{ij}\, p_j}{\alpha} \quad (5\text{-}5)$$

and the interference range is:

$$R_{I_j}(p) = \frac{PL_{ij}\, p_j}{\beta} \quad (5\text{-}6)$$

where interference power is assumed negligible only if it exceeds a threshold β at a receiver. The interference range is higher than the transmission range $R_I(p) > R_T(p)$, since $\beta < a$ [71].

Based on the interference conditions at every SU, there may be three different types of SUs, i.e.:

- **Supported SUs** - physically in the transmission range of one SAP and not interfered from other SAPs.
- **Interfered SUs** - in the transmitting range of one or more SAPs or transmitting range of one SAP and interference range from one or more SAPs.
- **Out of range SUs** - outside of every SAPs' transmitting range.

The problem of spectrum sharing now becomes a problem of *maximizing the number of supported SUs while enabling primary user protection from excessive interference*. The spectrum sharing strategy uses a Nash Bargaining Solution (NBS) cooperative approach to achieve the optimum solution [72]. The result of the cooperative game is that each participant increases its profit or at least one participant increases, while the profits of the others do not decrease. Consequently, the cooperative game can increase the profit of the whole system. In other words, it can achieve Pareto optimum.

5.2.2.3 Proposed spectrum sharing strategy

The spectrum sharing strategy is formulated and observed as a cooperative game where players bargain on their power transmission levels. In the beginning of the game, every SU associates to only one SAP and every SU chooses to associate to the SAP whose received signal power is highest at that moment. The SUs that are in transmission range of two or more overlapping SAPs are candidate relay SUs envisioned to be able to connect to more than one SAP. The spectrum sharing strategy itself adopts two separate approaches, i.e.:

- *Power Allocation Algorithm (PAA)* and
- *Combined Channel and Power Allocation Algorithm (CCPAA)*.

In the PAA approach, the cooperating SAPs bargain on their transmission powers in order to maximize the number of supported SUs, while guaranteeing that the SAPs' transmission powers will not overcome the permitted transmission power retrieved from the database for the targeted real terrain.

The CCPAA approach stems from the PAA additionally introducing a channel allocation among the SAPs. Namely, throughout the game in the PAA method, there can be a situation where the transmission areas of two SAPs overlap in more than 40%. This proves to be inefficient as the power optimization solely would require that the overlapping SAPs decrease their transmission powers leading to increasing the number of out of range SUs. Therefore, the CCPAA method finds the highly overlapping SAPs in the system prior to the beginning of the bargaining game between the players. Then, all SAPs that satisfy the overlapping condition (defined as minimum 40%) will undergo a channel allocation procedure that allocates *proportional amount of available spectrum* according to the number of connected SUs at each of the overlapping SAPs.

The proposed spectrum sharing strategy may operate in two distinct cooperation modes:

- ***Cooperation mode I*** envisions that cooperative groups are formed from overlapped first neighbours only. This means that the power optimization is performed only for smaller groups of overlapping SAPs.
- ***Cooperation mode II*** includes a wider group of overlapping SAPs in the cooperation, not only the closest neighbours. This means that the power optimization is performed for larger groups of cooperative SAPs.

The bargaining game assumes *N* players, which are the SAPs in this scenario. Let *S* denote the set of possible joint strategies or states, *d* represents the agreement to disagree and solve the problem competitively and *U* is the multiuser function where $U : S \cup \{d\} \rightarrow R^N$. The NBS sets a function that assigns a pair of $(S \cup \{d\}, U)$ and the corresponding solution is obtained by maximizing the Nash function [72] over all possible states:

$$S = \arg\max_{s \in S \cup \{d\}} \prod_{n=1}^{N} (U_n(s) - U_n(d)) \quad (5\text{-}7)$$

The Nash function $F(s): S \cup \{d\} \to R$ is defined as:

$$F(s) = \prod_{n=1}^{N} (U_n(s) - U_n(d)) \quad (5\text{-}8)$$

The disagreement point for all users is defined as:

$$d = \min_{s_{-i} \in S} \max_{s_i \in S_i} u_i(s_i, s_{-i}) \quad (5\text{-}9)$$

After formulating the problem, the following subsection will provide insight into the actual behaviour of the proposed spectrum sharing strategy and its possibilities for practical deployments.

5.2.2.4 Simulation results

The performance evaluation of the proposed spectrum sharing strategy for WiFi-like secondary usage of TV white spaces focuses on the benefits of using joint power and channel allocation vs. plain power allocation when performing spectrum sharing in the targeted scenario. The scenario setup parameters are given in Table 5-2. The simulation analysis is conducted with SAPs ranging from 5 to 25 and SUs number from 20 to 180 randomly distributed in an area of 2400 x 2400 m. The transmitting power is set to 100 mW at the beginning. The available channels are distributed to the SAPs according to the information for available 8 Mhz TV channels from the centralized database. The number of available channels ranges from 1 to 5 available channels per pixel in the chosen terrain. The simulations are conducted for the PAA and CCPAA approaches, respectively.

Table 5-2. Simulation parameters

No. of SAPs	**No. of SUs**	**Rx. Sensitivity threshold (α)**	**Interference threshold (β)**	**Simulation area**
5 to 25	20 to 180	-85 dBm	- 93 dBm	2400 x 2400 m

Fig. 5-11 depicts the performance of the PAA approach in terms of average increase of the number of supported SUs for different number of SAPs and different number of SUs. It is clear that the algorithm achieves peak values for 20 SAPs and 60 SUs in the specific simulated system. Higher values of SAPs and SUs lead to decrease of the performances. The PAA approach underperforms for lower number of SAPs (negative values for the increase in number of supported SUs when SAPs = 5). Namely, when the number of SAPs is lower, it is expected that they will rarely overlap in the scenario. As the primary system protection mechanism yields lower transmission power for every SAP, this would result in many coverage gaps in the targeted scenario leaving many SUs out of range.

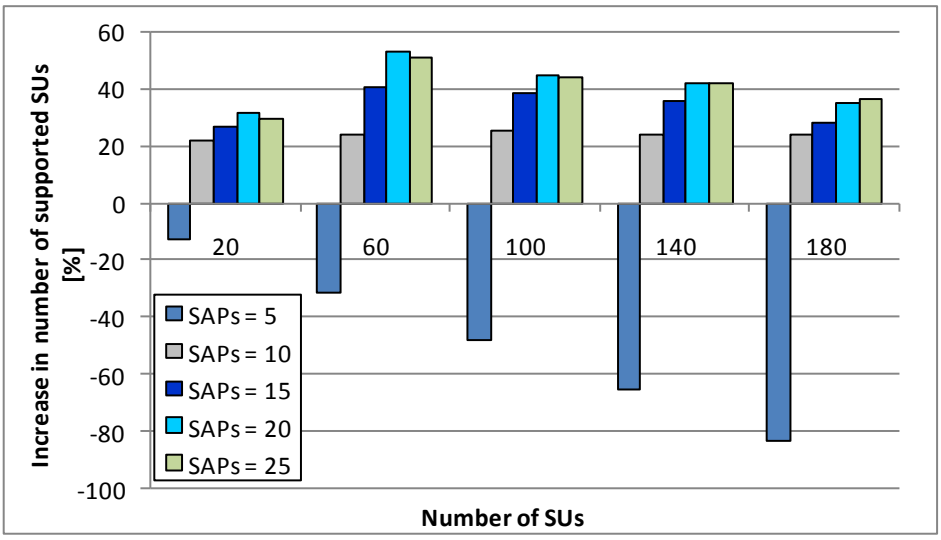

Fig. 5-11: Average number of increased supported SUs for different number of SAPs and SUs for the PAA method

Fig. 5-12 evaluates the CCPAA algorithm. It is evident that CCPAA outperforms PAA providing constant performance increase for higher number of SAPs (>=15). Also, compared to PAA, the CCPAA approach provides better performances for lower number of SAPs (smaller decrease of number of supported SUs for SAP = 5).

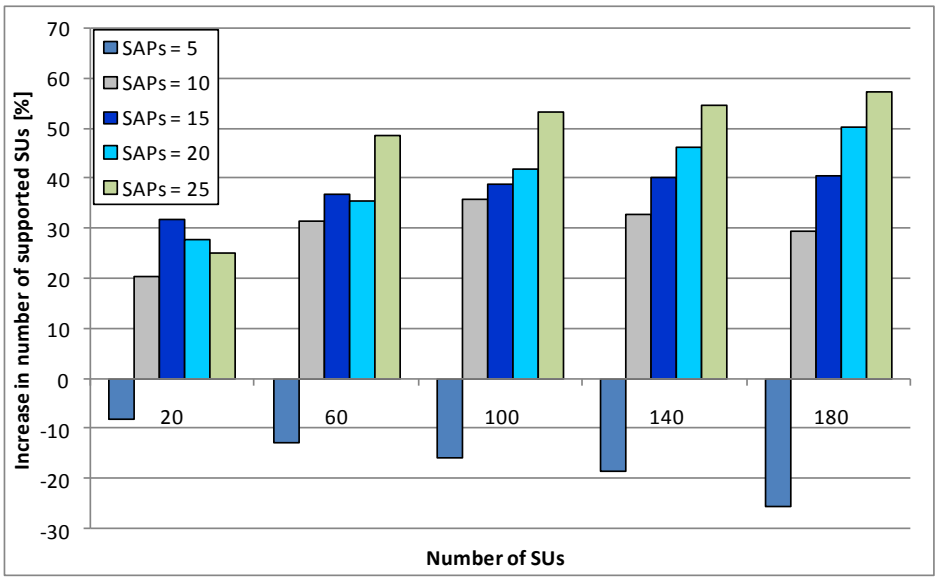

Fig. 5-12: Average number of increased supported SUs for different number of SAPs and SUs for the CCPAA method

Fig 5-13 depicts the effect of the different cooperation modes in the spectrum sharing strategy. The figure shows the relative ratio of Cooperation mode II vs. Cooperation mode I implemented in the PAA and CCPAA approaches. It is clear that the increased cooperation shows better performances for the PAA approach. This effectively leads to a conclusion that higher cooperation level among secondary systems can provide increased number of supported SUs.

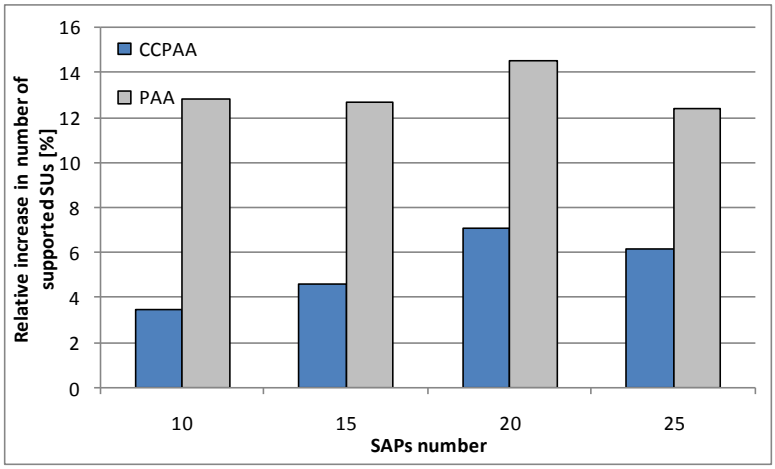

Fig. 5-13: Relative ratio of Cooperation mode II vs. Cooperation mode I implemented in the PAA and CCPAA approaches

This subsection introduced a spectrum sharing strategy that allows multiple cooperative secondary systems to efficiently and reliably share available spectrum. The targeted scenario and the subsequent analysis rely on a practically envisioned scenario stemming from WP5 work.

5.3 **Concluding remarks**

Spectrum sharing strategies are important aspects of secondary spectrum access enabling coexistence among primary and secondary systems. They must provide efficient and reliable secondary spectrum usage by multiple secondary systems without violating the primary users. Therefore, the QUASAR project targets spectrum sharing strategies that rely on database based spectrum opportunity detection which fosters aggregate interference management in the most efficient manner.

This section introduced and analyzed the benefits of using cooperation among multiple secondary systems when performing spectrum sharing. The cooperation allows multiple secondary systems to effectively share and use the available spectrum without jeopardizing the primary system. The proposed methods specifically target and fit within the QUASAR objectives.

The presented NCBC strategy decreases the computational complexity of NCBF making it suitable for real time spectrum sharing. The results show that even for low channel correlation the system performance satisfies the minimal requirements for modern communication systems. It is a theoretical model aimed at showing the benefits of NCBF with lower complexity and its practical deployment would require further analysis regarding the primary users' protection criteria. The proposed spectrum sharing strategy for multiple WiFi-like secondary users coexisting in TVWS uses NBS and effectively combines power and channel allocation to increase the number of supported secondary users. The strategy achieves increase in the number of supported SUs, while at the same time provides primary system protection from excessive interference. Low number of secondary access points results in poor sharing performance because of the primary system protection criteria forcing the secondary access points to limit their transmission power (limited coverage). The combination of power and channel allocation provides higher increase in the number of supported SUs than the usage of power allocation only. The effect of the cooperation is more emphasized in the cases when only power allocation is applied in the spectrum sharing scheme. It shows that the effect of cooperation can overcome the benefits of the combined power and channel allocation.

6 Conclusions

We consider cognitive radio networks where more than one secondary user (or secondary system) intends to operate in the spectrum band owned by the primary system. Since the aggregated interference from the secondary users is the bottleneck for secondary communication, estimating it and controlling it to an acceptably low level is of crucial importance for the secondary users to efficiently share the available opportunity. In this deliverable, we study the impact of allowing the multiple secondary users to interact with each other on potential interference reduction and performance enhancement. We have the following observations.

1) Due to the nature of wireless communications, the performance of the secondary system is in general severely affected by the fading phenomenon. Thus to guarantee a certain QoS, a large secondary transmit power might be demanded. Such a requirement leads to high interference to the primary system. Alternatively, to limit the interference below a certain level, satisfactory secondary communications may not be achievable. However, this issue can be effectively addressed by considering the concept of *cooperative communications* among secondary users, i.e. permitting certain secondary users to serve as relays for other secondary users to combat the negative impact of fading. In Chapter 2 we proposed two secondary relaying strategies and showed their throughput and error performance improvement over systems without considering user cooperation.

2) To protect primary system, the total aggregated interference from multiple secondary users is required to be kept below certain specified level. If only the probability distribution of the interference is available, normally the maximally allowed aggregated interference is set to a much lower level, i.e. to introduce an additional fixed margin. Such a fixed margin does not take into account the number and locations of secondary users and is decided using worst case assumptions. This requirement leads to a large margin and an overly constrained secondary transmit power allocation. In Chapter 3 we proposed an adaptive power allocation strategy to improve the situation. The strategy *jointly* assigns powers to multiple secondary users. As a result, the margin of the interference threshold can be adaptively tuned according to the actual environment. A better secondary system performance, over what can be achieved with the worst case assumptions, can thus be attained.

3) The spectrum sensing process' inability of deriving needed reliability for practical deployments leads to the databases being a preferred approach by the regulatory bodies in static environments (e.g. TVWS). However, the process of spectrum sensing may prove vital for accurate and up-to-date databases population especially or fast and efficient spectrum vacancy evaluation in more dynamic environments (e.g. protection of unregistered PMSE devices, etc.). Therefore, highly reliable spectrum sensing process can still serve as a solid complementary (not competitive) approach to databases. Compared with single-band spectrum sensing, multi-band spectrum sensing approaches can significantly increase the opportunity detection probability, especially when sensing decision can be reached through cooperation among multiple secondary users. In Chapter 4 we introduced and analyzed four cooperative multi-band spectrum sensing schemes. The cooperation among the secondary users effectively yields improved opportunistic throughput, higher energy efficiency, robustness, increased sensitivity etc.

4) Spectrum sharing among secondary users is another crucial aspect of CR networks with multiple secondary users. Without a proper sharing strategy, the coexistence of multiple secondary users in the vacant spectrum would in fact result in poor spectrum utilization. The spectrum sharing efficiency can be improved by conducting *cooperative communications* among different secondary

users: users with sufficient available spectrum bands can act as bridges (relays) for other users' communications. In addition, different users may exchange data on interference measurements or other relevant parameters, which are then used in the sharing process. In Chapter 5 we proposed two such cooperative sharing strategies (with database based spectrum opportunity detection). In both cases the cooperation yields improved system performances in terms of high resources utilization and reliable primary users' protection.

Certainly requiring different users to interact with each other may demand high system complexity in terms of sophisticated design of transmission, signalling, and scheduling etc. However, the results we provided in this deliverable (although they may require extra channel knowledge, high sensing time, or high energy consumption due to sensing) explicitly demonstrate the substantial performance gain that can be achieved via user cooperation. Thus we conclude that seeking secondary-user cooperation can serve as a promising solution to reduce interference and improve performance in next-generation CR systems. The strategies proposed and analyzed in this deliverable would pave the way for further research on approaches to realizing more efficient and reliable cooperation among secondary users or systems.

Appendix A

A.1 Proof of Theorem 2-1

First, we rewrite problem (2-4) in epigraph form

$$\begin{aligned} \min \quad & -t \\ \text{s.t.} \quad & h_1 = t - C_1 \le 0 \\ & \vdots \\ & h_K = t - C_K \le 0 \\ & h_{K+1} = \sum_{i=1}^{K} \varphi_i P_i \le \gamma \end{aligned}, \tag{A-1}$$

We now show that for the optimization problem (A-1) strong duality holds and therefore, primal and dual optimal variables must satisfy the KKT conditions [73]. To do so, we show that (A-1) satisfies the *linear independent constraint qualification* (LICQ) conditions [74] and hence, the duality gap of this problem is zero.

Constraints $h_{i,j} = 1,\ldots,K+1$ of problem (A-1) are said to satisfy the LICQ conditions if matrix

$$\mathbf{D}h = \left[\nabla_{P^*} h_1, \ldots, \nabla_{P^*} h_{K+1}\right]$$

has full column rank, i.e., the gradients of the active constrains are linearly independent at the optimal point $\left(P_1^*,\ldots,P_K^*\right)$.

The matrix of gradients has the following form

$$\mathbf{D}h = \begin{bmatrix} -A_{11} & B_{12} & \cdots & B_{1,L_b} & 0 & 0 & \cdots & 0 & \varphi_1 \\ 0 & -A_{22} & B_{23} & \cdots & B_{2,1+L_b} & 0 & \cdots & 0 & \varphi_2 \\ B_{31} & 0 & -A_{33} & B_{34} & \cdots & B_{3,2+L_b} & \cdots & 0 & \varphi_3 \\ \vdots & & & & & & \ddots & & \vdots \\ 0 & \cdots & 0 & B_{K,K-1-L_f} & \cdots & B_{K,K-1-L_f} & 0 & -A_{K,K} & \varphi_3 \\ 1 & \cdots & 1 & 1 & \cdots & 1 & \cdots & 1 & 0 \end{bmatrix} \tag{A-2}$$

Where

$$A_{i,i} = \frac{g_{i,i+1}}{\left(\sigma^2 + \sum_{\substack{k=j-L_f \\ k\neq i+1}}^{j+L_b} g_{k,i+1} P_k\right) \ln 2}, \tag{A-3}$$

$$B_{i,i} = \frac{P_j g_{i,j+1} g_{j,j+1}}{\left(\sigma^2 + \sum_{\substack{k=j-L_f \\ k\neq j+1}}^{j+L_b} g_{k,j} P_k\right)\left(\sigma^2 + \sum_{\substack{k=j-L_f \\ k\neq j \\ k\neq j+1}}^{j+L_b} g_{k,j+1} P_k\right) \ln 2}. \tag{A-4}$$

Since $g_{i,j}, \forall i,j$ are positive, non-zero with high probability and i.i.d., σ^2 and $P_i, \forall i,j$ are strictly positive, then $A_{i,j}$ and $B_{i,j}$ are also independent and strictly positive with high probability.

Therefore, for a set of optimal powers (P^*_1 , ..., P^*_K) matrix $\mathbf{D}h$ in (A-2) has full rank with high probability and hence, the LICQ conditions are satisfied. Thus, the KKT conditions are necessary conditions for a solution to be optimal.

We next show that the KKT conditions for (A-1) have a unique feasible solution only when all link capacities are equal and then maximized, such that ASI constraint (2-3) is met with equality.

The Lagrangian for (A-1) can be written as

$$L = -t + \sum_{i=1}^{K} \lambda_i \left(t - C_i\right) + \omega\left(\sum_{i=1}^{K} \varphi_i P_i - \gamma\right). \tag{A-5}$$

From (A-5) we can write down the KKT conditions for a solution to be optimal

$$\frac{\partial L}{\partial P_i} = 0, \quad i = 1,\ldots,K\,, \tag{A-6}$$

$$\frac{\partial L}{\partial t} = 0\,, \tag{A-7}$$

$$h_j \le 0, \quad j = 1,\ldots,K+1\,, \tag{A-8}$$

$$\lambda_i \ge 0, \quad \omega \ge 0, \quad i = 1,\ldots,K\,, \tag{A-9}$$

$$\lambda_i h_i = 0, \quad i = 1,\ldots,K\,, \tag{A-10}$$

$$\omega h_{K+1} = 0\,, \tag{A-11}$$

Taking partial derivatives from (A-5) we get the optimality conditions (A-6) and (A-7) of form

$$\frac{\partial L}{\partial P_i} = \varphi_i \omega - A_{i,i}\lambda_i + \sum_{j=i-L_f-1}^{i+L_b} B_{i,j}\lambda_j = 0\,, \tag{A-12}$$

$$\frac{\partial L}{\partial t} = -1 + \sum_{i=1}^{K} \lambda_i = 0\,, \tag{A-13}$$

where $A_{i,i}$ and $B_{i,j}$ are the same as in (A-3) and (A-4) respectively.

We have only one negative component in each of the K equations (A-12) and hence, all λ_i's have to be strictly positive in order to satisfy $\frac{\partial L}{\partial P_i} = 0, \forall i$. Otherwise, any $\lambda_i = 0$ will immediately lead to $\lambda_i = 0, \forall j \neq i$ and hence, (A-13) will not be satisfied.

Finally, if $\omega = 0$, we will get a linear system of equations

$$\mathbf{M}_{K+1,K+1}\left(\mathbf{D}h\right)\boldsymbol{\lambda} = \mathbf{0}\,, \tag{A-14}$$

where $\boldsymbol{\lambda} = \left[\lambda_i,\ldots,\lambda_K\right]^T$, $\mathbf{M}_{K+1,K+1}\left(\mathbf{D}h\right)$ is the minor sub-matrix to the entry $\left(K+1,K+1\right)$ of matrix $\mathbf{D}h$ in (A-2). Since $\mathbf{D}h$ has full column rank, the system (A-14) has a single trivial solution $\boldsymbol{\lambda} = \mathbf{0}$ which does not satisfy (A-13) and hence is not feasible.

All this leads us to the conclusion that the KKT conditions have a unique optimal solution corresponding to $C_1 = \ldots = C_K$ and $\sum_{i=1}^{K} \varphi_i P_i = \gamma$. Thus, the end-to-end throughput of a

tandem network with the ASI constraint (2-3) is maximized if and only if all the link capacities are equal and constraint (2-3) is satisfied with equality.

A.2 Proof in Section 4

CMSS with EGC optimization problem:

$$\text{Objective function}: \quad O(\tau_i, N) = \max_{\tau_i, N} \sum_{i=1}^{K} \frac{T - \frac{K \cdot N \cdot b_{egc}}{R_c} - \tau_c^{'} - K \cdot \tau_i}{T} \cdot r(i) \cdot P_{H_0}(i) \cdot (1 - P_{fa}(i))$$

$$\text{Constraint function 1}: \quad C_1(\tau_i, N, \lambda_i) = P_d(i) = Q_{nm}\left(\sqrt{\tau_i \cdot f_s \sum_{i=1}^{N} \gamma_i}, \sqrt{\lambda_i}\right) \geq \alpha^{'} \qquad \forall i \in \{1..K\}$$

$$\text{Constraint function 2}: \quad C_2(\tau_i, N, \lambda_i) = P_{fa}(i) = \frac{\Gamma(N \cdot \tau_i \cdot \frac{f_s}{2}, \frac{\lambda_i}{2})}{\Gamma(N \cdot \tau_i \cdot \frac{f_s}{2})} \leq \beta \qquad \forall i \in \{1..K\}$$

Lemma 4-1: *The minimal number of cooperative nodes and minimal sensing time that satisfy the first constraint function maximize the objective function.*

Proof of Lemma 4-1: If τ_i^* and N^* are the minimal sensing time and the number of cooperating nodes, chosen so that $P_d(i) = \alpha^{'}$, (i.e. $C_1(\tau_i^*, N^*, \lambda_i^*) = \alpha^{'}$), while τ_i^{**} and N^{**} are some other parameters, chosen so that the $P_d(i) > \alpha^{'}$, (i.e. $C_1(\tau_i^{**}, N^{**}, \lambda_i^*) > \alpha^{'}$), then $C_1(\tau_i^{**}, N^{**}, \lambda_i^*) > C_1(\tau_i^*, N^*, \lambda_i^*)$. The validity of the last statement implies that $\tau_i^{**} > \tau_i^*$ and/or $N^{**} > N^*$ (this was first supposed at the beginning). It is obvious that $O(\tau_i^{**}, N^{**}, \lambda_i^*) < O(\tau_i^*, N^*, \lambda_i^*)$, because the terms in the objective function with minus sign reduce the throughput. The last statement clearly shows that τ_i^* and N^* maximize the objective function. Based on this, the minimal τ_i and N that satisfy the detection probability maximize the throughput.

Lemma 4-2: *The second constraint function maximizes the detection probability when equality is achieved.*

Proof of Lemma 4-2: If τ_i^*, N^* and λ_i^* are the sensing time, the number of cooperating nodes and the detection threshold, respectively, that satisfy $P_{fa}(i) = \beta$ (i.e. $C_2(\tau_i^*, N^*, \lambda_i^*) = \beta$) and $\tau_i^*, N^*, \lambda_i^{**}$ are the same parameters that satisfy $P_{fa}(i) < \beta$ (i.e. $C_2(\tau_i^*, N^*, \lambda_i^{**}) < \beta$), then $C_2(\tau_i^*, N^*, \lambda_i^{**}) < C_2(\tau_i^*, N^*, \lambda_i^*)$ and $\lambda^{**} > \lambda^*$. The properties of the Generalized Marqum Q function yield that $C_1(\tau_i^*, N^*, \lambda_i^{**}) < C_1(\tau_i^*, N^*, \lambda_i^*)$. Thus, λ_i^* maximizes the detection probability.

References

[1] QUASAR Deliverable D4.1 "Sharing strategies for unaware secondary systems," public deliverable, 31 March 2012. Available online: http://www.quasarspectrum.eu/downloads/public-deleverables.html

[2] J. Mitola III and G. Maguire Jr., "Cognitive radio: Making software radios more personal," *IEEE Personal Commun.*, vol. 6, no. 4, pp. 13-18, Aug. 1999.

[3] I. Akyildiz, W.-Y. Lee, M. Vuran, and S. Mohanty, "A survey on spectrum nanagement in cognitive radio networks," *IEEE Commun. Magazine*, vol. 46, no. 4, pp. 40-48, Apr. 2008.

[4] J. Sachs, I. Maric, and A. Goldsmith, "Cognitive cellular system within the TV spectrum," *IEEE DySPAN 2010*, Singapore, 6-9 Apr. 2010.

[5] G. Kramer, I. Maric, and R. D. Yates, *Cooperative Communitions*, Foundations and Trends in Networking, 2006

[6] European Conference of Postal and Telecommunications Administrations (CEPT), "Draft ECC report 159: Technical and operational requirements for the possible operation of cognitive radio systems in the white spaces of the frequency band 470-790 MHz," September 2010. Available online at: http://www.ero.dk/D9634A59-1F13-40D1-91E9-DAE6468ED66C?frames=no&

[7] Y. Wang and J. Garcia-Luna-Aceves, "Spatial reuse and collision avoidance in ad hoc networks with directional antennas," *IEEE GLOBECOM 2002*, Taipei, Taiwan, Nov. 2002.

[8] P. Elias, A. Feinstein, and C. Shannon, "A note on the maximum flow through a network," *IRE Trans. Inf. Theory*, vol. 2, no. 4, pp. 117–119, Dec. 1956.

[9] M. Xiao and M. Skoglund, "Design of network codes for multiple-user multiple-relay wireless networks," *IEEE International Symposium on Information Theory (ISIT)*, Seoul, Korea, June 2009.

[10] C. Wang, M. Xiao, and M. Skoglund, "Diversity-multiplexing tradeoff analysis of coded multi-user relay networks," *IEEE Trans. Commun.*, vol. 59, no. 7, pp. 1995-2005, Jul. 2011.

[11] L. Zheng and D. N. C. Tse, "Diversity and multiplexing: A fundamental tradeoff in multiple-antenna channels," *IEEE Trans. Inform. Theory*, vol. 49, no. 5, pp. 1073-1096, May 2003.

[12] R. Narasimhan, "Individual outage rate regions for fading multiple access channels," *IEEE International Symposium on Information Theory (ISIT)*, Nice, France, Jun. 2007.

[13] T. M. Cover and J. A. Thomas, *Elements of Information Theory*. Wiley, 1991.

[14] M. Grant and S. Boyd "CVX: Matlab Software for Diciplined Convex Programming", Available online: http://cvxr.com/cvx/

[15] L. Fenton, "The sum of log-normal probability distributions in scatter transmission systems," *IRE Trans. Comm. Syst.*, vol. 8, no. 1, March 1960.

[16] QUASAR Deliverable D2.4 "Detection performance with multiple secondary interference," public deliverable, 31 March 2012. Available online: http://www.quasarspectrum.eu/downloads/public-deleverables.html

[17] QUASAR Deliverable D4.3 "Combined secondary interference models," public deliverable, 31 Mar. 2012. Available online: http://www.quasarspectrum.eu/downloads/public-deleverables.html

[18] P. Pirinen, "Statistical power sum analysis for nonidentically distributed correlated lognormal signals," in *The 2003 Finnish signal processing symposium (FINSIG'03)*, Tampere, Finland, May 19, 2003.

[19] QUASAR Deliverable D1.2 "Regulatory feasibility assessment," public deliverable, 31 December 2010. Available online: http://www.quasarspectrum.eu/downloads/public-deleverables.html

[20] QUASAR Deliverable D5.3 "Methods and tools for estimating spectrum availability: case of multiple secondary user," public deliverable, 31 March 2011. Available online: http://www.quasarspectrum.eu/downloads/public-deleverables.html

[21] QUASAR Deliverable D2.2 "Methodology for assessing secondary spectrum usage opportunities – final report," 31 December 2010. Available online: http://www.quasarspectrum.eu/images/stories/Documents/deliverables/QUASAR_D2.2.pdf

[22] A. Gorcin, K.A. Qaraqe, H. Celebi, and H. Arslan, "An adaptive threshold method for spectrum sensing in multi-channel cognitive radio network," *In Proc. IEEE 2010 17th International Conference on Telecommunication (ICT 2010),* pp. 425-429, Doha, Qatar, 4-7 Apr., 2010.

[23] M. Sanna and M. Murroni, "Nonconvex optimization of collaborative multiband spectrum sensing for cognitive radios with genetic algorithms," *International Journal of Digital Multimedia Broadcasting*, Vol. 2010, Article ID 531857, 12 pages, 2010, doi:10.1155/2010/531857

[24]R. R. Chen, K. H. Teo and B. Farhang-Boroujeny, "Random access protocols for collaborative spectrum sensing in multi band cognitive radio networks," *IEEE Journal on Selected Topics in Signal Processing*, vol. 5, no. 1, pp. 124-136, Feb. 2011.

[25]Z. Quan, S. Cui, A. H. Sayed, and H. V. Poor, "Optimal multiband joint detection for spectrum sensing in cognitive radio networks," *IEEE Transactions on Signal Processing,* Vol. 57, No. 3, pp. 1128–1140, Mar. 2009.

[26]S. M. Mishra, R. Tandra, and A. Sahai, "The case for multiband sensing," *The 45th Annual Allerton Conference on Communication, Control, and Computing,* The Allerton House, University of Illinois, Sept., 2007.

[27]Z. Quan, S. Cui, A. H. Sayed, and H. V. Poor, "Wideband spectrum sensing in cognitive radio networks," *In Proc. of IEEE International Conference on Communication,* Beijing, China, May 2008.

[28]P. Paysarvi-Hoseini and N. C. Beaulieu, "Optimal wideband spectrum sensing framework for cognitive radio systems," *IEEE Transactions on Signal Processing*, vol. 59, No. 3, pp. 1170 – 1182, Mar. 2011.

[29]W. Zhang, J. Yang, Q. Yan and L. Zhang "Optimal multiband spectrum sensing in cognitive radio," *IEICE Electronics Express,* vol. 7, No. 20, pp. 1557-1563, Oct. 2010.

[30]Z. Quan, S. Cui, H. V. Poor and A. H. Sayed, "Collaborative wideband sensing for cognitive radios," *IEEE Signal Processing Magazine*, vol. 25, no. 6, pp. 60–73, Nov. 2008.

[31]H. Su and X. Zhang, "Cross-layer based opportunistic MAC protocols for QoS provisionings over cognitive radio wireless networks," *IEEE J. on Sel. Ar. Commun.*, Vol. 26, No. 1, Jan. 2008.

[32]K. Liu and Q. Zhao, "Link throughput of multi-channel opportunistic access with limited sensing," *Proc. IEEE ICASSP*, Las Vegas, Nevada, U.S.A., Apr. 2008.

[33]A. Banaei and C. N. Georghiades, "Throughput analysis of a randomized sensing scheme in cell-based ad-hoc cognitive networks," *Proc. IEEE ICC*, Dresden, Germany, Jun. 2009.

[34]Q. Zhao and B. Krishnamachari, "Structure and optimality of myopic sensing for opportunistic spectrum access," *Proc. IEEE ICC*, Glasgow, Scotland, Jun. 2007.

[35]Y. Chen, Q. Zhao, and A. Swami, "Joint design and separation principle for opportunistic spectrum access," *Proc. IEEE ACSSC*, Oct. 2006.

[36]Q. Zhao, L. Tong, A. Swami, and Y. Chen, "Decentralized cognitive MAC for opportunistic spectrum access in ad hoc networks: A POMDP framework," *IEEE J. on Sel. Ar. Commun.,* Vol. 25, No. 3, Apr. 2007.

[37]S. Tang and B. L. Mark, "Modeling and analysis of opportunistic spectrum sharing with unreliable spectrum sensing," *IEEE Trans. Wir. Commun.*, Vol. 8, No. 4, Apr. 2009.

[38]H. Su, and X. Zhang, "Design and analysis of a multi-channel cognitive MAC protocol for dynamic access spectrum networks," *Proc. IEEE MILCOM*, San Diego, CA, Nov. 2008.

[39]K. Koufos, K. Ruttik, and R. Jäntti, "Feasibility of voice service in cognitive networks over the TV spectrum," *Proc. IEEE CrownCom*, Cannes, France, Jun. 2010.

[40]H. Lee and D. H. Cho, "VoIP capacity analysis in cognitive radio system," *IEEE Commun. Lett.*, Vol. 13, No. 6, Jun. 2009.

[41]K. Ruttik, K. Koufos, and R. Jäntti, "Detection of unknown signals in fading environment," *IEEE Commun. Lett.*, Vol. 13, No. 7, Jul. 2009.

[42]J. Shen, T. Jiang, S. Liu, and Z. Zhang, "Maximum channel throughput via cooperative spectrum sensing in cognitive radio networks," *IEEE Trans. Wir. Commun.*, Vol. 8, No. 10, Oct. 2009.

[43]R. Fan and H. Jiang, "Optimal multi-channel cooperative sensing in cognitive radio networks," *IEEE Trans. Wir. Commun.*, Vol. 9, No. 3, Mar. 2010.

[44]W-Y. Lee and I. Akyildiz, "Optimal spectrum sensing framework for cognitive radio networks," *IEEE Trans. Wir. Commun.*, Vol. 7, No. 10, Oct. 2008.

[45]Y. Pei, Y. C. Liang, K. C. Teh, and K. H. Li, "Sensing-throughput tradeoff for cognitive radio networks: A multiple-channel scenario," *Proc. IEEE PIMRC, Istanbul*, Turkey, Sep. 2010.

[46]Y. Chen, "Optimum number of secondary users in collaborative spectrum sensing considering resources usage efficiency," *IEEE Commun. Lett.*, vol. 12, no. 12, pp. 877-879, Dec. 2008.

[47]D. Pisinger, "Algorithms for Knapsack Problems," *Ph.D. dissertation*, Dept. Comput. Sci., Univ. Copenhagen, Feb. 1995.

[48]A. Mariani, A. Giorgetti, and M. Chiani, "SNR wall for energy detection with noise power estimation," *In proceedings of IEEE ICC*, Kyoto, Japan, 2011.

[49]C. E. Shannon, "Communication in the presence of noise," *In Proceedings of the Institute of Radio Engineers*, vol. 37, pp. 10–21, 1949.

[50]Y.-C. Liang, Y. Zeng, E. C. Y. Peh, and A. T. Hoang, "Sensing-throughput tradeoff for cognitive radio networks," *IEEE Transactions on Wireless Communications*, vol. 7, no. 4, pp. 1326–1337, 2008.

[51]C. Cormio and K. R. Chowdhury, "A survey on mac protocols for cognitive radio networks," *Ad Hoc Netw.*, vol. 7, pp. 1315–1329, Sept. 2009.

[52]T. V. Krishna and A. Das, "A survey on mac protocols in osa networks," *Comput. Netw.*, vol. 53, pp. 1377–1394, Jun. 2009.

[53]A. D. Domenico, E. C. Strinati, and M. D. Benedetto, "A survey on mac strategies for cognitive radio networks," *Communications Surveys & Tutorials*, IEEE, pp. 1–24, Dec. 2010.

[54]B. Jankuloska, M. Pavloski, M. Zahariev, V. Atanasovski, L. Gavrilovska, "Efficient spectrum utilization: a cognitive approach," *MTA Review*, Bucharest, Romania, 2011.

[55]Q. Zhang, J. Jia, and J. Zhang, "Cooperative relay to improve diversity in cognitive radio networks," *IEEE Communications Magazine*, vol. 47, no. 2, pp. 111–117, Feb. 2009.

[56]J. Jia, J. Zhang, and Q. Zhang, "Cooperative relay for cognitive radio networks," in Proc. *IEEE INFOCOM* 2009, Apr. 2009, pp. 2304–2312.

[57]E. Telatar, "Capacity of multi-antenna Gaussian channels," *Eur. Trans. Telecommun.*, vol. 10, Nov. 1999, pp. 585–598.

[58]G. J. Foschini and M. J. Gans, "On limits of wireless communications in a fading environment when using multiple antennas," *Wireless Pers. Commun.*, vol. 6, Mar. 1998, pp. 311–335.

[59]D. Gesbert, M. Kountouris, R. W. Heath, Jr., C.-B. Chae and T. Salzer, "Shifting the MIMO paradigm: From single user to multiuser communications," *IEEE Sig. Proc. Mag.*, vol. 24, no. 5, Oct. 2007, pp. 36–46.

[60]C.-B. Chae, D. Mazzarese, N. Jindal and R. W. Heath, Jr., "Coordinated beamforming with limited feedback in the MIMO broadcast channel," *IEEE Jour. Select. Areas in Comm.*, vol. 26, no. 8, Oct. 2008, pp. 1505–1515.

[61]K.-K. Wong, "Maximizing the sum-rate and minimizing the sum-power of a broadcast 2-user 2-input multiple-output antenna system using a generalized zeroforcing approach," *IEEE Trans. Wireless Comm.*, vol. 5, no. 12, Dec. 2006, pp. 3406–3412.

[62]C. B. Peel, B. M. Hochwald, and A. L. Swindlehurst, "A vectorperturbation technique for near capacity multiantenna multiuser communication part I: channel inversion and regularization," *IEEE Trans. Comm.*, vol. 53, no. 1, Jan. 2005, pp. 195–202.

[63]S. Jing, D. Tse, J. B. Soriaga, J. Hou, J. E. Smee and R. adovani, "Multicell downlink capacity with coordinated processing," *Eurasip Jour. Wireless Comm. and Networking*, 2008.

[64]H. Dahrouj and W. Yu, "Coordinated beamforming for the multi-cell multi-antenna wireless system," *Proc. of Conf. on Info. Scien. And Systems*, Mar. 2008, pp. 429–434.

[65]C.-B. Chae, S.-h. Kim and R.W. Heath, "Network coordinated beamforming for cell-boundary users: Linear and nonlinear approaches," *Proc. Of Selected Topics in Signal Processing*, Dec. 2009, pp.1094-1105.

[66]V. Rakovic, V. Atanasovski and L. Gavrilovska, "Clustered network coordinated beamforming for cooperative spectrum sharing of multiple secondary systems," *4th International Workshop on Cognitive Radio and Advanced Spectrum Management (CogArt 2011)*, Barcelona, Spain, Oct. 2011.

[67]V. Erceg et al., "TGn Channel Models," IEEE 802.11 document 802.11-03/940r4, 2004.

[68]3GPP Technical Specification 36.101 "LTE; E-UTRA; UE Radio transmission and Reception."

[69]B. Jankuloska, V. Atanasovski and L. Gavrilovska, "Combined power/channel allocation method for efficient spectrum sharing in TV white space scenario" *4th International Workshop on Cognitive Radio and Advanced Spectrum Management (CogArt 2011)*, Barcelona, Spain, Oct. 2011.

[70]QUASAR Deliverable D5.2 "Methods and tools for estimating spectrum availability: case of single secondary user," public deliverable, 31 December 2011. Available online: http://www.quasarspectrum.eu/downloads/public-deleverables.html

[71]A. T. Hoang and Y. C. Liang, "Downlink channel assignment and power control for cognitive radio networks using game theory," *IEEE Transactions on wireless communications*, Aug. 2008.

[72]L. Wang, X. Xu, W. Xu, Z. He and J. Lin, "A nash bargaining solution based cooperation pattern for open spectrum cognitive radio networks," *IEEE International Conference on Wireless Information Technology and Systems (ICWITS),* 2010.

[73]S. Boyd and L. Vandenberghe, *Convex Optimization*. Cambridge University Press, Mar. 2004.

[74]R. Henrion, "On constraint qualifications," *Journal of Opt. Th. and App.*, vol. 72, pp. 187–197, 1992.